Surface Plasmon Resonance Immunosensor Using Au Nanoparticle for Detection of Beta Agonist

A thesis submitted
for
the degree of Doctor of Philosophy

by

Dulal Chandra Kabiraz

to

Division of Environmental Materials Science
Graduate School of Environmental Science
HOKKAIDO UNIVERSITY
July 2017

Acknowledgement

First of all, I would like to express my outmost appreciation and thanks to my supervisor Associate Professor Toshikazu Kawaguchi for his extensive guidance, effective discussion and scholastic advice throughout my PhD research work. This work would not have been completed without his constant encouragement and motivation. Besides my supervisor, I would like to express my deepest appreciation and sincere thanks to the honorable members of the dissertation committee, Professor Sunitz Tanaka, Professor Vasudevan P. Biju, and Professor Masashi Takahashi for their constructive feedback and insightful comments of this thesis.

Next, I wish to thanks to Professor Ichizo Yagi for providing support, facilitation and opportunities in Yagi laboratory. I also grateful to Dr. Kou Nakata and Dr. Masaru Kato, Assistant Professors, for their constructive suggestions during my laboratory activities. I am greatly indebted to Associate Professor Ken-ichi Yamazaki for providing instrument to carry out my experiments.

Thanks are also extended to all the members of Yagi and Kawaguchi groups, especially to Dr. Suherman and Dr. Yusuke Sato for their kind assistance during my experiments. My highest appreciation also goes to USHIO INC. for remarkable cooperation.

Last but not least, I would like to express my deepest gratitude and sincere thanks to my mother for her sacrifice, patience and precious support in shaping up my educational career. I sincerely thank to my beloved wife Sutapa Devnath, my father in-law and my mother-in law for their encouragement, cooperation and optimistic mental support during my stay in Sapporo, Japan.

Sapporo Author

July 2017

Table of contents

Title: Surface Plasmon Resonance Immunosensor Using Au Nanoparticle for Detection of Beta Agonist

Chapter 1: Introduction **1**

1.1 General introduction 1

1.2 The concept of immunoassay and its application 2

1.3 Analytical method using immunoreaction **5**

1.3.1 Radioimmunoassay (RIA) 5

1.3.2 Enzyme-linked immunosorbent immunoassay (ELISA) 5

1.3.3 Immunochromatographic immunoassay 6

1.3.4 Electrochemical biosensor 7

1.3.5 Quartz crystal microbalance (QCM) biosensor 8

1.3.6 Chemilumenescent immunosensor 10

1.3.7 Surface plasmon resonance (SPR) biosensor 11

1.4 SPR biosensor and its application **12**

1.4.1 Design of immunosurface for SPR-immunosensing 12

1.4.2 Detection principles 16

1.4.3 β-agonists as target antigen 19

1.4.4 Recent advancement in analysis of β-agonists 21

1.5 Objective and outline of the thesis **23**

1.5.1 Objective of the thesis 23

1.5.2 Outline of the thesis 24

1.6 References 26

Chapter 2: Experimental **38**

2.1 Materials and chemicals 38

2.2 Surface plasmon resonance (SPR) **39**

2.2.1 Excitation of surface plasmons 39
2.2.2 Basic principle of SPR 42
2.2.3 SPR set-up 45
2.3 UV-visible measurement 47
2.4 X-ray photoelectron spectroscopy 47
2.5 Preparation of Au substrates 48
2.6 References 49
Chapter 3: Mechanism of Surface Plasmon Resonance Sensing by Indirect Competitive Inhibition Immunoassay Using Au Nanoparticle Labeled Antibody **52**
3.1 Introduction 51
3.2 Preparation of AuNP labeled antibody 54
3.3 Characterization of the Ab-AuNP conjugate 55
3.4 Fabrication of immunosurface 56
3.5 Immunoassay format 57
3.6 Results and Discussion **58**
3.6.1 Immunoassay using the Ab-AuNP conjugate 58
3.6.2 Evaluation of affinity constants 61
3.7 Summary 68
3.8 References 69
Chapter 4: Strategy of Signal Amplification and Sensitivity Enhancement **72**
4.1 Introduction 72
4.2 Fabrication of immunosurface 75
4.3 Immunoassay 77
4.4 Results and discussion **77**
4.4.1 Clenbuterol detection by using secondary immunoreaction 77
4.4.2 Evaluation of affinity constant 83
4.5 Summary 87

4.6 References 88

Chapter 5: A Sensitive Detection of Clenbuterol in Urine Sample by Using Surface Plasmon Resonance Biosensor **92**

5.1 Introduction 92

5.2 Fabrication of immunosurface 94

5.3 Urine sample pretreatment 94

5.4 Immunoassay format 96

5.5 Results and discussion 97

5.5.1 Comparison of filtration process 97

5.5.2 pH effect on secondary immunoassay 99

5.5.3 Inhibition effect 102

5.5.4 Clenbuterol detection 103

5.6 Summary 105

5.7 References 106

Chapter 6: Summary and Conclusion **109**

6.1 Summary and Conclusion 109

Chapter 1. Introduction

1.1 General introduction

There are billions of people who want a better quality of life. In fact, it is highly related to several factors such as disease detection [1,2], drug discovery [3], control of environment pollution [4,5], food quality and homeland security [6,7]. In particular, toxic agents including heavy metals, toxins, organic pollutants and food additives cause more than 200 diseases, ranging from infectious diseases to cancers [8]. For example, diarrheal disease (both food borne and water borne) kills at least 2,000,000 people annually [9]. In addition, annually approximately 600 million people or 1 out of 10 people all over the world become sick after ingesting contaminated food. Among them, 420,000 thousand people die including 125,000 children aged less than 5 years [9]. Therefore, reliable detection and quantification of toxic agents in food and drinking water are the first steps to ensure the quality of human health.

Quality of life is supported by the sensor technology. Biosensor, combining with a biorecognition element and a suitable transducer represents a promising technique for the detection of toxins in food and water samples. This technique relies upon the immunoassay based on the detection of antibody-antigen (Ab-Ag) interaction. Biosensor provides several advantages such as miniaturization, easy to use, short response time and detection of analyte without separation process. Despite the extensive research conducted in the past 20 years, a few biosensors including glucose biosensor, pregnancy test biosensor and biochemical oxygen demand biosensor are available in market [10]. Although huge potentiality emerges in the area of food and the environmental monitoring, the lack of high sensitivity of detection techniques is a major challenge.

The main contaminants in food and the environment are small molecules. However, biosensor, which is suffers from low signal levels and low sensitivity in response to small molecules, because of the inefficiency of small molecules to generate sufficient signal upon biochemical reactions or recognitions (immunoreaction). To overcome this technical limitation, the incorporation of nanoparticle is a promising approach. Nanoparticles (NP) has some unique physical and chemical features such as redox property, surface fictionalization, optoelectronic property and conductivity [11]. Since government and screening agencies (e. g. FDA) demand a high sensitive detection technique in improving the quality of human health, the use of nanoparticles in biosensors can be a promising method for the development of a sensitive technique.

1.2 The concept of immunoassay and its application

Immune system is the natural defense system of body against foreign substances. At the invasion of foreign substances such as pathogens or toxins, immune responses are stimulated. Then specialized classes of proteins called antibodies (also called immunoglobulin) are secreted in blood to neutralize the invading organisms or toxic materials. The substance that stimulates the immune system to produce antibodies is termed antigen. The specific binding reaction between an antibody and the corresponding antigen is called an immunoreaction.

The term 'immunoassay' is used for tests that involve immunoreactions. In other word, immunoassay is a biochemical technique that uses antibodies as recognition elements for binding of analytes in samples. Therefore, the important step in the immunoassay is the molecular recognition of antigen by the corresponding antibody. As illustrated in Fig. 1.1, antibody consists of two light and two heavy chains, which are linked by disulfide bonds and form characteristic 'Y' shape. The

chains are divided into constant (Fc) and variable (Fab) regions; those are unique for each type of antibody. Therefore, an antibody can recognize only a specific antigen. According to the 'lock-key' model, an antibody interacts on a highly specific way with its corresponding antigen [12]. The interaction is reversible and governed by the low of mass action. Four types of forces assists the recognition as follows:

(1) Electrostatic interactions

(2) Van der Waals interactions

(3) Hydrogen bond interactions

(4) Hydrophobic interactions.

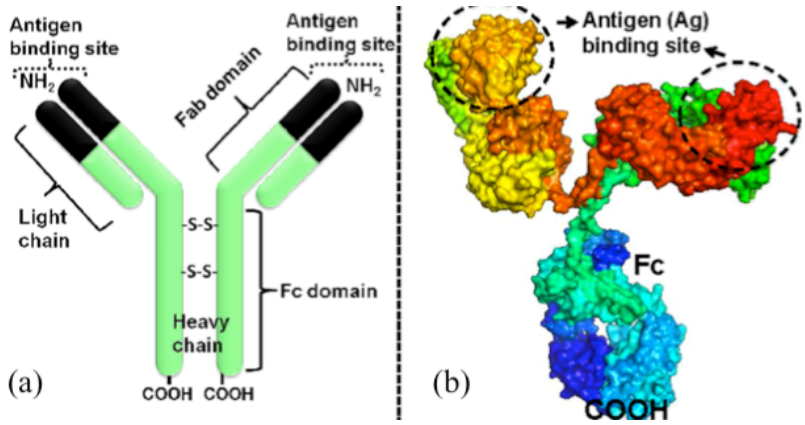

Fig. 1.1 The structure of an antibody (Ab): (a) diagrammatic presentation of an Ab with different regions displayed; (b) three-dimensional view of an Ab (PDBcode: 1IGT) [12].

Antibodies are the key factors for the successful immunoassay. Usually, monoclonal and polyclonal antibodies are used in immunoassay. Those antibodies are produced in immunized animals such as rabbits, mice or goats. Animals can be stimulated to produce different antibodies with different epitopes against a specific antigen, and are termed as polyclonal antibodies [13]. Polyclonal antibodies can

recognize multiple epitopes of one antigen. Furthermore, polyclonal antibodies are inexpensive to be produced. In contrast, monoclonal antibodies are produced from identical immune cells that are all clones of a unique parent cell and are expensive [14].

The principle of immunoassay was first introduced by Yalow and Berson et al. [15] for the determination of insulin and by Ekins et al. [16] for the determination of thyroxin in the late 1950s. Since then, there has been an increasing interest in immunoassay development and has become a popular analytical technique in different applications, from environmental monitoring and drug analysis to food sciences [17-21]. Some application fields of immunoassay are summarized in Table 1.1. Immunoassays are usually employed for one of the following purposes:

- To identify the presence or absence of particular chemical substance.
- To estimate the amount of a particular substance, within a range of interest.
- For real time monitoring of the changes in concentration of an analyte.

Table 1.1 Application fields of immunoassay.

Application field	Detection objects	Ref.
Food quality and safety analysis	Food additives, pesticide residues, pathogens, toxins	[22−26]
Biomolecular interaction studies	Antigen-antibody, protein-protein	[22,27−31]
Pharmaceutical analysis	Macromolecular biomolecules, metabolites, biomarkers, low molecular weight drugs	[32]
Environmental monitoring	Organochlorine pesticides, aromatic hydrocarbon, Heavy metals and real time monitoring of the growth of toxic algae in sea water	[33−35]
Medical diagnostics	Cancer markers, hormones, Hepatitis B-virus, Allergy markers, heart attack markers	[33,35−40]

1.3 Analytical methods using immunoreaction

1.3.1 Radioimmunoassay (RIA)

Radioimmunoassays use radioactive isotopes, usually tritium (^{3}H) or iodine-125 (^{125}I) as labels to detect either the antigen or antibody. Miles and Hales et al. [41] published their first report on radioimmunoassay technique for monitoring insulin in human plasma. As shown in Fig.1.2, two antibodies are used and one is radio labeled. In this system, the sample is incubated with a specific antibody attached to a substrate. After the formation of antibody-antigen complex, a radioactive antibody is added. The amount of radioactivity is directly proportional to the amount of antigen. The major advantages of RIA are higher sensitivity, easy signal detection and rapid assay. However, RIA possesses concerns on occupational safety [42].

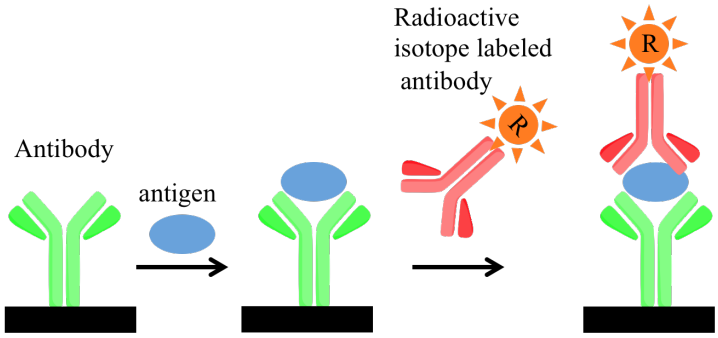

Fig. 1.2. The principle of radioimmunoassay [23].

1.3.2 Enzyme-linked immunosorbent assay (ELISA):

In the early 1970s, ELISA technique was adopted for the detection of environment pollutants such as dithiothreitol (DDT), malathion and aminotriazole in ecosystem [43]. Over the next decade, this method has been developed and widely used for food and environmental monitoring [44-48]. ELISA employs the basic immunoassay concept of an antigen binding to its specific antibody [24,25]. Antigen or antibody in liquid phase is immobilized, usually in 96-well microtiter plates (special absorbent

plates). The ELISA method follows some steps, shown in Fig. 1.3. The first step is to coat ELISA plate with antibody against antigen of interest. In the next step, a sample solution-containing antigen is added. The antibody already bonded to the plate captures antigen. In step 3, an antibody labeled with enzyme (usually horseradish peroxidase or alkaline phosphatase) is added [47,48]. Finally, a substrate (e.g. 5-amino salicylic acid, orthophenylenediamine, p-nitrophenyl phosphate etc.) is added to the plate. During the enzyme–substrate reaction, the substrate is converted into a colored product. Therefore, quantification of target analyte is based on color changes. ELISA is simple and low cost, but this technique suffers from low sensitivity of the photometric measurement, long time for enzyme-substrate reaction (> 1 h) and poor stability of the labeled enzymes [49].

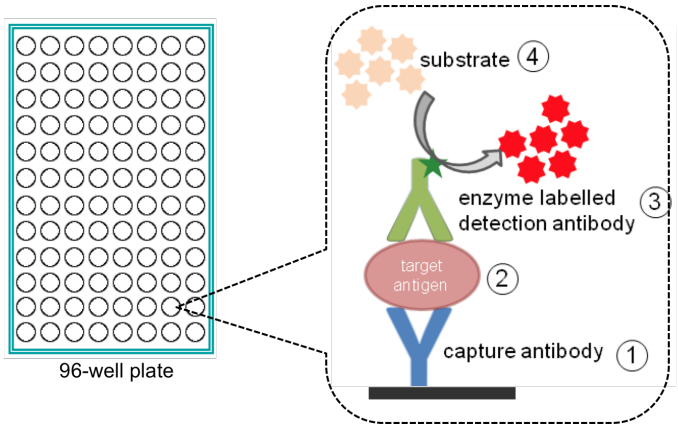

Fig. 1.3. The ELISA method showing the steps in the assay [47].

1.3.3 Immunochromatographic assay (ICA):

This assay principle involves flow of liquid containing analyte through a porous membrane (nitrocellulose) to an absorbent pad [50-52]. The basic principle of immunochromatographic assay is presented in Fig. 1.4. When a sample solution is dropped at the sample pad, it moves forward by capillary action. After reaching at the conjugation pad, it dissolves and reacts with the colloidal Au-labeled reagents. It then

further moves to an area on the test line where antigens or antibodies attached. If the compounds formed between samples and the Au-labeled reagents specifically reacts with the antigens or antibodies, they will accumulate in test line. This causes a color change, which is visible to the naked eye.

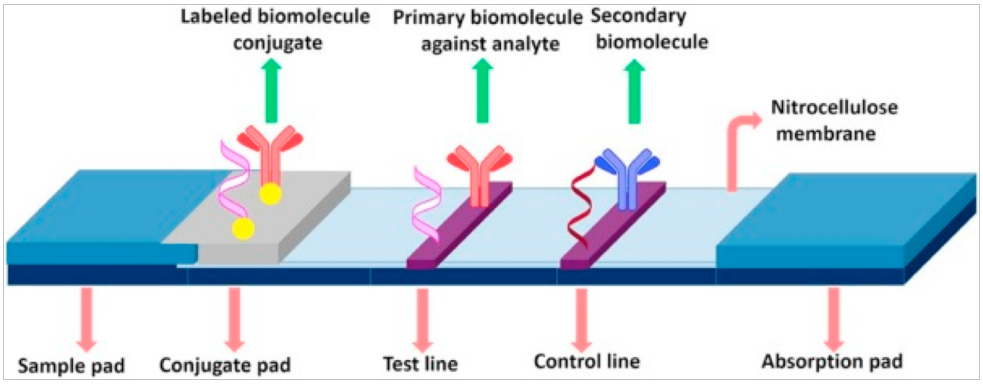

Fig.1.4. The principle of immunochromatographic assay [50].

This technique is rapid (within 5 min) and simple for qualitative screening, but needs large volume of samples [51,53]. The practical application of this method is often restricted by relatively low sensitivity, especially for the analysis of food contaminants such as chemical pesticides and antibiotic residues [54].

1.3.4 Electrochemical biosensor

Electrochemistry studies an electron transfer that takes place at the interface of an electrode and the electrolyte or species in solution. Biorecognition elements (e.g. antibody or antigen) linked with electrode act as electrochemical transducer. Based on the signal generation principle, the electrochemical biosensors are mainly classified as amperometric, voltametric, impedimetric and capacitometric [19,55,56]. Although the immunoreaction can change the electrochemical signal, the change is relatively small. For successful development of immunoassay, high affinity antibodies, enzyme labeled antibodies, quantum dots (QDs) or nanoparticle (NP)

labeled antibodies are usually employed [57–61]. For example, Idegami et al. [62] applied secondary antibody labeled Au-nanoprticle for signal amplification for the detection of human chorionic gonadotropin (hCG) hormone (antigen) by using differential pulse voltametry (DPV). The immunoreaction on the electrode surface and oxidation of AuNP upon applied voltage is illustrated in Fig. 1.5 A. As seen in Fig. 1.5 B, the signal increases proportionally with the increase in antigen concentration. Electrochemical biosensor provides several advantages such as high sensitivity, low cost and low power requirement. However, this technique suffer from insufficient matching of redox partner with the target analytes, lack of strong background signal and low sensitivity [19,63].

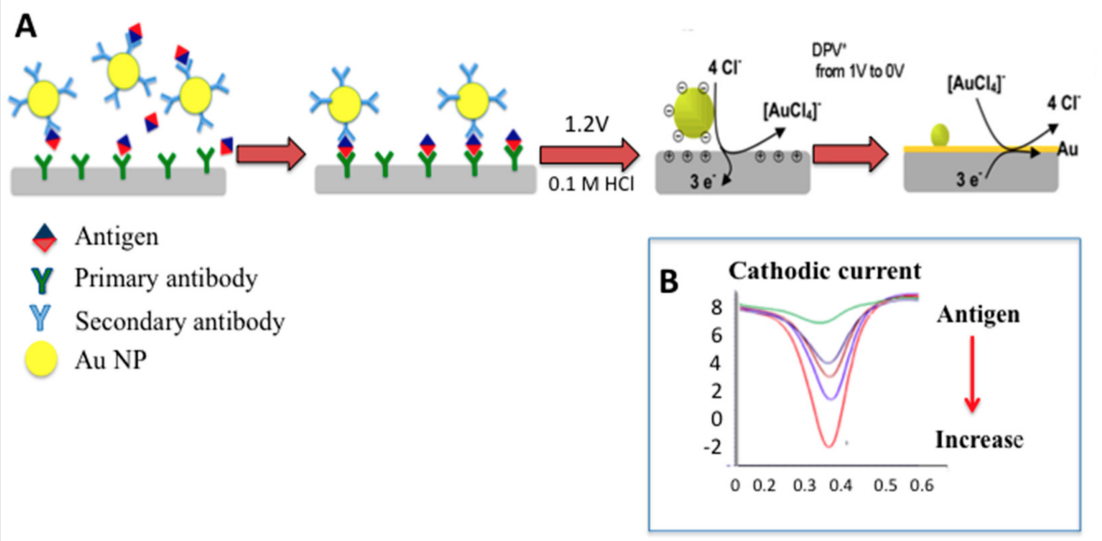

Fig. 1.5. The schematic presentation of electrochemical immunoassay by using secondary Ab labeled with AuNP [64].

1.3.5 Quartz crystal microbalance (QCM) biosensor

QCM is basically a mass-sensing sensor. The principle of QCM-biosensor relies upon the piezoelectric effect [65] of the crystal. Fig. 1.6 represents the QCM immunoassay. When a quartz crystal is subjected to an AC potential, a mechanical oscillation is generated. The frequency change of such oscillation is correlated to

the mass change on the material surface. The frequency change (Δf_x) can be explained by the Sauerbrey equation [66].

$$\Delta f_x = -\frac{f_0^2}{F_q \rho_q} m \qquad (1.1)$$

Where F_q is the constant of crystal frequency, f_0 is the resonance frequency of the quartz resonator, ρ_q is the material density and m is the mass per unit area. Such biosensor utilizes antigen or antibody immobilized sensor surface for the measurement of the change in frequency. When immunoreaction is occurred onto the sensor surface, the resonance frequency decreases due to formation of antibody-antigen complex. The change in frequency (Δf_x) is linearly proportional to the mass (Δm) of the absorbed molecules per unit area. Recently, Karczmarczyk et al. [67] developed a QCM-biosensor for the detection of small molecule ochratoxin A by using antibody labeled with AuNP to achieve high sensitivity. However, reported limit of detection (LOD) was only 0.16 ngmL^{-1}. Therefore, the use of QCM for the detection of trace biological target is still encumbered by its relatively low intrinsic sensitivity [68-71].

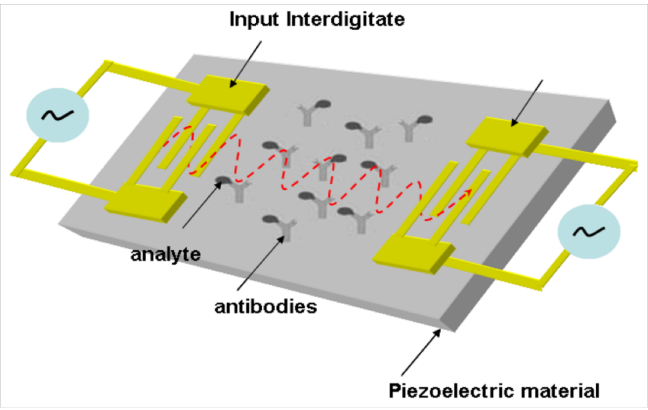

Fig. 1.6. The schematic illustration of QCM immunoassay [72].

1.3.6. Chemiluminescent immunoassay

Chemiluminescent immunoassay, combining with chemiluminscent system and immunoreaction, is a detection technology for the determination of analyte in sample. This technique measures the signal or response from the emission of chemiluminescent (CL) light produced by molecules that are excited by chemical energy and detected by a light detector. The most widely used system among CL reaction is the luminol-H_2O_2-horseradish peroxidase. Phenol or derivative compounds act as an enhancer of the CL reaction. Since it was first reported by Woodhead et al. [73], chemiluminescence immunoassay has drawn attention to researchers in different fields such as clinical diagnosis [74], food safety [75], prevention of radiation damage [76] and environmental analysis [77]. For example, Guan's group [78] demonstrated a developed chemiluminescence immunoassay based on Fe_3O_4 magnetic nanoparticle to detect human chorionic gonadotropin (hCG). The reported process required time consuming step such as washing and labeling as seen from Fig 1.7. This technique provides some advantage such as simple instrumentation, wide dynamic range and very low limit of detection. However, chemiluminescent immunoassay suffers from considerable background issues [19].

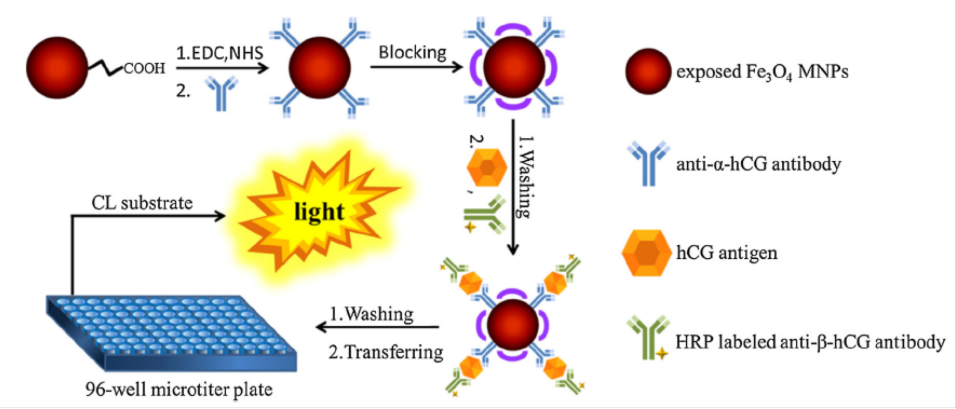

Fig. 1.7. The schematic diagram of chemiluminescent immunoassay for hCG [78].

1.3.7. Surface plasmon resonance (SPR) biosensor [56-85]

SPR biosensor is an optical sensor based on excitation of surface plasmon at thin metal (Au) film [33,79]. A beam of incident light can couple with the surface plasmon under certain condition and generating an evanescent electromagnetic wave, which decay exponentially within 300 nm from the metal Au surface [79]. SPR biosensor measures the refractive index (RI) changes (smaller than 10^{-5}) due to binding analyte onto the sensor surface with a time resolution of few seconds [80]. The sensor response is characterized by the wavelength (λ) or angle (θ) of the minimum reflectivity [80,81]. The basic principle of SPR biosensor is illustrated in Fig. 1.8.

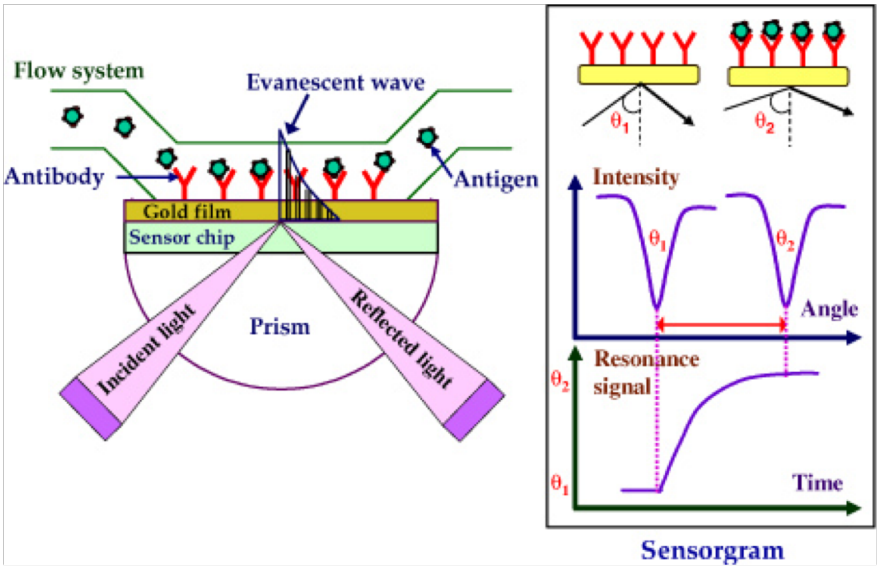

Fig. 1.8. The schematic view of typical SPR biosensor [79].

In SPR-biosensing, a solution containing target analyte is flowed over the sensor surface where probe molecules are immobilized. The capture of analyte by molecular recognition of the sensor surface alter its refractive index and resulted in SPR angle shift. From the angle shift calculation (Δθ) the reacted amount of analyte on that surface (1 mdeg~ 10 RU~ 1 ng cm^{-2}) can be calculate [82]. Since the first

application of SPR technology for a biosensor for the detection of gas by Nylander and Liedberg et al. [83,84] in 1983, SPR biosensors have attracted increasing attention and have been widely used in various fields including biomolecular interaction monitor [85], pharmaceutical development [33], medical diagnostics [33,85–88], environmental monitoring [33, 89–91], food safety [33,92–94], and homeland security [33,95–98]. For example, Muira's group [95-98] studied SPR biosensors for the detection of TNT, which has carcinogenic effect and usually used in landmines. Most of their sensor could detect as few as 10 $pgmL^{-1}$ in less than 20 min, without labeling or enrichment step.

In the scope of the thesis, I will focus on SPR biosensor as it provides several advantages such as:

- Label-free detection
- High sensitivity
- Rapid and real-time analysis
- Relatively simple procedures
- Small amount of sample solution
- Miniaturization
- Immunoassay provides high selectivity

1.4 SPR biosensor and its application

1.4.1 Design of immunosurafce for SPR-immunoasensing

SPR biosensors commonly use antibodies or antigen as bioreceptors to recognize its complementary target. The classification of strategies for the sensor surface fabrication onto both unmodified and functionalized Au-substrate is difficult. Because the diversity of activation process and the singularity of each recognition

event. To date, several sensor surface fabrications strategy has been introduced. A brief summery of some SPR immunosensors have been developed for various application are listed in Table. 1.2.

(i) Adsorption

Direct adsorption onto Au-surfaces is simple and easy to perform; therefore, it is the most employed sensor surface fabrication approach for decades [79,93,94]. This adsorption is generally relies on hydrophobic, electrostatic, hydrogen binding and Van der Waals forces [79]. Antibody or analyte-protein conjugate can be immobilized onto Au-surface for the detection of analyte of interest. For instance, Shankaran et al. [79] have been developed immunosensor by physical adsorption of the conjugates for the detection of analytes such as methampthamine and they reported high sensitivity. However, physical adsorption is an uncontrolled and non-specific process that may cause the sensor surface inactivation. Furthermore, there is a possibility to degrade the sensor surface [95]. As a result, the stability and the reproducibility of the assay will be decreased.

Table 1.2. SPR immunosurface fabrication technique

Fabrication method	Analyte	Biomolecule/ interfacial structure	Detection range	Regeneration/stability	Ref.
Physical Adsorption	Morphine (MO)	Au/MO–BSA conjugate	0.1–10 ppb	Glycine-HCl 10 cycles	[79,97]
Dextran	Estradiol	Au-Dextran/estradiol oligoethylene derivatives	2.5 ppm	NaOH and MeCN 200 cycles	[79,87,97]
Self-assembly	TNT	Au/PEG-NH_2 SAM/ TNPh-β-alinine	0.008-30 ppb	Pepsine 100 cycles	[98]
Protein A or G	2,4-dichlorophenol	Au/Gold binding peptide/proteins	20 ppb	New chip for each measurement	[104]
Biotin-steptavidin	c-reactive protein (CRP)	Au/biotin-streptavidin/ biotinylated anti CRP/CRP	2–5 ppm	-	[106]
Polymer or membrane	Domoic acid	Au/SAM/MIP polymer	5 ppb	0.2% SDS–HCl 30 cycles	[110]

(ii) Dextran platform

The special conformation of dextran based-layer provides multiple binding sites. Therefore, a high density of immobilized receptors is expected. The immobilization of antibodies or antigen can be achieved through amide coupling chemistry. Prior to immobilization, the carboxylic groups of dextran are activated by carbodiimide bonding [92]. Subsequently, the antibody or analyte-conjugates are covalently attached to the surface via the amine group. This type of platform has been traditionally used in SPR biosensing, especially through Biacore carboxymethyl (CM) dextran sensor surface [96-98]. However, such surface faced problem regarding non-specific adsorption, when real sample for example plasma or serum is analyses. Another possible difficulty is the mass transfer limitation, which may lead wrong kinetic information [79].

(iii) Self-assembly

The formation of self-assembled monolayer (SAM) is simple and straightforward. In particular, SAM of alkanethiols on Au surface provides a convenient and flexible route to fabricate a stable and ordered layer of biological molecule on a variety of substrate [79]. Therefore, covalently binding of receptor (antibodies or antigen) to previously chemically modified substrate is widely used immobilization method for monitoring immunoreactions [99-102]. One of the most important advantages of immunosurface fabricated by using SAM method is reduction of non-specific adsorption [79].

(iv) Protein A or protein G

Fabrication of sensor surface via Protein A and Protein G binding is a common strategy to achieve site-oriented immobilization of antibodies onto sensor surface [103-105]. Antibody-binding proteins are generally attached to Au-surface with self-assembled monolayer or dextran-hydrogel coupling. The Fc part of antibody

covalently binds with the protein. Therefore, the antigen-binding sites stay away from the sensor surface. Consequently, a stable and accessible immunosurface can be achieved, which is capable to recognize its complementary target. For example, Waswa et al. [105] attached protein A onto carboxymethylated (CM) dextran layer via amide-coupling reaction. Subsequently they immobilized polyclonal *S. enterica* antibody to protein A in order to prepare sensor surface for the detection of *S. enterica* in milk. One of the important limitations of this modification process is the high cost and the requirement of a linker to immobilize the protein A or G [79].

(v) Biotin-avidin coupling

The immobilization of bioreceptors via biotin-avidin coupling is generally employed when the amine or thiol coupling is unsuitable [92]. Biotin (MW 244 Da) has carboxylic acid group, which can covalently bind with a wide range of macromolecules (e.g. proteins, peptides, oligonuclides and antibodies) while maintaining its binding affinity towards avidin or avidin related molecules such as steptavidin. Steptavidin has four binding sites and it forms a layer over a biotynilated surface (e.g. biotynilated BSA). The steptavidin-immobilized surface then captures the biotynilated antibody. This method is a common choice in order to control the receptor orientation and signal enhancement due to high binding capacity [106-108]. However, one significant limitation is the requirement of chemically modifying the biotynilated antibody. Therefore, the cost and required time are increased for the analysis.

(iv) Polymer matrix

The fictionalization of the SPR sensor surface via polymers provides a versatile and heterogeneous three-dimensional matrix for capturing receptors by adsorption or covalent coupling. Poly (p-xylylene) polymers and polymer brushes of

(poly (2-hydroxyethyl methacrylate) (poly (HEMA)) and poly[oligo(ethylene glycol) methacrylate-co-glycidyl methacrylate] (POEGMA-co-GMA)) are used in the fabrication process [109,110].

Among these sensor surface fabrication methods mentioned above, self-assembly (SAM) shows great advantages in terms of surface oriented monolayer, high stability and easy preparation.

1.4.2 Detection principle

The selection of detection principle basically depends on the size of analyte (antigen) molecule and characteristic of analyte, which has to be detected. The common assay principles are (a) direct detection, (b) sandwich detection, (c) competitive detection and (d) indirect competitive inhibition format. Each assay format has its own advantages and limitations in terms of sensitivity, availability of suitable reagents, assay time, required sample volume and application [33,111]. An overview of different assay formats used in SPR biosensor for various application fields are summarized in Table 1.3.

(a) Direct assay format

With a direct assay format (Fig. 1.9-a), antibodies (Ab) are immobilized onto the substrate [83,111]. Upon injection the sample containing anlyte of interest, analyte can directly binds to the Ab onto sensor surface. Therefore, the binding response is proportional to the mass of antigen. By the use of such simple direct assay format, Indyk et al. have reported a detection limit of 16.8 ppb (ng/mL) for IgG in milk [121]. This assay format is appropriate for large molecule (Molar mass > 10 kDa), because small molecule (Molar mass < 1000 Da) have insufficient mass to produce a detectable change in refractive index at the sensor surface [33,111].

Table.1.3 Overview of detection format used in SPR immunoassay.

Application	Detection format	Analyte	Detection matrix	LOD	Ref.
Food quality and food safety analysis	inhibition	antibiotics	Poultry	0.005 µg/kg	[112]
	sandwich	Allergen	Chocolate	1 µg/g	[113]
	sandwich	staphylococcal enterotoxin B	Milk	0.5 ng/ mL	[114]
	Inhibition	Thiabendazole	Orange sample	0.13 µg/L	[115]
	competitive	staphylococcal entrotxin A	Raw eggs	1 ng/mL	[116]
Environmental monitoring	direct	Cu+	Buffer	62 pM	[117]
	inhibition	atrazin	Water	20 pg/mL	[118]
	inhibition	Bisphenol A	Buffer	10 ng/mL	[104]
Clinical diagnosis	sandwich	Hormon (hCG)	Urine	46 mIU/ mL	[119]
	sandwich	Prostate-specific antigen	Buffer	0.15 ng/mL	[120]
	Direct	Antibody (IgG)	Milk	16.8 ng/mL	[121]
	inhibition	insulin	Buffer	1 ng/mL	[122]
Biothreat	direct	E.Coli O157	Apple juice	10^2-10^3 cfu/mL	[105]
	sandwich	Staphylococcus aureus	Buffer solution	10^5 cfu/mL	[123]

Note: Inhibition=Indirect competitive inhibition assay

(b) Sandwich assay format

The direct immunoassay can further improve by employing secondary antibody and antibody-antigen-antibody complex is formed, which is called sandwich immunoassay (Fig. 1.9-b). Therefore, this assay format consists of two recognition steps; first one is primary immunoreaction and the next one is secondary immunoreaction. Concentration of analyte is proportional to the signaling intensity of the immunocomplex generated by the secondary immunoreaction. Based on this assay principle, Homola et al. [114] have analyzed milk sample for the detection of staphylococcal enterotoxin B and more than 10-times lower detection limit with a magnitude of 0.5 ng mL^{-1} compared to the direct immunoassay was reported. This assay format produced high signal and high sensitivity; hence it gained popularity in the immunosensing. However, it should be noted that this assay requires two distinct

antibodies that simultaneously binds with the target analyte. In addition, this format is applicable for large molecule (> 5000 Da) such as protein, bacteria and viruses those has a minimum of two distinct epitopes [111]. Therefore, those two fundamental limitations hinder its wide application.

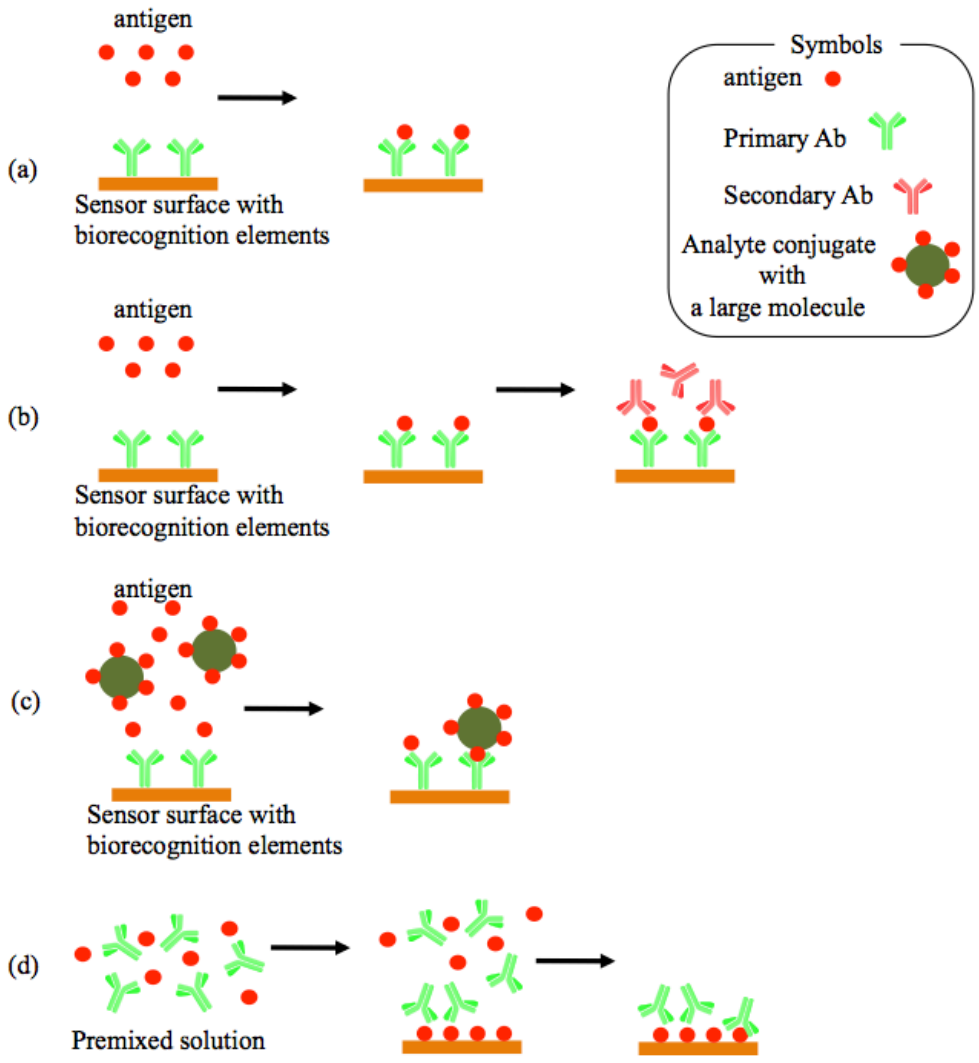

Fig. 1.9. The principle of assay formats used in SPR biosensor [33].

(c) **Competitive immunoassay**

Figure 1.9-c presents the principle of competitive assay format, in which sensor surface is antibody immobilized sensor surface. Exposure of this sensor to a solution of the analyte of interest mixed with a conjugate analyte, the analyte and its conjugate analogue compete for the binding sites of the sensor surface [112]. The

analyte blocks the ability of the analyte conjugate to bind because that binding site on the antibody is already occupied. Therefore, the binding signal of the test sample is inversely proportional to the concentration of analyte. When analyte is introduced to the sensor surface after the injection of analyte conjugate, this assay format is called as competitive displacement assay [124]. Upon injection of analyte, displacement of analyte conjugate from the sensor surface is occurs. This format is easy to use. However, the binding affinity of surface-bound and solution-phase analyte needs to be comparable [111].

(d) Indirect competitive inhibition immunoassay

In this assay (Fig. 1.9-d), antigen or analyte of interest is immobilized onto sensor chip via an appropriate monolayer or an analyte-carrier protein (such as BSA). Then, the analyte and its corresponding antibody are premixed. In this step, a portion of antibody will bind to the analyte in the premixed solution. Hence, unreacted antibody bind with the analyte onto sensor surface. There are two immunoreactions occurs in the indirect competitive inhibition immunoassay. One is solution immunoreaction and another is sensor surface immunoraection. The SPR transducer monitors the sensor surface immunoreaction between antibody and analyte at the interface and translates the changes in dielectric constant into output signal. As the SPR biosensor recognizes the binding of heavy weight antibody; therefore, a high signal is expected [111]. Indirect competitive inhibition immunoassay is useful [33,111] for analyte (such as toxins, β-agonists) with single epitope and molar mass less than 1,000 Da.

1.4.3 β-agonists as target antigen

The agriculture and live stock sector of many countries are under threatened due to several environmental problems. Furthermore, some countries need to import

food products such as meet and grains from other countries due to food-insufficiency. Table 1.4 represents food sufficiency rate in fiscal year in 2014 and target for 2025 in Japan [125]. This report also stated that approximately 60% of the total consumption has been imported from other countries. Another report shows that Japan imports approximately 700,000 metric tons of beef, which is about 17 % of the global import [126]. The inspection rate in term of food safety conducted in Japan to check the quality of imported food is approximately 20 % [127].

Table 1.4. Food –sufficiency rate in Japan.

Item	Fiscal year-2014	**Fiscal year-2025 (Target)**
Calorie basis	39	45
Production value basis	64	73
Animal feed	27	40

Beta-adrenergic agonists or β-Agonists (MW is less than 300 Da) are among the commonly prescribed drugs for the treatment of respiratory diseases and asthma [128-131]. However, due to their potential roles in increasing muscle to fat ratio, β-agonists are illegally used in animals as growth promoters [132-137]. Clenbuterol (Fig. 1.10) is the most common and one of the most potent β-adrenergic agonist used in meat farming for such purpose. It may be added to animal feeds as growth promoter with a dose level 5 to 10 times higher than the therapeutic dose (0.8 ug/kg body weight per day) for economic benefit [138-140]. After consumption of meet, clenbuterol can be easily stored in human tissues, and result in many serious health problems such as headache, nervousness, tremor, rhinitis, blood pressure, heart palpitations etc. [141-143]. Recently, many countries including EU, USA, China and Japan have strictly banned the use of clenbuterol for growth promoting agent [144].

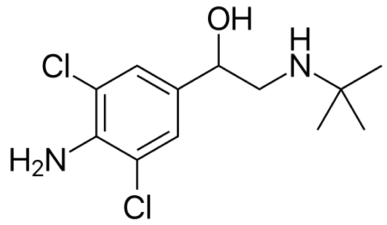

Fig. 1.10. Chemical structure of Clenbuterol.

The doping issue is also a burning issue in the sports sector such as World Cup Football, Olympics game, etc. Despite several attempts have been taken by concerned authority such as International Association of Athlete Federations (IAAF), International Olympic Committee (IOC) to keep free sports from doping, recent report didn't indicated any signs of decreasing trend [145]. Recent reports on meat consuming by athletes in China have shown an increased risk of unintentional doping with the banned chemical clenbuterol [146, 147]. Therefore, inspection services for food safety are particularly interested in β-agonists.

1.4.4 Recent advancement in analysis of β-agonists

To date, analysis of β-agonists is performed by traditional analytical methods including chromatography combined mass spectroscopy [148] and enzyme-linked immunosorbant immunoassay (ELISA) [149,150]. These technologies provide high sensitivity, but can't meet the requirement of on-site and rapid detection. In contrast, SPR biosensor received increased attention as it provides many advances are discussed earlier. Some recent studies are summarized in Table 1.5. In general, indirect competitive inhibition immunoassay is adopted, as β-agonists are small molecules. For example, Wu et al. [164] prepared sensor surface by conjugating clenbuterol (Clb) to BSA conjugate, which provides large number of reaction sites. As a result, a high response can be obtained. However, the reported LOD was 4.5 ppm by using anti-clenbuterolpolyclonal Ab in buffer solution. Most importantly,

they could not avoid the non-specific adsorption. In another example, Gao et al. [149] applied the same strategy and assay format for the detection of ractopamine and achieved sensitivity as low as 0.12 ppb in pork liver sample. In order to improve sensitivity, Yao et al. [160] explored a new immobilization strategy and prepared three-dimentional immobilization of clenbuterol. The limit of detection was obtained 6.32 ppm. Most recently, Suherman et al. [161-163] constructed immunosurface through immobilization of Clb onto self-assembled monolayer via amide coupling reaction. The estimated limit of detection was as low as 3 ppt for unlabeled anti-clenbuterol antibody (primary Ab). Therefore, high sensitivity is requested for the practical application. Recent developments of analytical techniques for β-agonists detection have been listed in Table 1.5.

Table: 1.5 Summery of analytical technologies of β-agonists.

Analytical Techniques	Sample	Targets	LOD	Ref.
Gas chromatography with Mass spectrometry	Urine	Clenbuterol, metoprolol and propranolol	0.08-0.1ng mL^{-1}	[148]
ELISA	swine kidney, liver, meat and feed	Phynylethanolamine A	0.003 ng mL^{-1}	[149]
	Animal tissue	Clenbuterol	100–25 pg mL^{-1}	[150]
Immunochromato-graphic assay	Swine urine	Clenbuterol and rectopamine	1 ng mL^{-1}	[151]
	Swine urine	Salbutamol, cimbuterol, Terbutaline, clenbuterol, and brombuterol	0.43 ng mL^{-1}	[152]
Colorimetric assay	Human urine	clenbuterol	2.8×10^{-11} M	[153]
	Swine feed	Ractopamine and salbutamol	1×10^{-10} M	[154]
Electrochemical sensor	Feed	Clenbuterol	1 ng L^{-1}	[155]
	Pork	Eight β-agonists	0.58-1.46 ng mL^{-1}	[156]
	Pork	Clenbuterol	0.22 ng mL^{-1}	[157]
	Spiked	Ractopamine	1×10^{-10} M	[158]
Chemilumenescence assay	Liver	Clenbuterol	120 ng mL^{-1}	[159]
SPR biosensor	Buffer	Clenbuterol	6.32 µg mL^{-1}	[160]
	Buffer	Clebuterol	0.3 ng mL^{-1}	[161]
	Buffer	Rectopamine salbutamol	10 pg mL^{-1} 5 pg mL^{-1}	[162, 163]
	Buffer	Clenbuterol	6.25-50 µg mL^{-1}	[164]
	Pork	Clenbuterol	2.75 ng mL^{-1}	[165]

1.5 Objective and outline of the thesis

1.5.1 Objective of the thesis

SPR biosensor is a suitable candidate as it provides a numerous advantages over other kinds of analytical method. However, the SPR biosensor is not commercialized so far, because a common SPR instrument is larger than a microwave oven in kitchen. Although the compact SPR biosensor has been commercialized, its sensitivity is lower than laboratory oriented common SPR instrument. The lack of high signal and high sensitivity for detecting a small analyte at a low concentration is a major impediment to SPR biosensor.

When small molecule such as β-agonists is target, the indirect competitive inhibition immunoassay is useful. Although a high SPR signal is expected using this immunoassay format, only 5 mdeg was reported using monoclonal Ab [161]. Whereas, 10 mdeg signal drift could be observed due to physical change such as temperature and pressure. Furthermore, LOD obtained by previous study [161-165], is far above for practical application. Thus, I investigated the signal enhancement and sensitivity improvement of the immunoassay. In the past reports, the SPR immunosensing with Au nanoparticles provides a high sensitivity [33]. However, the use of AuNP for sensor surface modification could not produced a high sensitivity of the indirect competitive inhibition immunoassay. Therefore, it is hypothesized that monoclonal Ab labeled with AuNP (Ab-AuNP conjugate) as a biorecognition element could improve the sensitivity. However, it is believed that the total size of Ab-AuNP conjugate becomes a larger than the unlabeled antibody. Hence, the mobility of AuNP-antibody must be altered. Since affinity constant of immunoreaction is a key factor of sensitivity, thus it is assumed that large size Ab-AuNP conjugate would affect the immunoreaction. Therefore, I investigated the relationship between the

affinity constants of immunoreaction and LOD of indirect competitive inhibition immunoassay. In this thesis, I used clenbuterol (a small analyte) as a target analyte.

As the primary immunoraection could not generate sufficient SPR signal, therefore I proposed secondary immunoreaction in the indirect competitive inhibition immunoassay. It was reported [161-163] that the sensitivity of the primary immunoreaction was determined by the affinity constant of the immunosurface. Thus, it is inferred here that the affinity constant of the sensor surface also influenced on the secondary immunoreaction. Aiming to elucidate this effect on the secondary immunoreaction, the low and high affinity constant sensor surfaces were employed.

Even though the high sensitivity was realized in an ideal condition, there are challenges for real sample analysis as it contains many kinds of inhibitors. In addition, pH of sample may affect the SPR response. However, this information for secondary immunoassay is still lacked. Thus, I investigated the pH effect in secondary immunoassay. It should be noted that an important step for biological sample analysis is the pretreatment. The present filtration process takes long times (more than 1 h) and need organic solvent. To overcome this limitation, alternative filtration process is needed. In order to test the developed immunoassay and filtration process for the practical application, urine sample was analyzed.

1.5.2 Outline of the thesis

The main body of the thesis includes 6 chapters.

In **chapter 1**, the present situation of environmental problems and its adverse effects on human beings are described. Also, inadequacy of classical methodologies to overcome the environmental assessments and monitoring is mentioned. Because this thesis focused on SPR, the principle and its application are reported. In addition,

the sensors using an immunoassay are introduced to deal with environmental challenges. The scope and outline of the thesis have briefly are summarized.

In **chapter 2**, the instrument and their principle are described in briefly. In particular, SPR configuration and the sensor surface fabrication process are introduced. Experimental condition of SPR, UV-Vis spectroscopy, and X-ray Photoelectron Spectroscopy (XPS) is mentioned.

In **chapter 3**, I discuss clenbuterol immunosensing by using the anti-clenbuterol Ab (mouse IgG) and anti-clenbuterol Ab labeled with AuNP (Ab-AuNP conjugate). The sensor surface fabrication procedure, anti-clenbuterol Ab labeling processes its characterization is described here. Using indirect competitive inhibition immunoassay, the sensing performance of Ab and Ab-AuNP conjugate are compared for the detection of clenbuterol. To identify the key factors in determining the LOD of the immunoassay, the affinity constants of surface immunoreaction (K_1) and solution immunoreaction (αK_2) is evaluated. According to the modified Langmuir isotherm, the simulation plot of LOD with respect to K_1 and αK_2 are constructed. The simulation plot clarifies the LOD determination factor of the indirect competitive inhibition immunoassay.

In **chapter 4**, I propose the secondary immunoreaction in indirect competitive inhibition immunoassay aiming to achieve high signal and sensitivity. To understand the effect of sensor surface affinity constant on the secondary immunoreaction, a low and a high affinity constant sensor surface are febricated. The SPR response and the obtained sensitivity for clenbuterol immunosensing are compared. In order to calculate the affinity constant for the secondary immunoreaction, the Langmuir isotherm is modified. After secondary immunoreaction, the sensor surfaces are characterized by using XPS study. Furthermore, the sensing performance of unlabeled

anti-mouse IgG (secondary Ab) and anti-mouse IgG labeled with AuNP (Ab_2-AuNP) are compared. The obtained results are discussed based on surface concentration and affinity constant calculation.

Chapter 5 describes a highly sensitive immunosensing of clenbuterol in a real urine sample. Urine sample filtration processes (physical and chemical filtration) and the obtained results are compared. The clenbuterol spiked urine sample is analyzed by using secondary immunoreaction with Ab_2–Au NP conjugate. The obtained sensitivity is also compared with the ideal buffer solution.

In chapter 6, the concept of the sensitivity determination factor is summarized. Based on the kinetic analysis, the strategy for the design of the highly sensitive immunoresensing is discussed. Further, toward to a practical use of immunosensor, the pretreatment method for a real urine sample is proposed.

1.6. References

[1] R.M. Kaplan, A.N. Vidyashankar, Vet. Parasitol. 186 (2012) 70–78.

[2] P.F. Kiku, M. V Yarygina, Achiev. Life Sci. 8 (2014) 16–22.

[3] G. Toth, C. Szigeti, Ecol. Indic. 60 (2016) 283–291.

[4] R. Tang, J.M. Clark, T. Bond, N. Graham, D. Hughes, C. Freeman, Environ. Pollut. 173 (2013) 270–277.

[5] D. Pimentel, Environ. Dev. Sustain. 14 (2012) 151–152.

[6] H.O. Johnson, S.C. Gupta, A.V. Vecchia, F. Zvomuya, J. Environ. Qual. 38 (2009) 1018–1030.

[7] Center for Disease Control and Prevention, Tracking and reporting food borne disease outbreaks in 2013, at www.cdc.gov.

[8] K. Fukuda, Bull World Health Organ. 93 (2015) 212.

[9] http://www.who.int/bulletin/volumes/93/4/15-154831/en/

[10] R. Romero-González, Anal. Methods. 7 (2015) 7193–7201.

[11] T. Dhewa, Oct. Jour. Env. Res. Vol. 3 (2015) 212–218.

[12] S.C.B. Gopinath, T.H. Tang, M. Citartan, Y. Chen, T. Lakshmipriya, Biosens. Bioelectron. 57 (2014) 292–302.

[13] M. Russo, N. Starobinas, P. Minoprio, A. Coutinho, M. Hontebeyrie-Joskowicz, Ann. l'Institut Pasteur / Immunol. 139 (1988) 225–236.

[14] F. Xu, K. Ren, Y. Yang, J. Gue, G. Ma, Y. Liu, Y. Lu, X. Li, J. Integr. Agric. 14 (2015) 2282–2295.

[15] R.S. Yalow, S.A. Berson, Nature 184 (1960) 1648–1649.

[16] R.P. Ekins, Clin. Chim. Acta. 5 (1960) 453–459.

[17] H. Jiang, X. Weng, D. Li, Microfluid. Nanofluid. 10 (2011) 941–946.

[18] T.K. Christopoulos, E.P. Diamandis, Past, present, and future of immunoassays: In Immunoassay, (1996) Academic Press, San Diego, CA.

[19] X. Pei, B. Zhang, J. Tang, B. Liu, W. Lai, D. Tang, Anal. Chim. Acta. 758 (2013) 1–18.

[20] A.T. Pereira, P. Novo, D.M.F. Prazeres, V. Chu, J.P. Conde, Biomicrofluidics. 5 (2011) 102–113.

[21] G. Shan, C. Lipton, S.J. Gee, B.D. Hammock, Immunoassay, Handbook of Residual Analytical Methods for Agrochemicals, John Wiley & Sons, Ltd. Chichester (2002) 623–679.

[22] R. Karlsson, J. Mol. Recognit. 17 (2004) 151–161.

[23] M. Piliarik, L. Parova, J. Homola, Biosens. Bioelectron. 24 (2009) 1399–1404.

[24] A. Rasooly, J. Food Prot. 64 (2001) 37–43.

[25] R. Verma, B.D. Gupta, Food Chem. 166 (2015) 568–575.

[26] Z. Zhu, M. Feng, L. Zuo, Z. Zhu, F. Wang, L. Chen, J. Li, G. Shan, S. Luo, Biosens. Bioelectron. 65C (2014) 320–326.

[27] E. Danelian, A. Karlen, R. Karlsson, S. Winiwarter, A. Hansson, S. Lofas, H. Lennernas, M.D. Hamalainen, J. Med. Chem. 43 (2000) 2083–2086.

[28] R. Hoffrogge, H. Mikschofsky, B. Piechulla, Chronobiol. Int. 20 (2003) 543–558.

[29] R.B.M. Schasfoort, A.J. Tudos, Handbook of Surface Plasmon Resonance, Royal Society of Chemistry, Cambridge, 2008.

[30] A. Szabo, L. Stolz, R. Granzow, Curr. Opin. Struct. Biol. 5 (1995) 699–705.

[31] S. Shi, L. Wang, R. Su, B. Liu, R. Huang, W. Qi, Z. He, Biosens. Bioelectron. 74 (2015) 454–460.

[32] I.A. Darwish, Int. J. Biomed. Sci. 2 (2006) 217–235.

[33] J. Homola, Chem. Rev. 108 (2008) 462–493.

[34] L.S. Goh, T. Ichimiya, K. Watanabe, N. Shinomiya, 2016 26th International Conference on: IEEE, 2012, pp. 418–422.

[35] C. Ayela, F. Roquet, L. Valera, C. Granier, L. Nicu, M. Pugniere, Biosens. Bioelectron. 22 (2007) 3113–3119.

[36] J.W. Chung, S.D. Kim, R. Bernhardt, J.C. Pyun, Sens. Actuators, B (2005) 416–422.

[37] J.W. Chung, R. Bernhardt, J.C. Pyun, Sens. Actuators, B 118 (2006) 28–32.

[38] A.J. Haes, R.P. Duyne, Expert Rev. Mol. Diagn. 4 (2004) 527–537.

[39] S. Rupp, M. von Schickfus, S. Hunklinger, H. Eipel, A. Priebe, D. Enders, A. Pucci, Sens. Actuators, B 134 (2008) 225–229.

[39] A. Ahmed, J.V. Rushworth, J.D. Wright, P.A. Millner, Anal. Chem. 85 (2013) 12118–12125.

[40] T.A. Petrie, J.E. Raynor, D.W. Dumbauld, T.T. Lee, S. Jagtap, K.L. Templeman, D.M. Collard, A.J. Garcia, Sci. Transl. Med. 2 (2010) 45–60.

[41] L. E. M. Miles, C. N. Hales, J. Biochem. 108 (1968) 611–618.

[42] A. H. Schuurs, B. K. Weemen, Clin. Chim. Acta. 81(1977) 1–40.

[43] S.D. Gan, K.R. Patel, J. Invest. Dermatol. 133 (2013) 1–3.

[44] S. Aydin, Peptides. 72 (2015) 4–15.

[45] M. Hatamifar, N. Mosavari, J. Kazemi, Int. J. Mycobacteriology. 5 (2016) S188.

[46] S. Nagaraj, S. Ramlal, J. Kingston, H. V. Batra, Int. J. Mycobacteriology. 237 (2016) 136–141.

[47] S. Ling, Q. Chen, Y. Zhang, R. Wang, N. Jin, J. Pang, S. Wang, Biosens. Bioelectron. 71 (2015) 256–260.

[48] S. Parween, P. Nahar, Biosens. Bioelectron. 63 (2015) 605–608.

[49] S.Y. Toh, M. Citartan, S.C.B. Gopinath, T.H. Tang, Biosens. Bioelectron. 64 (2015) 392–403.

[50] J. Sui, H. Lin, L. Cao, Z. Li, Food Agric. Immunol. 20 (2009) 125–137.

[51] E.B. Bahadir, M.K. Sezgintürk, TrAC - Trends Anal. Chem. 82 (2016) 286–306.

[52] K. Meng, W. Sun, P. Zhao, L. Zhang, D. Cai, Z. Cheng, Biosens. Bioelectron. 55 (2014) 396–399.

[53] A. Geertruida, T. Posthuma, J. Korf, A. Amerongen, Anal. Bioanal. Chem. 393 (2009) 569–582.

[54] X. Li, P. Li, Q. Zhang, R. Li, W. Zhang, Z. Zhang, Biosen. Bioelectron. 49 (2013) 426–432.

[55] X. Sun, Y. Zhu, X. Wang, Food Control. 28 (2012) 184–191.

[56] J. Zhou, J. Zhuang, M. Miro, Z. Gao, G. Chen, D. Tang, Biosens. Bioelectron. 35 (2012) 394–400.

[57] L. Zeng, Q. Li, D. Tang, G. Chen, M. Wei, Electrochim. Acta. 68 (2012) 158–165.

[58] J. Wu, Y. Yan, F. Yan, H. Ju, Anal. Chem. 80 (2008) 6072–6077.

[59] J. Zhang, J. Lei, R. Pan, C. Leng, Z. Hu, H. Ju, Chem. Commun, 47 (2011) 668–670.

[60] C. Leng, J. Wu, Q. Xu, G. Lai, H. Ju, F. Yan, Biosens. Bioelectron, 27 (2011) 71–76.

[61] A. Santos, J. J. Davis, P. R. Bueno, J. Anal. Bioanal Tech. (2014) S7.

[62] K. Idegami, M. Chikae, K. Kerman, N. Nagatani, T. Yuhi, T. Endo, E. Tamiya, Electroanalysis, 20 (2008) 14–21.

[63] X. Pei, B. Zhang, J. Tang, B. Lui, W. Lai, D. Tang, Anal. Chim. Acta. 758 (2013) 1–18.

[64] K. Yamanaka. M.C. Vestergaard, E.Tamiya, Sensors 16 (2016) 1–16.

[65] P. Curei, J.C.R. Curie, Acad. Sci. 91 (1880) 294–295.

[66] Sauerbrey, Z. Phys. 155 (1959) 2333–2338.

[67] A. Karczmarczyk, K. Haupt, K.H. Fellera, Talanta 166 (2017) 193–197

[68] D. Tang, Q. Li, J. Tang, S. Su, G. Chen, Anal. Chim. Acta. 686 (2011) 144–149.

[69] D. Tang, R. Yuan, Y. Chai, Analyst 133 (2008) 933–938.

[70] S. Kurosawa, J. Park, H. Aizawa, S. Wakida, H. Tao, K. Ishihara, Biosens. Bioelectron. 22 (2006) 473–481.

[71] D. Tang, D. Zhang, D. Tang, H. Ai, J. Immunol. Methods. 316 (2006) 144–150.

[72] Y. Zhou, C. Chiu, H. Liang, Sensors 12 (2012) 15036–15062.

[73] J.S. Woodhead, I. Weeks, Pure Appl. Chem.57 (1985) 7.

[74] W. Baeyens, S. Schulman, A. Calokerinos, Y. Zhao, A. Campana, K. Nakashima, D. De Keukeleire, J. Pharmaceut. Biomed. 17 (1998) 941–953.

[75] Z. Fu, H. Liu, H. Ju, Anal. Chem. 78 (2006) 6999–7005.

[76] Z. Yang, Z. Xie, H. Liu, F. Yan, H. Ju, Adv. Funct. Mater. 18 (2008) 3991–3998.

[77] C. Wang, J. Wu, C. Zong, J. Xu, H. Ju, Chin. J. Anal. Chem. 40 (2012) 3–10.

[78] Z. Zhanga, Y. Guana, T. Xiab, J. Dua, T. Lia, Z. Suna, C. Guob, Colloids and Surfaces A: Physicochem. Eng. Aspects 520 (2017) 335–342.

[79] D.R. Shankaran, N. Miura, J. Phys. D: Appl. Phys. 40 (2007) 7187–7200.

[80] J. Homola, S.S. Yee, G. Gauglitz, Sens. Actuators B 54 (1999) 3–15.

[81] J. Homola, S. Yee, D. Myszka, in: F.S. Ligler, C.A.R. Taitt (Eds.), Surface Plasmon Resonance Biosensors, Elsevier, The Netherlands, 2002, pp. 207–251.

[82] E. Estenberg, B. Persson, H. Rooks, C. Urbaniczky, J. coll. Int. Sci. 143 (1991) 513–526.

[83] B. Liedberg, C. Nylander, I. Lunstrom, Surface plasmon resonance for gas detection and biosensing, Sens. Actuators 4 (1983) 299–304.

[84] C. Nylander, B. Liedberg, T. Lind, Gas detection by means of surface plasmon resonance, Sens. Actuators 3 (1982) 79–88.

[85] F. Long, A. Zhu, H. Shi, Sensors 13 (2013) 13928–13948.

[86] Y. H. Liang, C.C. Chang, C.C. Chen, Y. Chu-Su, C.W. Lin, Clin. Biochem. 45 (2012) 1689–1693.

[87] J. S. Mitchell, Y. Wu, C. J. Cook, L. Main, Steroids, 71 (2006) 618–631.

[88] R.L. Rich, D.G. Myszka, J. Mol. Recog. 18 (2005) 431–478.

[89] K.E. Komolov, I.I. Senin, P.P. Philippov, K.W. Koch, Anal. Chem. 78 (2006) 1228–1234.

[90] M. Karkar, M. Chamtouri, J. Moreau, M. Besbes, M. Canva, Sens. Actuators B 191 (2014) 115–121.

[91] G.J. Wegner, A.W. Wark, H.J. Lee, E. Codner, T. Saeki, S. Fang, R.M. Corn, Anal. Chem. 76 (2004) 5677–5684.

[92] J. Martinez-Perdiguero, A. Retolaza, L. Bujanda, S. Merino, Talanta 119 (2014) 492–497.

[93] S.M. Yo, D.K. Kim, S.Y. Lee, Talanta 132 (2015) 112–117.

[94] P.K. Maharana, R. Jha, S. Palei, Sens. Actuators B 190 (2014) 494–501.

[95] K. Nagatomo, T. Kawaguchi, N. Miura, K. Toko, K. Matsumoto, Talanta 79 (2009) 1142–1148.

[96] K. Matsumoto, A. Torimaru, S. Ishitobi, T. Sakai, H. Ishikawa, K. Toko, N. Miura, T. Imato, Talanta 68 (2005) 305–311.

[97] N. Miura N, K. Ogata K, G. Sakai, T. Uda, N. Yamazoe Chem. Lett. 26 (1997) 713–714.

[98] T. Kawaguchi, D. R. Shankaran, S. J. Kim, K. V. Gobi, K. Matsumoto, K. Toko, N. Miura, Talanta 72 (2007) 554–560.

[99] S. K. Vashist, E.M. Schneider, J.H. Luong, Analyst 139 (2014) 2237–2242.

[100] Z. Altintas, Y. Uludag, Y. Gurbuz, I.E. Tothill, Talanta 86 (2011) 377–382.

[101] E. Mauriz, S. Carbajo-Pescador, R. Ordoñez, M.C. García-Fernández, J.L. Mauriz, L.M. Lechuga, Analyst 139 (2014) 1426–1435.

[102] W. C. Tsai, I.C. Li, Sens. Actuators B Chem. 136 (2009) 8–12.

[103] U. Bilitewski, Anal. Chim. Acta. 568 (2006) 232–247.

[104] N. Soh, T. Tokuda, T. Watanabe, K. Mishima, T. Imato, T. Masadome, Y. Asano, S. Okutani, O. Niwa, S. Brown, Talanta 60 (2003) 733–745.

[105] J.W. Waswa, C. DebRoy, J. Irudayaraj, J. Food proess Eng. 29 (2006) 273–385.

[106] G. Gupta, P.K. Singh, M. Boopathi, D. V Kamboj, B. Singh, R. Vijayaraghavan, Thin Solid Films. 519 (2010) 1171–1177.

[107] S.A. Walper, P.A.B. Lee, E.R. Goldman, G.P. Anderson, J. Immunol. Methods. 388 (2013) 68–77.

[108] E. de Juan-Franco, J.M. Rodríguez-Frade, M. Mellado, L.M. Lechuga, Talanta 114 (2013) 268–275.

[109] P.T. Charles, E.R. Goldman, J.G. Rangasammy, C.L. Schauer, M.S. Chen, C.R. Taitt, Biosens. Bioelectron. 20 (2004) 753–764.

[110] H. Vaisocherová, V. Ševců, P. Adam, B. Špačková, K. Hegnerová, A. de los Santos Pereira, C. Rodriguez-Emmenegger, T. Riedel, M. Houska, E. Brynda, J. Homola, Biosens. Bioelectron. 51 (2014) 150–157.

[111] D.R. Shankaran, K.V. Gobi, N. Miura, Sens. Actuators B 121 (2007) 158–177.

[112] B.J. Yakes, K.M. Kanyuck, S.L. DeGrasse, Anal. Chem. 86 (2014) 9251–9255.

[113] I. Mohammed, W.M. Mullett, E.P.C. Lai, J.M Yeung, Anal. Chim. Acta. 444 (2001) 97–102.

[114] J. Homola, J. Dostalek, S. Chen, A. Rasooly, S. Jiang, S.S. Yee, Int. J. Food Microbial. 75 (2002) 61–69.

[115] M.C. Estevez, J. Belenguer, S. Gomez-Montes, J. Miralles, A.M. Escuela, A. Montoya, L.M. Lechuga, analyst 137 (2012) 5659–5665.

[116] M.B. Medina, Rapid Methods Autom. Microbiol. 14 (2006) 119 –132.

[117] E.S. Forzani, H. Zhang, W. Chen, N. Tao, Environ. Sci. Technol., 39 (2005) 1257–1262

[118] M. Farré, E. Martínez, J. Ramón, A. Navarro, J. Radjenovic, E. Mauriz, L. Lechuga, M.P. Marco, D. Barceló, Anal. Bioanal Chem. 388 (2007) 207–214.

[119] J.W. Chung, R. Bernhardt, J.C Pyun, J. Immunol Methods. 311 (2006) 178–188

[120] G.A. Besselink, Anal. Biochem. 333 (2004), 165–173.

[121] H.E. Indyk, E.L. Filonzi, L. W Gapper. J. AOAC. Int. 89 (2006) 898–902.

[122] K.V. Gobi, H. Iwasaka, N. Miura, Biosens. Bioelectron. 22 (2007) 1382–1389.

[123] A. Subramanian, J. Irudayaraj, T. Ryan, Sens. Actuators B 114 (2006) 192–198.

[124] J.A. Carter, E. Triplett, C.C. Striemer, B.L. Miller, Biosens. Bioelectron. 77 (2016) 1–6.

[125] http://english.agrinews.co.jp/?p=3704

[126] Ministry of Internal Affairs and Communications Japan, Statistics Bureau (2017), http://www.stat.go.jp/english/data/handbook/index.html.

[127] The Ministry of Health, Labor, and Welfare Japan (2017), http://www.mhlw.go.jp/english/topics/importedfoods/index.html.

[128] C. Crescenzi, S. Bayoudh, P.A.G. Cormack, T. Klein, K. Ensing, Anal. Chem. 73 (2001) 2171–2177.

[129] S. Liu, Q. Lin, X. Zhang, X. He, X. Xing, W. Lian, J. Huang, Sens. Actuators B 156 (2011) 71–78.

[130] H. Wang, Y. Zhang, H. li, B. Du, H. Ma, D. Wu, Q. Wei, Biosens. Bioelectron. 49 (2013) 14–19.

[131] X. Yang, F. Wu, D-Z. Chen, H-W. Lin, Sens. Actuators B 192 (2014) 529–535.

[132] E. Shishani, S.C. Chai, S. Jamokha, G. Aznar, M.K. Hoffman, Anal. Chim. Acta. 483 (2003) 137–145.

[133] S. Shen, Z. Li, P. He, Electrochem. Comm. 12 (2010) 876–881.

[134] G.S. Yang, M. Meng, R.M. Xi, H.Y. Aboul-Enein, Food Chem. 130 (2010) 1061–1065.

[135] Z. Li, Y. Wang, W. Kong, Z. Wang, L. Wang, Z. Fu, Sens. Actuators B 174 (2012) 355–358.

[136] J. Han, H. Gao, W. Wang, Z. Wang, Z. Fu, Biosens. Bioelectron. 48 (2013) 39–42.

[137] M. Regiart, M.A. Fernandez-Baldo, V.G. Spotorno, F.A. Bertolino, J. Raba, Biosens. Bioelectron. 41 (2013) 211–217.

[138] G.A. Mitchell, G. Dunnavan, J. Anim. Sci. 76 (1998) 208–211.

[139] M.W.F. Nielen, J.J.P. Lasaroms, M.L. Essers, J.E. Oosterink, T. Meijer, M.B. Sanders, Anal. Bioanal. Chem. 391 (2008) 199–210.

[140] J. Pleadin, T. Gojmerac, Z. Lipej, M. Mitak, D. Novose, N. Persl, Arch. Toxicol. 83 (2009) 979–983.

[141] G. Brambilla, T. Cenci, F. Franconi, R. Galarini, A. Macrì, F. Rondoni, M. Strozzie, A. Loizzo, Toxicol. Lett. 114 (2000) 47–53.

[142] G. Mazzanti, C. Daniele, G. Boatto, G. Manca, G. Brambilla, A. Loizzo, Toxicology 187 (2003) 91–99.

[143] J. Duan, D. He, W. Wang, Y. Liu, H. Wu, Y. Wang, M. Fu, S. Li, Talanta 115 (2013) 992–998.

[144] W. Zhang, P. Wang, X. Su, TrAC-Trends Anal. Chem. 85 (2016) 1–16.

[145] http://www.thestatszone.com/articles/athletics-should-the-records-be-reset-1.

[146] S. Guddat S, G. Höller, H. Geyer, 29th Cologne Workshop on Dope Analysis, Cologne, Germany; February 2011, p13–18.

[147] http://sportsillustrated.cnn.com/2011/more/wires/02/15/2080.ap.doping. clenbuterol. study.0711/index.html.

[148] W. Liu, L. Zhang, Z. Wei, S. Chen, G. Chen, J. Chromatogr. A 1216 (2009) 5340–5346.

[149] B. Cao, G. He, H. Yang, H. Chang, S. Li, A. Deng, Talanta, 115 (2013) 624–630.

[150] X. Ren, F. Zhang, F. Chen, T. Yang, Food Agr. Immunol. 20 (2009) 333–344.

[151] M.Z. Zhang, M.Z. Wang, Z.L. Chen, J.H. Fang, M.M. Fang, J. Liu, Anal. Bioanal. Chem. 395 (2009) 2591–2599.

[152] W. Xu, X. Chen, X. Huang, W. Yang, C. Liu, W. Lai, Talanta 114 (2013) 160–166.

[153] X. Zhang, H. Zhao, Y. Xue, Z. Wu, Y. Zhang, Y. He, X. Li, Z. Yuan, Biosens. Bioelectron. 34 (2012) 112–117.

[154] Y. Zhou, P. Wang, X. Su, H. Zhao, Y. He, Talanta 112 (2013) 20–25.

[155] P. Zhan, X.W. Du, N. Gan, Chinese J. Anal. Chem. 41 (2013) 828–834.

[156] X. Lin, Y. Ni, S. Kokot, J. Hazard. Mater. 260 (2013) 508–517.

[157] X. Yang, F.Wu, D.Z. Chen, H.W. Lin, Sens. Actuators B Chem. 192 (2014) 529–535.

[158] Y. Zhou, P.Wang, X. Su, H. Zhao, Y. He, Mikrochim. Acta 181 (2014) 1973–1979.

[159] J. Liu, L. Zeng, Z. Li, F. Gao, X. Huang, F. Li, Anal. Chim. Acta 638 (2009) 69–74.

[160] M. Yao, Y. Wu, X. Fang, Y. Yang, H. Liu, Anal. Biochem. 475 (2015) 40–43.

[161] Suherman, K. Morita, T. Kawaguchi, Appl. Surf. Sci. 332 (2015) 229–236.

[162] Suherman, K. Morita, T. Kawaguchi, Biosens. Bioelectron. 67(2015) 356–363.

[163] Suherman, K. Morita, T. Kawaguchi, Sens. Actuators B 210 (2015) 768–775.

[164] J. Wu, X. Liu, Y. Peng, J. Pharmacol. Toxicol. Methods. 69 (2014) 211–216.

[165] Y. Li, X. Mao, M. Zhao, P. Qi, J. Zhong, Eur. Food Res. Technol. 239 (2014) 195–201.

Chapter 2

Experimental

2.1 Materials and Chemicals

Clenbuterol hydrochloride and its corresponding antibody [mouse immunoglobulin (IgG) clenbuterol, clone 1F8B10B7] were supplied by LKT Laboratories, Inc. (USA) and Novus Biologicals (USA), respectively. Anti-mouse IgG (H+L) and anti-mouse IgG (H+L) labeled with Au- nanoparticle (40 nm, 2.14 x 10^{11} particle/ mL) were purchased from Jacson Immunoresearch Lab. Inc. and Cytodiagonestic, Canada, respectively. Phosphate-buffered saline (PBS, pH 7.4), 3,3′-dithiobis sulfosuccinimidyl propionate (DTSSP), and dithiobis succinimidyl propionate (DSP) were supplied by Thermos Scientific (USA). Colloidal Au (40 nm) was purchased from British BioCell International Solutions (UK). Borate-buffered saline (pH 8.5) and 10% bovine serum albumin (BSA) solution were purchased from KPL (USA) and Sigma–Aldrich (USA), respectively. Ethanol, potassium dihydrogen phosphate and ammonium chloride were all obtained from WAKO, Japan, respectively. Sodium dihydrogen phosphate, disodium hydrogen phosphate and ethanolamine were purchased from Kanto Chemical Co. Inc., Japan, respectively. Methanol and sodium sulfite were supplied by Dojindo, Japan and Nakali Tesque Inc. Kyoto, Japan. Sodium chloride and sodium hydroxide were purchased from Junsei Chemical Co., Ltd. (Japan). Refractive index-matching fluid (refractive index = 1.518) was obtained from Cargille Labs (USA). Minisart Syringe filter and monospin (CBA, amide, and C18) were supplied by Thermos Scientific and GL sciences (Japan). Deionized water (18.2 MΩ cm) was produced from a Millipore Milli-Q purification system. Urine sample of cow was collected from the field science center for Northern Biosphere, Hokkaido University.

2.2 Surface Plasmon Resonance (SPR)

2.2.1 Excitation of surface plasmons

Surface Plasmons (SPs) are electron clouds oscillation that occurs at specific material interfaces, such as metal-dielectric interfaces. A light wave can couple to a surface plasmon if the component of light's wave vector is matches with the propagation constant of the surface plasmon.

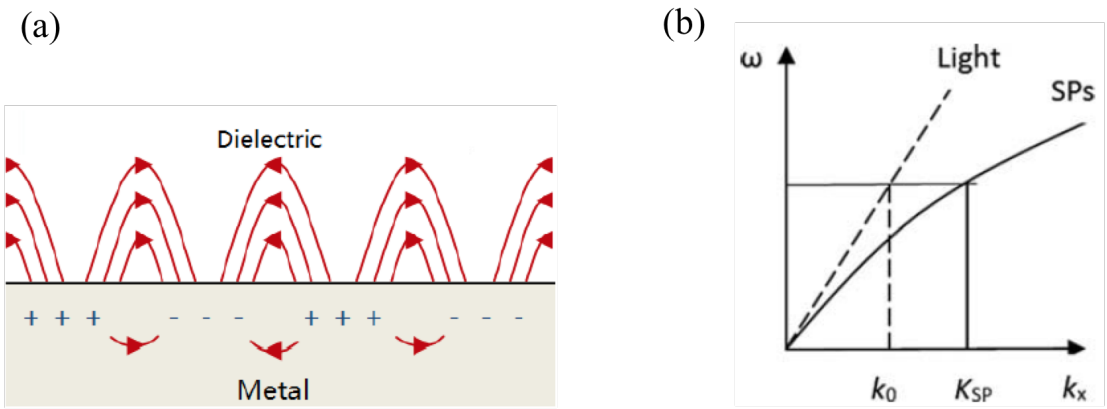

Fig. 2.1. (a) The concept of SPR and (b) dispersion curve of light in vacuum and surface plasmon [1].

The excitation of surface plasmon by light is denoted as SPR (Fig.2.1). The dispersion curve is illustrated, where surface plasmon mode shows the momentum mismatch problem. Fig.2.1 (b) indicated that the momentum of surface plasmon mode is always lying beyond the light line. Therefore, the propagation constant (k_{sp}) of a surface plasmon at a metal-dielectric interface is larger than the free-space photon (k_0) of the same frequency (ω). Thus, surface plasmons cannot be excited directly by the light incident onto a smooth metal surface. As a consequence, special techniques (coupling devices) are essential to couple photons with surface plasmon. These techniques are known as the configuration of SPR, a brief description as follows:

Otto configuration

The Otto configuration is illustrated in Fig. 2.2 (a), where the order of layer is prism, air gap (dielectric) and metal layer. When the angle of the incident light is greater than the critical angle, the evanescent field can tunnel through the air gap and coupled with the surface plasmon of metal surface. The coupling is highly depends on the air gap; therefore, prism and metal surface should be very close to each other. This configuration is useful in the study of single crystal metal surfaces and adsorption phenomenon on them [2]. One of the important advantages of this configuration is temperature independent. However, applications where fluids and solutions are concerned, this configuration is no longer effective, due to the gap between the metal and prism [3-5].

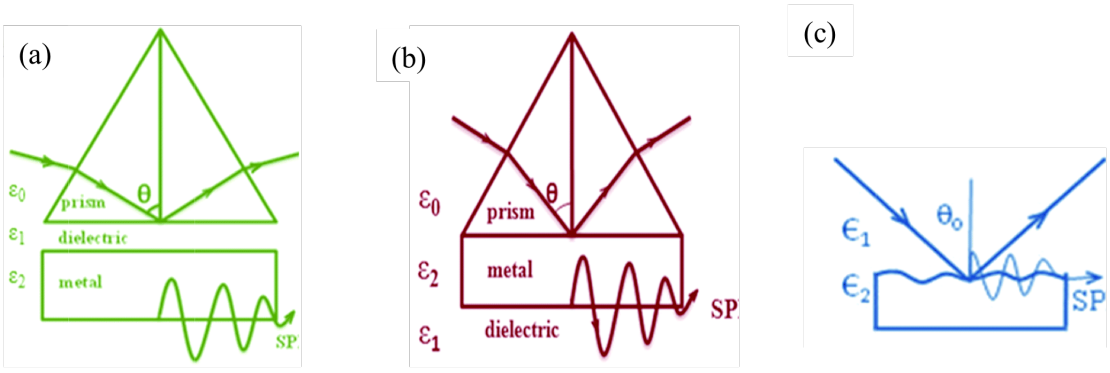

Fig. 2.2. SPR configuration (a) Otto configuration, (b) Kretschmann configuration and (c) grating configuration [6].

Kretschmann configuration

In 1968, Kretschmann-Raether [6,7] gave geometry for the excitation of surface plasmon on a smooth surface, where a metal layer (e.g. Au, thickness approximately 50 nm) is sandwiched between the prism and the dielectric. The arrangement is schematically presented in Fig 2.2 (b). In the Kretschmann configuration, a metal film

(e.g. Au) is illuminated with a single wavelength light through a high refractive index prism at an angle of incidence is greater than the critical angle for attenuated total reflection (ATR) and generating an evanescent wave [8-10]. This evanescent wave propagates along the interface between the prism and the metallic film with propagation constant. The coupling condition can be expressed by:

$$k_x = \frac{2\pi}{\lambda_0} n_p \sin\theta \qquad \text{(Eq. 2.1) [11]}$$

Where k_x is the wave vector component along the x-axis of the incident light, λ_0 is the wavelength in vaccum, n_p is the refractive index of the prism and θ is the incident angle. Therefore, the wave vector component of evanescent field can be adjusted with the propagation constant of surface plasmon by controlling the angle of incident light. The optical excitation of surface plasmon results in a drop in the intensity of the reflected light. This configuration is applied in sensing performance, mostly for SPR biosensor techniques.

Diffraction grating configuration

Fig. 2.2 (c) presented the diffraction grating configuration. An incident light comes from the dielectric medium on a metallic grating and diffracted. The wave vectors from diffraction grating are larger in magnitude than the incident light wave vector. The surface plasmon wave matched with the incident beam by diffraction at a rectangle metal grating [7, 11-14]. This method is suitable for spectral filtering applications.

In practical application, Kretschmann configuration has gained much attention to the scientist because the Otto and the diffraction grating configurations need high nanotechnology to set-up.

2.2.2 Basic principle of SPR

When the incident light travels through a high refractive index medium-1 (n_1) to a low refractive index medium-2 (n_2), a part of incident light will be refracted and remained will be reflected. The angel of refracted light can be calculated from the Snell's law:

$$n_1 \sin\theta_i = n_2 \sin\theta_r \qquad \text{(Eq. 2.2)}$$

where θ_i is the angle of incident light and θ_r is the angle of refracted light. At a certain angle of incident light, the light will be refracted along the boundary. This angle is called critical angle (θ_c). When the incident light passes through the angle above critical angle, total internal reflection (TIR) occurs, where all light is reflected into the high refractive index medium (medium 1) in the Fig. 2.3. There is another condition, at Brewster angle, a portion of light transmitted in the low refractive index medium. This transmitted light is polarized.

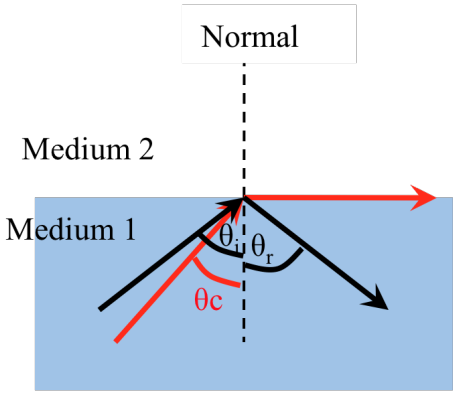

Fig. 2.3. Schematic illustration of total internal reflection. Medium 1 is the high refractive index medium and medium 2 is the low refractive index medium [15].

At the total internal reflection condition, evanescent wave (transmitted wave) is generated. In SPR configuration, glass chip covered with a thin film of noble metal (Au) is coupled with the prism by using refractive index matching oil. The conduction

band electron (Plasmon) of Au film is possible to resonate with the evanescent wave. According to the Fresnel theory [16], the interaction between plasmon of Au film and the evanescent wave can be explained. The reflection and transmission coefficient for wave parallel or perpendicular to the plane of incident light (Fig.2.4) can be expressed as;

$$r_{II} = \frac{\tan(\theta_i - \theta_t)}{\tan(\theta_i + \theta_t)} \text{ (Parallel reflection)} \qquad \text{(Eq. 2.3) [16]}$$

$$r_{\perp} = -\frac{\sin(\theta_i - \theta_t)}{\sin(\theta_i + \theta_t)} \text{ (Perpendicular reflection)} \qquad \text{(Eq. 2.4)[16]}$$

$$t_{II} = \frac{2\sin\theta_t \cos\theta_i}{\sin(\theta_i + \theta_t)\cos(\theta_i - \theta_t)} \text{ (Parallel transmission)} \qquad \text{(Eq. 2.5)[16]}$$

$$t_{\perp} = \frac{2\sin\theta_t \cos\theta_i}{\sin(\theta_i + \theta_t)} \text{ (Perpendicular transmission)} \qquad \text{(Eq. 2.6)[16]}$$

The surface plasmon can be exited by the evanescent wave and this phenomenon is called surface plasmon resonance (SPR). When the surface plasmon wave is resonantly matched to the evanescent wave, the surface plasmon resonance occurs and the evanescent wave becomes enhanced. As a result, the intensity of the reflected light is decreased sharply. The propagation of the evanescent electromagnetic field is confined to the metal-dielectric interface (Fig.2.5). The magnitude of the parallel wave vector of the evanescent wave, k_{eva}, is expressed as;

$$k_{eva} = \frac{2\pi}{\lambda} n_{prism} \sin\theta \qquad \text{(Eq. 2.7)[11]}$$

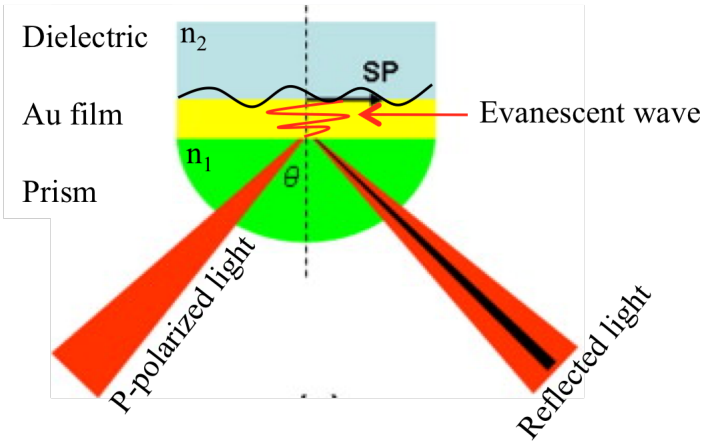

Fig. 2.4. Schematic illustration of evanescent wave generation [13].

The magnitude of the wave vector of the surface plasmon (k_{sp}) is related to the dielectric constants of the dielectric media and Au-film. For a non-absorbing media, the dielectric constant equals the square of the refractive index, $\varepsilon=n^2$, where ε is the dielectric constant and n is the refractive index. Therefore, k_{sp} is can be determined by refractive index of the dielectric media (n_2) and the refractive index of Au-film. The relationship is as follows:

$$k_{sp} = \frac{2\pi}{\lambda}\sqrt{\frac{n_2^2 n_{Au}^2}{n_2^2 + n_{Au}^2}} \qquad \text{(Eq. 2.8)[17]}$$

where n_2 is the refractive index n_{Au} is the refractive index of the Au-film. One requirement for the SPR is that k_{sp} equals to k_{eva}. Thus using Eq. 2.2 and 2.3 gives

$$\theta_{SPR} = \frac{1}{n_{prism}}\sin^{-1}\sqrt{\frac{n_2^2 n_{Au}^2}{n_2^2 + n_{Au}^2}} \qquad \text{(Eq. 2.9)[17]}$$

where n_{prism} is the refractive index of prism. The angle required for the resonance, θ_{SPR}, is related to n_2 when n_{Au} is fixed. Adsorption of any chemical species onto the SPR sensor changes the refractive index of metal-dielectric interface and the resonance angle changes accordingly. Therefore, the changes of θ_{SPR} can be used to analyze the adsorption-desorption or association-dissociation activities that take

places onto the SPR sensor surface. A schematic representation of adsorption of chemical species onto Au surface and SPR angle change is represented in Fig. 2.5.

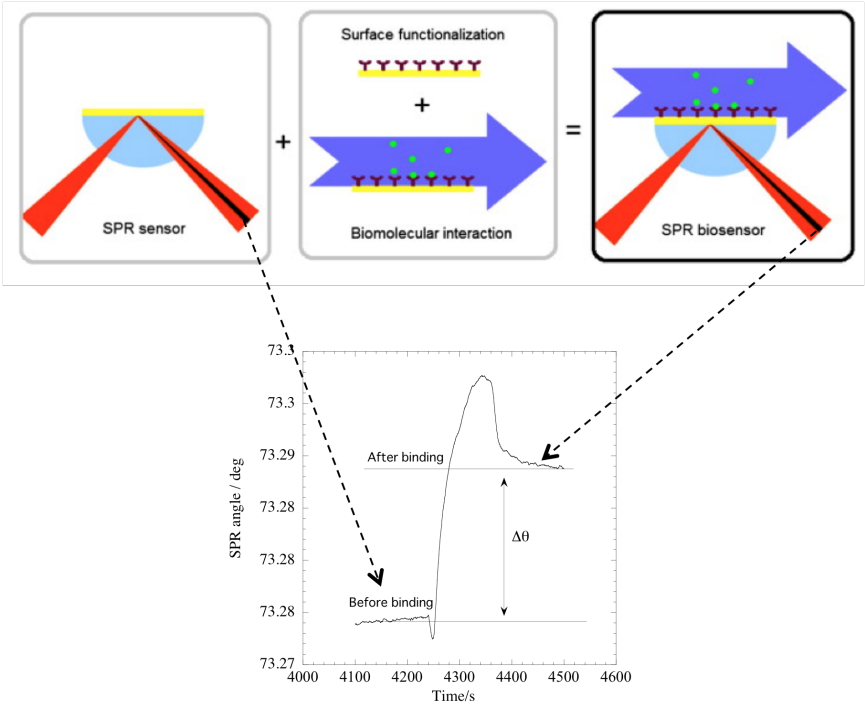

Fig. 2.5. A SPR sensor equipped with suitable surface fictionalization as biorecognition element (antibody, brown colored Y shaped) as transformed into SPR biosensor. Green dot is the analyte [11].

2.2.3. SPR set-up

This research mainly used SPR biosensor technique to examine immunoreaction. SPR experiments were performed using an SPR analyzer (SPR-670; Nippon Laser Electronics, Japan). The instrument employs a Kretschmann-attenuated total reflectance (ATR) configuration and incorporates computer controlled two flow cells (200 μL each) for independent analysis. A 200 μL injection loop is filled with the solutions through an injection valve. The solutions are pumped individually into the cells with a syringe pump (Fig. 2.6).

A prepared sensor chip (glass chip coated with an Au layer of 50 nm thickness) was mounted on the semi-cylindrical prism (refractive index = 1.515) of the SPR analyzer using a refractive index-matching fluid (refractive index = 1.51) to decrease the deformation of SPR images. A red light-emitting source (Ni–Cd laser beam, $\lambda = 670$ nm) reflected light onto the sensor chip at ATR angles, and the intensity of reflected light was recorded using a charge-coupled device camera. The reflectance angle at which the light intensity is the minimum, called the SPR angle, was recorded with respect to time on a personal computer. All the experiments were performed in an air-conditioned room (25 ± 1°C).

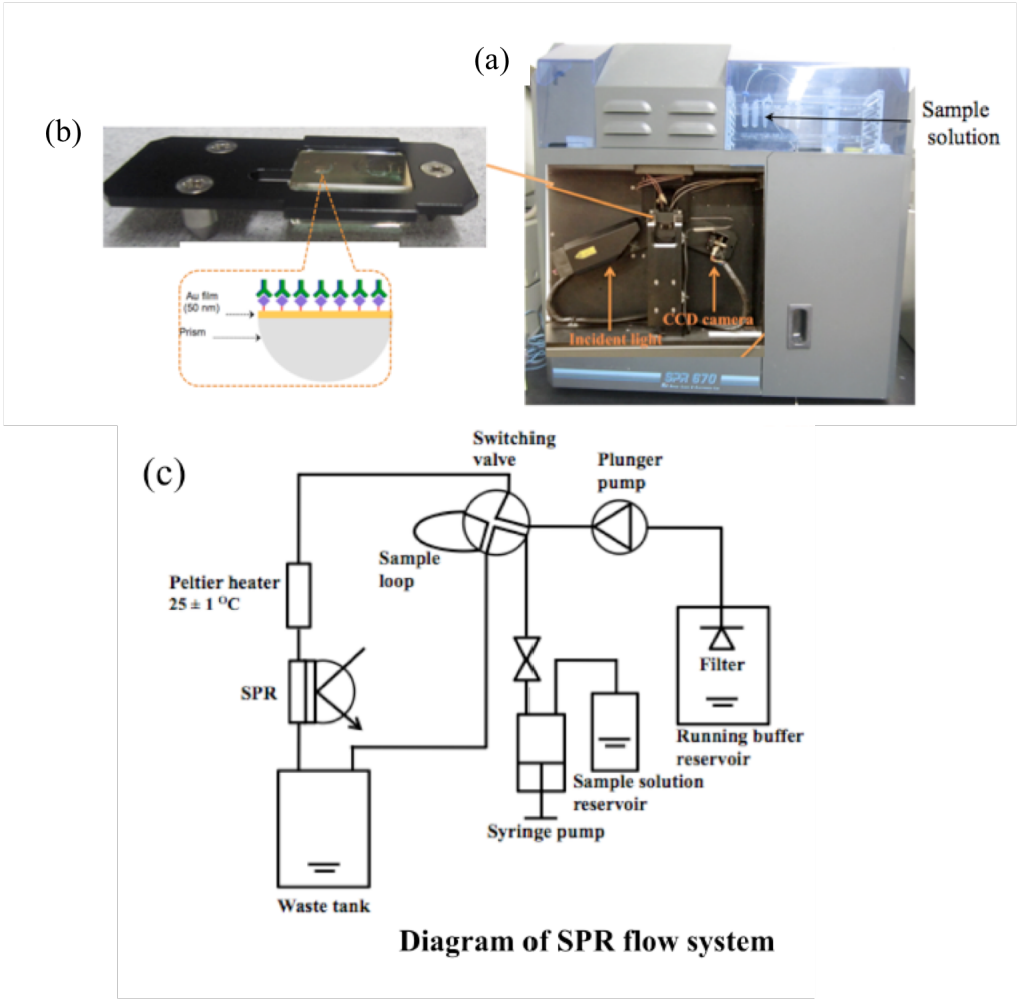

Figure 2.6. SPR 670 from Nippon Laser and Electronics-Japan: (a) sensing part, (b) Sensor surface onto prism, (c) diagram of SPR flow system.

2.3 UV-visible measurement

When incident light interact with metal nanoparticles (e.g., Au, Ag), the electromagnetic field of light induces a collective coherent oscillation of the surface conduction electrons of the metal nanoparticles in resonance with the frequency of light, in a phenomena known as Localized Surface Plasmon Resonance (LSPR). LSPR is sensitive to the refractive index change in the local dielectric environment. For spherical metal nanoparticles the Mie solution to Maxwell's equation can be use to describe the light absorption caused by LSPR. According to Mie theory, for well separated spherical nanoparticles with a radius *R*, the extinction cross section can be expressed as [20]:

$$C_{ext} = \frac{24\pi^2 R^3 N \varepsilon_m^{3/2}}{\lambda}\left[\frac{\varepsilon_i}{(\varepsilon_r + 2\varepsilon_m)^2 + \varepsilon_i^2}\right] \qquad \text{(Eq. 2.10)[20]}$$

where ε_m is the dielectric constant of the surrounding medium, ε_r and ε_i are the real and imaginary part of the dielectric function of the nanoparticle, respectively. N is the number of sphere per unit volume.

In this study, measurements of the light absorbed by the AuNP suspension were carried out using a UV-Vis spectrometer (U-3310 spectrophotometer; Hitachi, Japan). The instrument was baselined before accusation to remove any background absorbance arising from, for instance, the cuvette or buffer.

2.4 X-ray photoelectron spectroscopy

X-ray photoelectron spectroscopy (XPS) relies on photoelectric effect. The XP-spectra used for obtaining quantitative and qualitative information about the surface composition. When X-ray beam strikes to the sample surface with an ultra high vacuum condition, the core electron of atoms will absorb energy from X-ray [21].

When the energy of photon ($h\nu$) is higher than energy level of the orbital, because of the binding energy of the core electron is equal to the ionization energy the photoelectron emission will occur.

By using the Einstein relationship, the binding energy of the core electron can be expressed as following:

$$h\nu = E_b + E_k + \phi \qquad \text{(Eq. 2.11)[21]}$$

where hν is the energy of X-ray beam. ϕ is the work function of the sample. E_b is the binding energy of core level electron and E_k is the kinetic energy of photoelectron.

The XPS peak intensity can be estimated by using the following equation:

$$I = S \times I_x \times N_n \times \sigma i \times \exp\left[-d/\lambda_i \cos(\theta)\right] \qquad \text{(Eq. 2.12)[21]}$$

Here, S = Machine function

I_x = Intensity of the incident X-ray intensity

N_n = Number of the specific atom per the certain surface area

σ_i = cross-section area of an atom at i-state

λ_i = Mean of free path length of certain atom n at i-state

θ = Take of angle (angle between detector and the sample)

X-ray photoelectron spectra were obtained by using a Rigakudenki model XPS-7000 X-ray photoelectron spectrophotometer. The source of radiation was Mg Kα, and the power of the radiation source was 200 W. The chamber pressure was approximately 1.2×10^{-6} torr. The take-off angle was 90°. C1s peak at 285.0 eV was used to calibrate the binding energy.

2.5 Preparation of Au substrates

Glass chips (BK7, refractive index = 1.515, 20 mm × 13 mm × 0.7 mm from Matsunami Glass Ind., Ltd.) were used as the SPR sensor chips. These chips were cleaned with soapy water (10% Contrad 70, Decon Laboratories, Inc.) and acetone in an ultrasound bath for 30 min. After this process, the glass chips were rinsed using a copious amount of Milli-Q water. Then, the chips were dried using pure nitrogen gas (purity > 99.995%), following which light treatment (deep UV, λ = 172 nm) was performed to produce a hydrophilic surface. The glass chips were then placed in a sputtering system (JEOL, Japan). 50 nm Au film was deposited using the sputtering method. Sputtering was performed under 2.0–2.5 Pa. Finally, the prepared gold chip was loaded into the SPR instrument immediately after sputtering.

2.6 References

[1] X. Guo, J. Biophotonics. 7 (2012) 483–501.

[2] A. Otto, Zeitschri fur Physik, 216 (1968) 398–410.

[3] E.K. Akowuah, T. Gorman, S. Haxha, Opt. Express 17 (2009) 23511–23521.

[4] N.H. Salah, D. Jenkins, L. Panina, R. Handy, G. Phan, S. Awan, Smart Nanosys. Eng. Med. 2 (2012) 10–22.

[5] T. Iwata, Y. Mizutani, Opt. Express 18 (2010) 14480–14487.

[6] J. Jana, M. Ganguly, T. Pal, RSC Adv., 6 (2016) 86174–86211.

[7] J. Homola, Chem. Rev. 108 (2008) 462–493.

[8] A.K. Singh, S.C. Sharma, Opt. Laser Tech. 56 (2014) 256–262.

[9] Y. Mao, Y. Bao, W. Wang, Z. Li, F. Li, L. Niu, Am. J. Anal. Chem. 2 (2011) 589–604.

[10] C. Rhodes, S. Franzen, J. Appl. Phys. 100 (2006) 1–4.

[11] E. Wijaya, C. Lenaerts, S. Maricot, J. Hastanin, S. Habraken, J.Vilcot,

R. Boukherrou, S. Szunerits, Curr. Opin. Solid State Mater. Sci, 15 (2011) 208–224.

[12] J. Homola, I. Koudela, S.S. Yee, Sens. Actuators B 54 (1999) 16–24.

[13] M.C. Hutley, D. Maystre, Opt. Comm. 19 (1976) 431–436.

[14] L. B. Mashev, E.K. Popov, E.G. Loewen, Appl. Opt. 28 (1989) 2538–2541.

[15] Snell's law <http://en.wikipedia.org/wiki/Snell's law>.

[16] Fresnel's theory <www.teknik.uu.se/ftf/education/ftf2/Optics_FresnelsEqns.pdf>.

[17] Y. Tang, X. Zeng, J. Liang, J. Chem. Edu. 87(7) (2010) 742–746.

[18] A.J. Bard**,** L.R Faulkner, Electrochemical Method (Fundamental and Applications), 2nd edition, John Wiley and Sons, Inc. 2001, USA.

[19] Electrochemistry <http://en.wikipedia.org/wiki/Electrochemistry>.

[20] J. Cao, T. Sun. K. T. V. Grattan, Sensors and Actuators B 195 (2014) 332–351.

[21] D.J. O'Connor, B.A. Sexton, R.St.C. Smart, Surface Analysis Methods in Materials Science, 1992, Springer-Verlag.

Chapter 3

Mechanism of Surface Plasmon Resonance Sensing by Indirect Competitive Inhibition Immunoassay Using Au Nanoparticle Labeled Antibody

3.1. Introduction

Surface plasmon resonance (SPR) sensor is a signal transducer based on the optical method. Because its sensitivity for detection of protein reaches at pg cm^{-2} order, SPR biosensor has been widely investigated in the past decades [1,2]. To date, there are many review articles about SPR biosensors for environmental monitoring, fundamental biological studies, food safety, and clinical diagnosis [3-10]. However, only a few of these biosensors are commercially available [11]. The main challenge in the practical use of commercial SPR biosensors is posed by impurities in real samples, which interfere with the SPR signal [12]. Therefore, the pretreatment such as centrifuge, filtration, precipitation etc is needed for real sample measurement. I here consider that the sample dilution is one of approaches to avoid impurity interference. However, dilution method requests the extremely high sensitivity that is the lowest limit of detection (LOD) of low (sub-nanomolar) concentrations. In the past study, it was noticed that the affinity constants of the biochemical reactions on the sensor surface determined the sensitivity [13]. Therefore, I investigated sensitivity enhancement of the SPR biosensor in the present study.

I would like to discuss the LOD determination here. LOD is calculated from the calibration curve. The most frequently used format is a direct immunoassay [3]. This immunoassay uses an antibody (Ab)-immobilized sensor surface; an analyte is

injected and reacts with Ab on the sensor surface. The calibration curve shows the linear relation with the analyte concentration (Fig. 3.1 (A)). This format is preferred for large molecule detection such as proteins, nucleic acids, bacteria, and viruses [6,14]. In case of the detection of small analytes [molecular weight (MW) < 1,000 g mol^{-1}], indirect competitive inhibition immunoassay is useful [15-21]. Adrian Losoya-Leal *et al.* [18] reported the indirect competitive inhibition immunoassay for the detection of a small analyte amikacin (AK). They fabricated the sensor surface using amikacin-BSA conjugate (AK-BSA). AK-BSA conjugate was physically immobilized on Au-sensor chip. As the premixed solution of the Ab and the analyte is injected onto the sensor surface, SPR monitors the binding event of a high molar mass Ab instead of the analyte. Therefore, a high SPR signal change is expected. This calibration curve shows the sigmoid curve as shown in Fig. 3.1 (B).

Recently, in order to improve the LOD and SPR signal, localized surface plasmon resonance (LSPR) detection using Au-nanoparticles (AuNP) has drawn much attention by researchers [22-26]. Typically, two strategies are considered for SPR signal amplification: (1) sensor surface modification with AuNP and (2) labeling of a biorecognition part (such as an Ab) with AuNP. Both strategies use the coupling of LSPR and SPR with AuNP for signal and sensitivity improvement. Fig. 3.1 shows the calibration curves in the presence or absence of AuNP on the sensor surface. Detectable range of instrument is marked in figure. In a direct immunoassay (Fig. 3.1A), Liu et al. [24] demonstrated the detection of atrazine. They noticed that AuNP enhanced the SPR signal, and the LOD at the minimum value of the detectable range was improved. On the other hand, the LOD of the calibration curve of indirect competitive inhibition using AuNP-modified sensor surface did not change although the SPR signal was enhanced (Fig. 3.1B) [22]. Improvement in LOD of an indirect

competitive inhibition immunoassay means that the calibration curve needs to be shifted toward a lower analyte concentration. This shift is determined by the affinity constants of immunoreactions. Therefore, I studied the control method of the affinity constants. In this study, I assume that the AuNP labeling to Ab can control the affinity constant. It is believed that a large matter label could reduce the mobility of reactant. As a result, the affinity constants may be reduced. AuNP labeling of Ab is mainly used in sandwich immunoassays. Several researchers have reported the achievement of high sensitivities in the nanomolar to femtomolar range [23,27,28]. To date, there have been no reports on an indirect competitive inhibition immunoassay using Ab modified with AuNP as the signal amplification strategy.

In this study, I investigated the use of Ab modified with AuNP in an indirect competitive inhibition immunoassay for detecting clenbuterol (MW, 277 g mol^{-1}). The target analyte, clenbuterol is a member of the β-agonist family and is a problematic material for food safety. Although, commercial test kit can detect clenbuterol at a detection level of 25 ppt (25 pg mL^{-1}) in meat samples by enzyme-linked immunoassay (ELISA) [29], however, this technique is time (>1 h) and reagent consuming. Therefore, it is of vital importance to develop a detection process that is rapid and cost effective. Recently, we reported an LOD of 2 ppt for detecting clenbuterol using an indirect competitive inhibition immunoassay [13]. However, this sensitivity is insufficient for the real sample detection in diluted solution. Even worse, maximum change (5 mdeg) is too small for the miniaturized SPR instrument. Considering a use in paddock to judge the doping agent, the physical condition change such as temperature and pressure causes the SPR signal drift of approximately 10 mdeg. Therefore, I investigated a signal amplification strategy using the Ab modified with AuNP in this study.

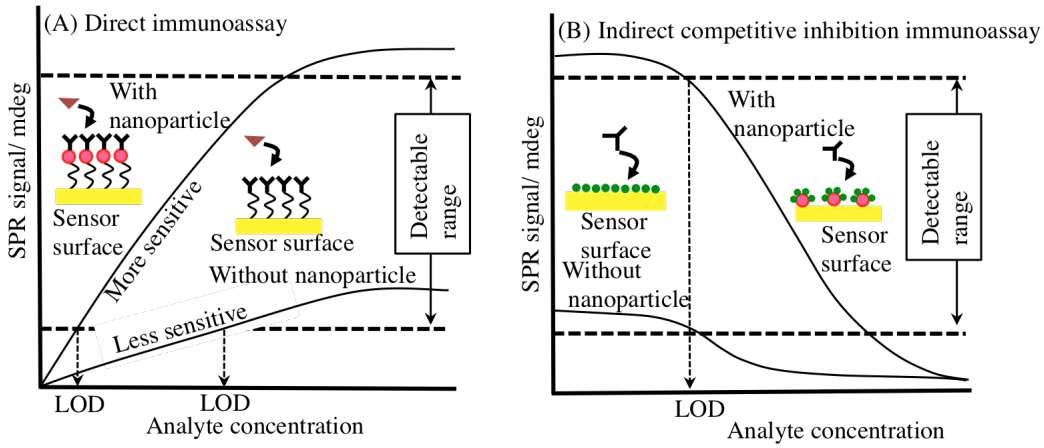

Fig 3.1. Comparison of calibration curves for the AuNP-labeled and unlabeled SPR biosensor (A) Direct immunoassay [24] and (B) indirect competitive inhibition immunoassay [18,22].

3.2 Preparation of AuNP labeled antibody

In this study, Abs covalently modified with AuNP (Ab-AuNP conjugate) was used for detection in an indirect competitive inhibition immunoassay. The 40-nm size of AuNPs was chosen because it provides the best signal amplification factor for the SPR sensing system [30].

The Ab-AuNP conjugate was prepared according to the literature [31]. pH of the colloidal-Au solution (1 mL) was adjusted to 8.5 with 40 μL of 50 mM borate buffer (pH 8.5). Then, 10 μL of 1 mM DTSSP in aqueous solution was added to the AuNP suspension. After 30 min of mixing at room temperature, the sulfo-*N*-hydroxy succinimidyl (NHS)-terminated AuNP suspension was centrifuged for 5 min at 7000 ×*g* to separate excess and unreacted DTSSP. AuNP was then resuspended in 2 mM borate buffer, and primary Ab (20 μg) was added. In this step, sulfo-NHS-terminated AuNP covalently binds to the side chain amino group of Ab. After standing for 90

min, the mixture was then centrifuged at 7000 ×*g* for 5 min. The supernatant was discarded. Next, the Ab-AuNP conjugate was resuspended in 2 mM borate buffer containing 1% BSA. The processes of resuspension and centrifugation were repeated once again to effectively remove excess reagent. The suspension was incubated for 30 min to allow BSA to block any unreacted sulfo-NHS ester and nonspecific binding sites. A small volume of concentrated NaCl (10%) was added to the suspension to reach a final concentration of 150 mM. Finally, a PBS + 10% ethanol solution was added to achieve the desired concentration. The prepared Ab-AuNP conjugate was either used immediately or stored overnight at 4°C.

3.3 Characterization of the Ab-AuNP conjugate

The Ab-AuNP conjugate solution was red because of light absorption in a specific wavelength range (Fig. 3.2). Measurement of the light absorbed by the AuNP suspension using a UV-Vis spectrometer (U-3310 spectrophotometer; Hitachi, Japan) showed a maximum absorption peak at 525.0 nm before conjugation, whereas the absorption peak was shifted to 531 nm for the Ab-AuNP conjugate solution. This shift was caused by a change in the local refractive index due to binding of Ab onto the sulfo-NHS end.

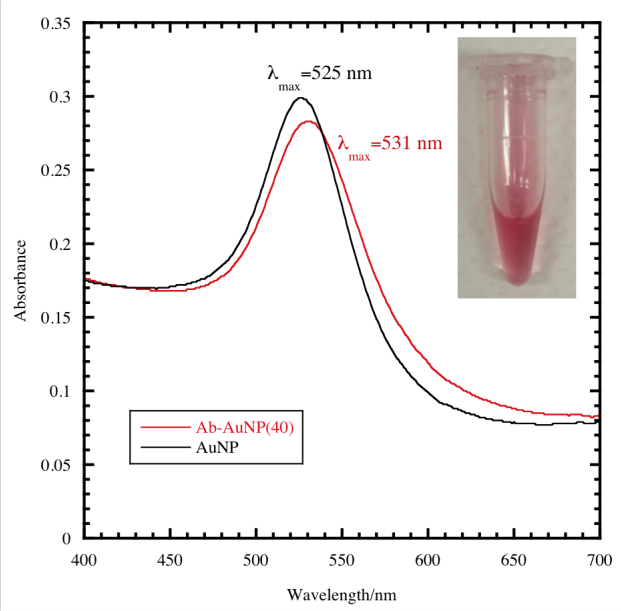

Fig. 3.2. Adsorption spectra after labeling of Abs with AuNPs.

Inset: Color of unlabeled Abs after AuNP labeling.

3.4. Fabrication of immunosurface

Fig. 3.3 illustrates the fabrication process of the immunosurface according to the self-assembly method. First, methanol was flowed over the sensor chip as a carrier solution. Once a stable baseline was achieved, a 5 mM DSP methanolic solution (200 μL) was injected onto the Au chip for 40 min at a flow rate of 5 μL min^{-1}. The Au surface was covered with a succinimidyl-terminated propenthiol monolayer. Clenbuterol (1000 ppm, 200 μL) in PBS solution was then injected onto the surface for 40 min. The NHS group was replaced with clenbuterol through an amide coupling reaction. Finally, to block unreacted NHS groups, ethanolamine (1000 ppm, 200 μL) in PBS solution was flowed over the surface as a blocking agent. The surface concentrations of succinimidyl propanethiol, immobilized clenbuterol, and ethanolamine were calculated from the observed angle shift as 3.3 ± 1.2 × 10^{-10} mol cm^{-2}, 1.1 ± 0.3 × 10^{-10} mol cm^{-2}, and 1.8 ± 0.4 × 10^{-10} mol cm^{-2}, respectively. The

reproducibility was confirmed by performing the same experiment five times.

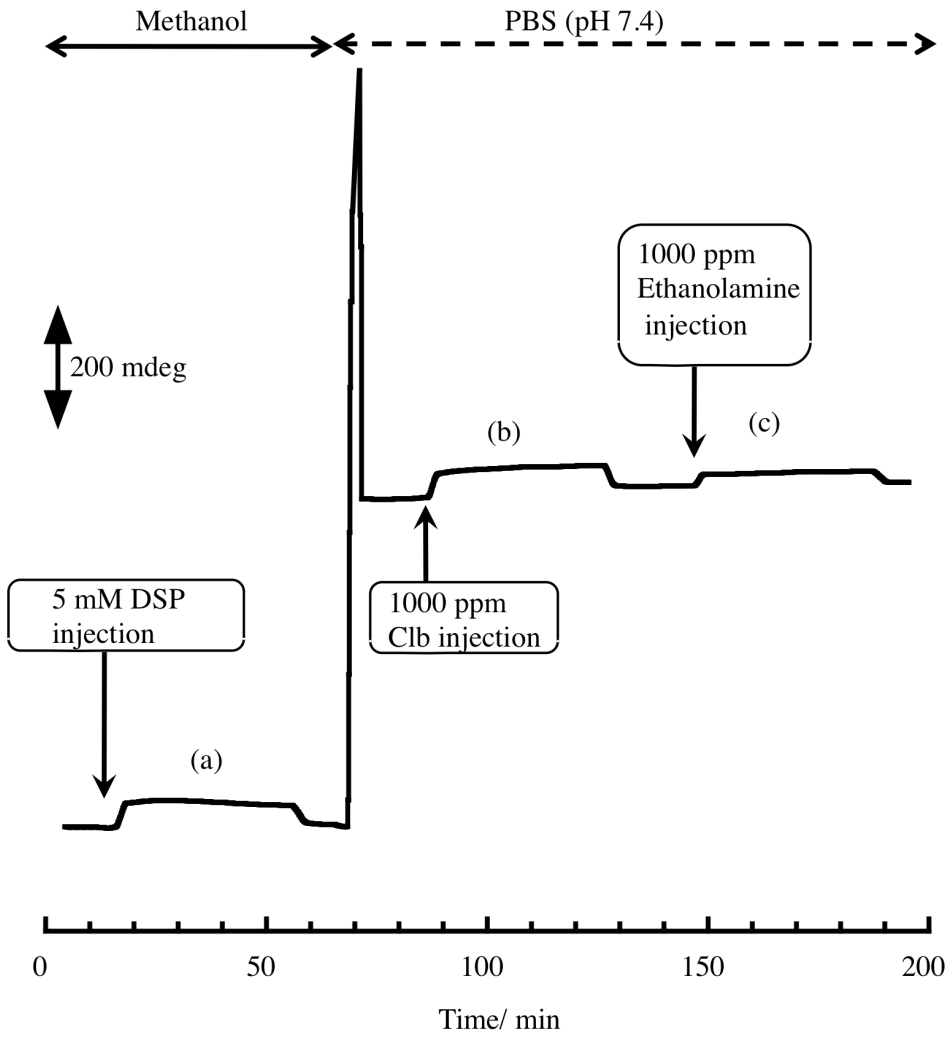

Fig. 3.3. SPR sensogram recorded during the fabrication process of the sensor surface (a) Self-assembly process of the succinimidyl-terminated propenthiol (DSP) monolayer, (b) immobilization of clenbuterol (Clb) by amide coupling reaction, and (c) blocking of the unreacted *N*-hydroxysuccinimidyl group with ethanolamine. Flow rate was 5 μL min^{-1}.

3.5 Immunoassay format

When analyte with a low molar mass is detected, the low mass of captured analyte could not generate sufficient response in direct immunoassay by SPR. Thus, SPR experiments were carried out using indirect competitive inhibition format. This

format utilizes the immunosurface immobilized with analyte instead of antibody (Ab) and the mass provided by the binding of primary antibodies. As a consequence, this format can produce much greater signal and sensitivity. According to the detection principle, a PBS solution containing of Ab-AuNP conjugate with a standard concentration was premixed with different concentrations of clenbuterol in PBS solution at the incubation process. During this process, a portion of the Ab-AuNP conjugate bonded to the clenbuterol in the sample solution. Then the sample solution was injected into the clenbuterol-immobilized sensor surface at a flow rate of 100 $\mu L \cdot min^{-1}$. The unbonded Ab-AuNP in the premixed solution will binds to the clenbuterol of the sensor surface, which is called primary immunoreaction. After the primary immunoreaction, the sensor surface was regenerated using 0.1 M NaOH solution. Therefore, the same sensor surface was used for the detection.

3.6 Results and Discussion

3.6.1. Immunoassay using the Ab-AuNP conjugate

Clenbuterol detection was performed using an indirect competitive inhibition immunoassay and Ab-AuNP conjugate. Fig. 3.4 shows the SPR sensogram recorded during immunosensing detection of the Ab-AuNP conjugate (1 ppm) for 0 to 1 ppb (1 ng mL^{-1}) of clenbuterol. Because of the refractivity difference between the running buffer (PBS) and sample solution, the SPR signal abruptly decreased after sample solution injection. For the calibration curve (Fig. 3.5), the angle shifts were calculated from the difference in the SPR signal before and after sample injection (from t = 150 s to t = 450 s). As shown in Fig. 3.4 (inset), the signal slightly decreased until regeneration solution injection because of the desorption of nonspecifically adsorbed Ab-AuNP conjugate from the sensor surface. The amount of nonspecifically adsorbed

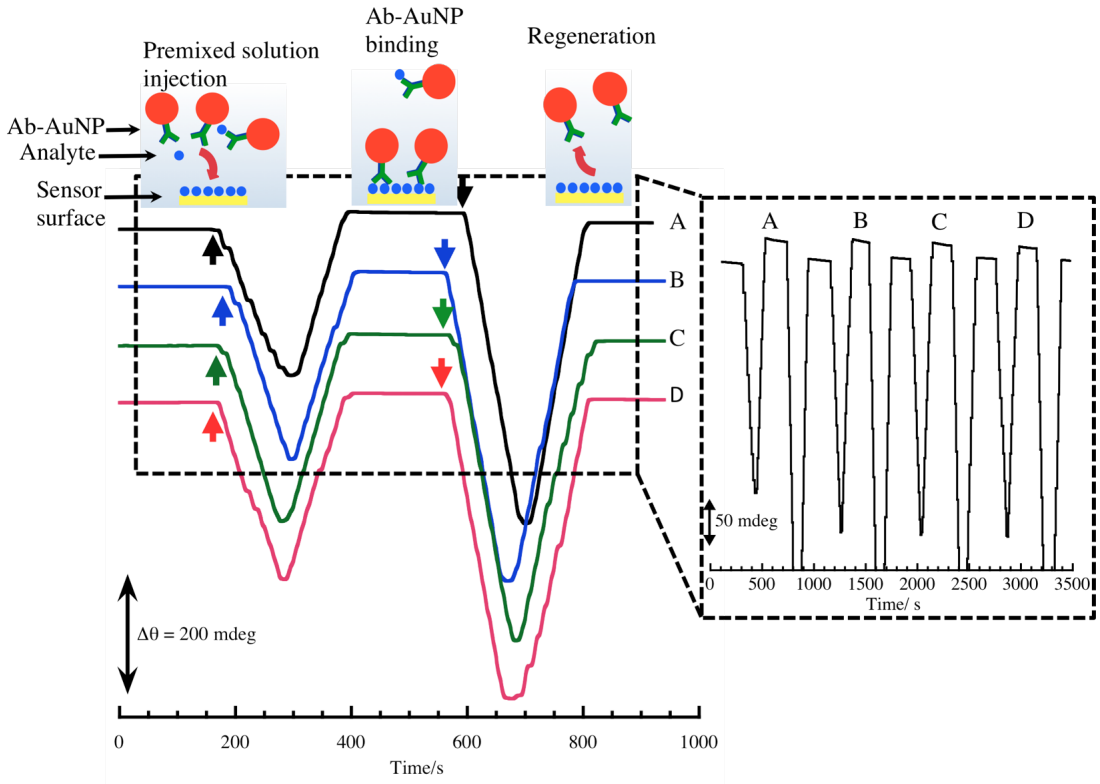

Fig. 3.4 SPR sensogram of the immunoreactions with clenbuterol and Ab-AuNP conjugate premixed solutions were comprised 1 ppm Ab-AuNP conjugate and the clenbuterol standard solutions [(A) 0 ppt clenbuterol and (B) 0.01 ppt, (C) 0.1 ppt and (D) 1 ppt clenbuterol]. Inset figure shows the full time-course measurement. Regeneration solution was 0.1 M NaOH. The flow rate of the carrier solution was 100 μL min^{-1}.

Ab-AuNP conjugate was estimated to be approximately 12.6 ± 4.0%. In support of this view, there is a recent report suggesting that the orientation of Ab molecules on the nanoparticle surface is not uniform [32]. For example, one set of Abs that is outwardly oriented on the AuNP surface has a high affinity for capturing analytes onto the sensor surface. Another set of Abs may be immobilized onto the AuNP surface with less affinity for antigen binding. Because the immobilized analyte is much smaller than Ab-AuNP, some conjugates may be deposited on the sensor

surface without strongly binding to the sensor surface because of the orientation of the Ab molecule on the nanoparticle surface. Therefore, the unbound or loosely bound conjugates are desorbed from the sensor surface when the running solution is switched from the sample solution to PBS.

It was also found that a regeneration solution of 0.1 M NaOH removed all Ab-AuNP conjugates from the sensor surface. The sensor surface could be used again, as illustrated in Fig. 3.4 (inset). The surface is robust because the sensor surface architecture consists of covalent bonds (S-Au, S-S, and NHCO).

A typical sigmoidal-type calibration curve of the indirect competitive inhibition immunoassay was obtained and is shown in Fig. 3.5. Because the amount of free Ab-AuNP conjugate decreased with increasing clenbuterol concentration, the angle shifts also decreased with increasing clenbuterol concentration. The highest angle shift (14.8 mdeg) was observed in the absence of clenbuterol because the free Ab-AuNP concentration was at the maximum. The angle shift was approximately 3-fold higher than that of unlabeled Ab (5 mdeg). The signal enhancement was caused by dielectric constant difference between unlabeled Ab and the Ab-AuNP conjugate.

The LOD has been typically defined at 85% of the maximum angle shift [13,15,22]. LOD of the immunoassay for the detection of clenbuterol was determined to be 0.05 ppt (0.05 pg mL^{-1}) using the Ab-AuNP conjugate. In contrast, LOD was only 2 ppt (2 pg mL^{-1}) for the unlabeled Ab, which was approximately 40 times higher than that of the Ab-AuNP conjugate. To the best of my knowledge, such extremely high sensitivity has not been reported for the detection of clenbuterol [ELISA: 100–25 pg mL^{-1} [28,33]; amperometry: 1.3 pg mL^{-1} [34]; fluorescence spectroscopy: 0.12 μg L^{-1} [35]; SPR: 2.0 μg L^{-1} [36]; spectral imaging SPR: 6.7–4.5 μg mL^{-1} [37]. Sensitivity enhancement can be explained by evaluation of affinity

constants of immunoreactions of the indirect competitive inhibition immunoassay. The detailed mechanism will be discussed in the next section.

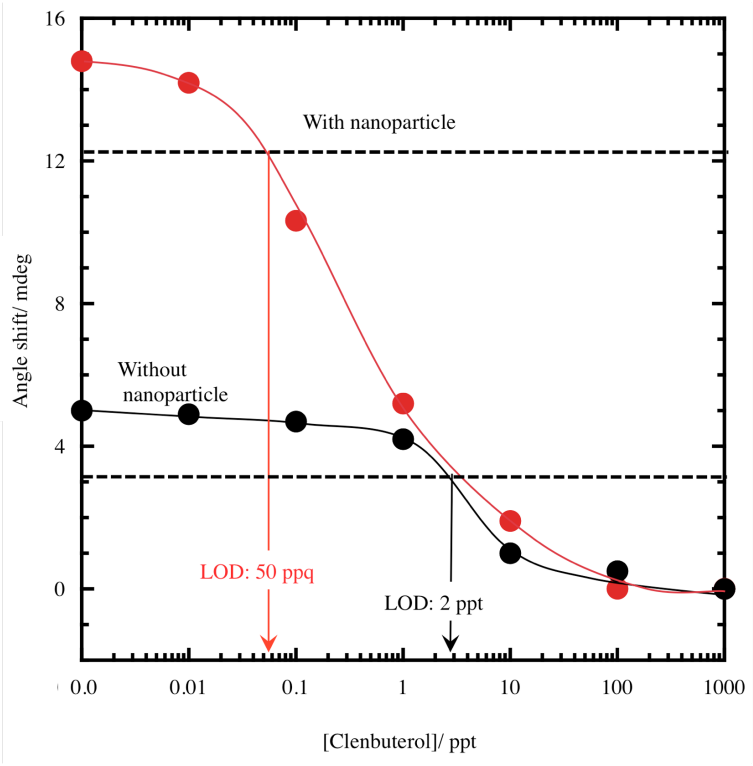

Fig. 3.5. Calibration curves for the detection of clenbuterol using unlabeled Ab and Ab-AuNP conjugate.

3.6.2. Evaluation of affinity constants

It is known that AuNP causes LSPR signal amplification. Because LSPR signal amplification complicates the estimation of an accurate reactant amount, no one has evaluated the affinity constant. However, our system does not cause the LSPR effect. Because the maximum surface concentration of AuNPs is very low (distance between particles is a sub-micrometer order), the electromagnetic wave coupling cannot be occurred. Therefore, I construct here the estimation of affinity constants of an indirect competitive inhibition immunoassay from the basic Langmuir adsorption isotherm.

The angle shift is a result of biomolecular interactions during the capture of the Ab-AuNP conjugate by the analyte immobilized on the sensor surface. In the indirect competitive inhibition immunoassay, Ab-AuNP conjugate solution is premixed with clenbuterol solution; the Ab-AuNP conjugate reacts with clenbuterol immobilized on the sensor surface (*Ss*) and clenbuterol in the premixed solution (*Clb*). Immunoreaction on the sensor surface can be denoted as follows:

$$Ab\text{-}AuNP + Ss \rightleftharpoons Ab\text{-}AuNP\text{-}Ss \quad (1)$$

Immunoreaction in the premixed solution can be expressed as:

$$Ab\text{-}AuNP + Clb \rightleftharpoons Ab\text{-}AuNP\text{-}Clb \quad (2)$$

The affinity constants for the surface immunoreaction and immunoreaction in the premixed solution were defined as K_1 and K_2, respectively.

$$K_1 = \frac{[Ab-AuNP-Ss]}{[Ab-AuNP][Ss]} \quad (3)$$

$$K_2 = \frac{[Ab-AuNP-Clb]}{[Ab-AuNP][Clb]} \quad (4)$$

where [*Ab-AuNP*] and [*Ab-AuNP-Clb*] in Eq. (3) and (4) indicates molar concentration (mol L^{-1}) of the Ab-AuNP conjugate solution and Ab-AuNP conjugate complex with clenbuterol in the premixed solution, respectively. [*Clb*] is the molar concentration of clenbuterol in the premixed solution. [*Ab-AuNP-Ss*] and [*Ss*] denotes the surface concentration [ng cm^{-2}] of Ab-AuNP conjugate reacted with the clenbuterol and that of free clenbuterol on the sensor surface, respectively. The surface immunoreaction of the Ab-AuNP conjugate with the sensor surface is modeled by the Langmuir adsorption isotherm. The Langmuir adsorption isotherm for SPR immunosensing is written as follows:

$$\frac{1}{\Delta\theta_{Ab-AuNP}} = \frac{1}{\Delta\theta_{Ab-AuNP,\max}} + \frac{1}{K_1[Ab-AuNP]\Delta\theta_{Ab-AuNP,\max}} \quad (5)$$

Here, $\Delta\theta_{Ab\text{-}AuNP}$ is the total angle shift for the standard concentration (2.6×10^{-14} M–2.6×10^{-12} M) of the Ab-AuNP conjugate and $\Delta\theta_{Ab\text{-}AuNP,\max}$ is the SPR angle shift when the maximum amount of the Ab-AuNP conjugate is bonded to the reaction site on the sensor surface. It is assumed that the SPR angle is proportional to the amount of Ab-AuNP captured onto the adsorption site (immobilized clenbuterol), and it is thought that the reacted amount could not be estimated by dielectric constant change of Ab-AuNP conjugate. Hence, the signal amplification magnitude is defined as "*A*". It is assumed that *A* is always the same (constant) under our experimental conditions. It is reasonable to wonder whether this assumption is true. $\Delta\theta_{Ab\text{-}AuNP,\max}$ is definitely overestimated because of dielectric constant change. Thus, the true maximum concentration must be lower than 1549 μm^2/Ab-AuNP estimated from $\Delta\theta_{Ab\text{-}AuNP,\max}$ (108 mdeg). Therefore, it is reasonable to assume that "*A*" is always constant. Hence, Eq. (5) can be rewritten as follows:

$$\frac{1}{A\Delta\theta_{Ab-AuNP}} = \frac{1}{A\Delta\theta_{Ab-AuNP,\max}} + \frac{1}{K_1[Ab-AuNP]A\Delta\theta_{Ab-AuNP,\max}} \qquad (6)$$

All the "*A*" terms can be canceled out in this equation. Therefore, it can be concluded that the dielectric constant change did not affect the determination of K_1. Hence, K_1 was estimated to be 3.0×10^{11} M^{-1}.

For the estimation of K_2 with "*A*," the following equation [13] can be used

$$\frac{1}{A\Delta\theta} = \frac{1}{A\Delta\theta_{1ppm,Ab-AuNP}} + \frac{\alpha K_2[Clb]_0}{K_1[Ab-AuNP]_{total}A\Delta\theta_{Ab-AuNP,\max}} \qquad (7)$$

where $[Ab\text{-}AuNP]_{total}$ denotes the total concentration (1 ppm) of Ab-AuNP conjugate. $[Clb]_0$ is the initial concentration of clenbuterol. Considering the reaction time of the immunoreaction in the premixed solution, the concentration of clenbuterol is $[Clb] = [Clb]_0 e^{-kt}$. In the Eq. (7), $\alpha = e^{-kt}$, where *k* is the reaction rate and *t* is the reaction time of the immunoreaction in premixed solution. Because "*A*" can also be canceled in this

equation, it is concluded that the dielectric constant change does not affect on αK_2 as well as K_1. αK_2 was calculated to be 2.9×10^{12} M^{-1} from the slope. K_1 and αK_2 of unlabeled Ab were estimated to be 4.8×10^8 M^{-1} and 1.0×10^8 M^{-1}, respectively (Fig. 3.6). Notably, K_1 and αK_2 of the Ab-AuNP conjugate were three and four orders of magnitude higher than those of unlabeled Ab, respectively. These differences in affinity constants can be easily explained by the molar concentration calculations of Eq. (3) and Eq. (4). The molecular mass of unlabeled Ab (MW 46.5 kg mol^{-1}) is four orders of magnitude lower than that of the Ab-AuNP conjugate (MW 390,000 kg mol^{-1}).

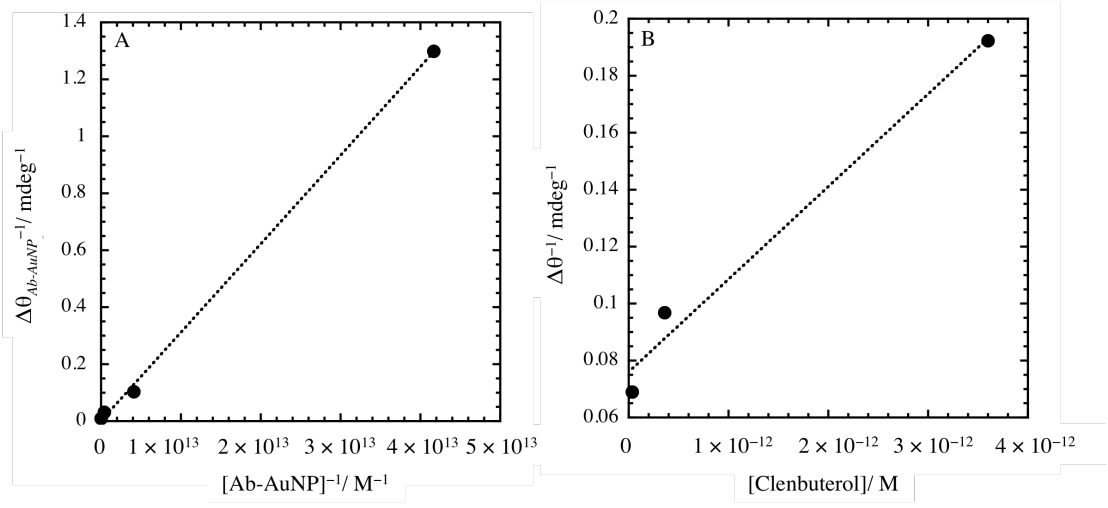

Fig. 3.6 Determination of the affinity constants (A) K_1 and (B) αK_2 of the indirect competitive inhibition immunoassay. The maximum angle shift, $\Delta\theta_{Ab\text{-}AuNP,max}$= 108.0 mdeg and $\Delta\theta_{1ppm,Ab\text{-}AuNP,max}$ = 14.8 mdeg.

In the premixed solution containing 1 ppm Ab or Ab-AuNP conjugate, the molar concentration of Ab-AuNP was four orders of magnitude lower than that of unlabeled Ab. Because [Ab-AuNP] was in the denominators of Eq. (3) and Eq. (4), the affinity constants became high. Size comparison revealed that [Ab-AuNP-Ss] is one order

smaller than [Ab-Ss]. Thus, the K_1 and αK_2 values of the Ab-AuNP conjugate were three and four orders of magnitude higher than those of unlabeled Ab, respectively.

Aiming to identify the determining factor of LOD, simulations were constructed. To compare the calibration curves, the SPR signals ($\Delta\theta$) were normalized to the percentage of the maximum angle shift ($\Delta\theta_{1\ ppm,\ Ab\text{-}AuNP}$) obtained in the absence of an analyte. The following equation can be derived from Eq. (7):

$$\frac{\Delta\theta}{\Delta\theta_{1ppm,Ab-AuNP}} = \left(1 + \frac{\alpha K_2 [Clb]_0 \Delta\theta_{1ppm,Ab-AuNP}}{K_1 [Ab-AuNP]_{total} \Delta\theta_{Ab-AuNP}}\right)^{-1} \quad (8)$$

The simulations of $\Delta\theta/\Delta\theta_{1ppm,Ab\text{-}AuNP}$ were plotted as functions of K_1 and αK_2, as illustrated in Fig. 3.7. The experimental results show good agreement with the theoretical curve (3.0×10^{11} M^{-1} and 2.9×10^{12} M^{-1} for K_1 and αK_2, respectively).

It was found that LOD shifted toward higher concentrations at higher K_1 values. In contrast, LOD shifted toward lower concentrations at higher αK_2 values. Thus, it was concluded that the balance of K_1 and αK_2 determines LOD of the indirect competitive inhibition immunoassay. To support this conclusion, The LOD simulation is constructed. The LOD is defined as the concentration of clenbuterol $[Clb]_0$ in the premixed solution that produces an SPR angle shift of 85% of $\Delta\theta/\Delta\theta_{1ppm,Ab\text{-}AuNP}$. In other words, the $[Clb]_0$ at 85% is the LOD. The equation to determine the LOD can be written as follows:

$$\frac{\Delta\theta}{\Delta\theta_{1ppm,Ab-AuNP}} = \frac{85}{100} = \left(1 + \frac{\alpha K_2 \mathrm{LOD} \Delta\theta_{1ppm,Ab-AuNP}}{K_1 [Ab-AuNP]_{total} \Delta\theta_{Ab-AuNP,\max}}\right)^{-1} \quad (9)$$

In the inverse form, it can be written as follows:

$$\frac{100}{85} = 1 + \frac{\alpha K_2 \mathrm{LOD} \Delta\theta_{1ppm,Ab-AuNP}}{K_1 [Ab-AuNP]_{total} \Delta\theta_{Ab-AuNP,\max}} \quad (10)$$

$$\frac{15}{85} = \frac{\alpha K_2 \mathrm{LOD} \Delta\theta_{1ppm,Ab-AuNP}}{K_1 [Ab-AuNP]_{total} \Delta\theta_{Ab-AuNP,\max}} \quad (11)$$

This equation can be rearranged as follows:

$$\mathrm{LOD} = \frac{15K_1[Ab - AuNP]_{total}\Delta\theta_{Ab-AuNP,\max}}{85\alpha K_2\Delta\theta_{1ppm,Ab-AuNP}} \qquad (12)$$

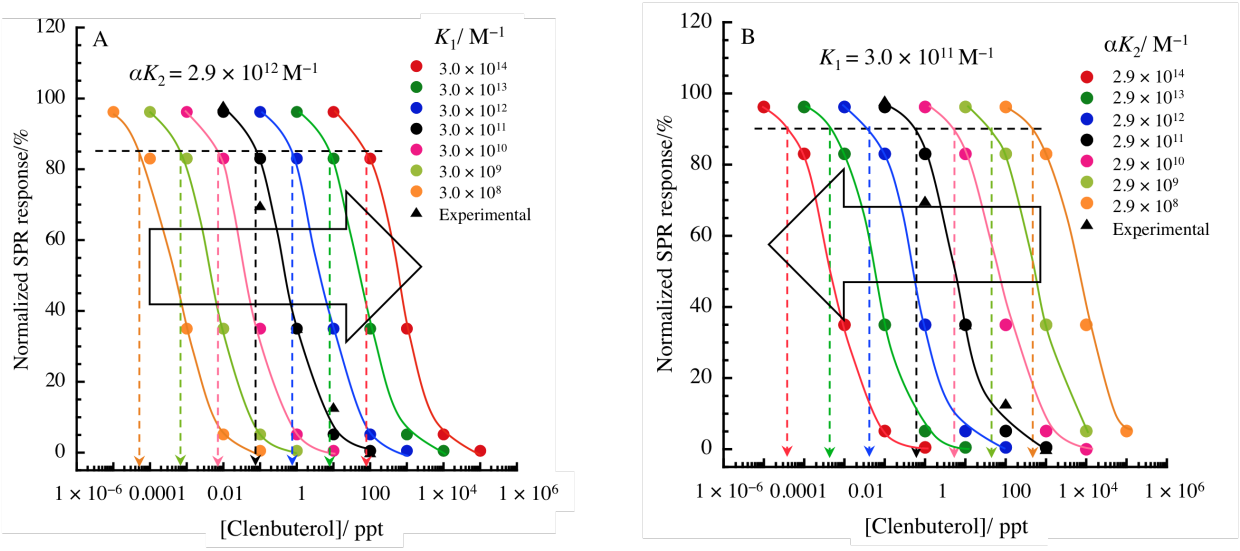

Fig. 3.7. Simulated calibration curves: Ab-AuNP conjugate in the indirect competitive inhibition immunoassay. Filled triangles are experimental data for Ab-AuNP. The simulation curves are calculated using Eq. (7), assuming (A) $\alpha K_2 = 2.9 \times 10^{12}\ \mathrm{M}^{-1}$ and (B) $K_1 = 3.0 \times 10^{11}\mathrm{M}^{-1}$.

LOD is plotted according to Eq. (12) with respect to K_1 and αK_2 in Fig. 3.8. The plot clearly shows that higher values of K_1 and lower values of αK_2 lead to higher values of LOD. Because this is a rising diagonal slope from the bottom left to top right, the same LOD could be obtained from the same order of K_1 and αK_2. To achieve LOD at the ppt (pg mL^{-1}) level, αK_2 must be one order of magnitude higher than K_1.

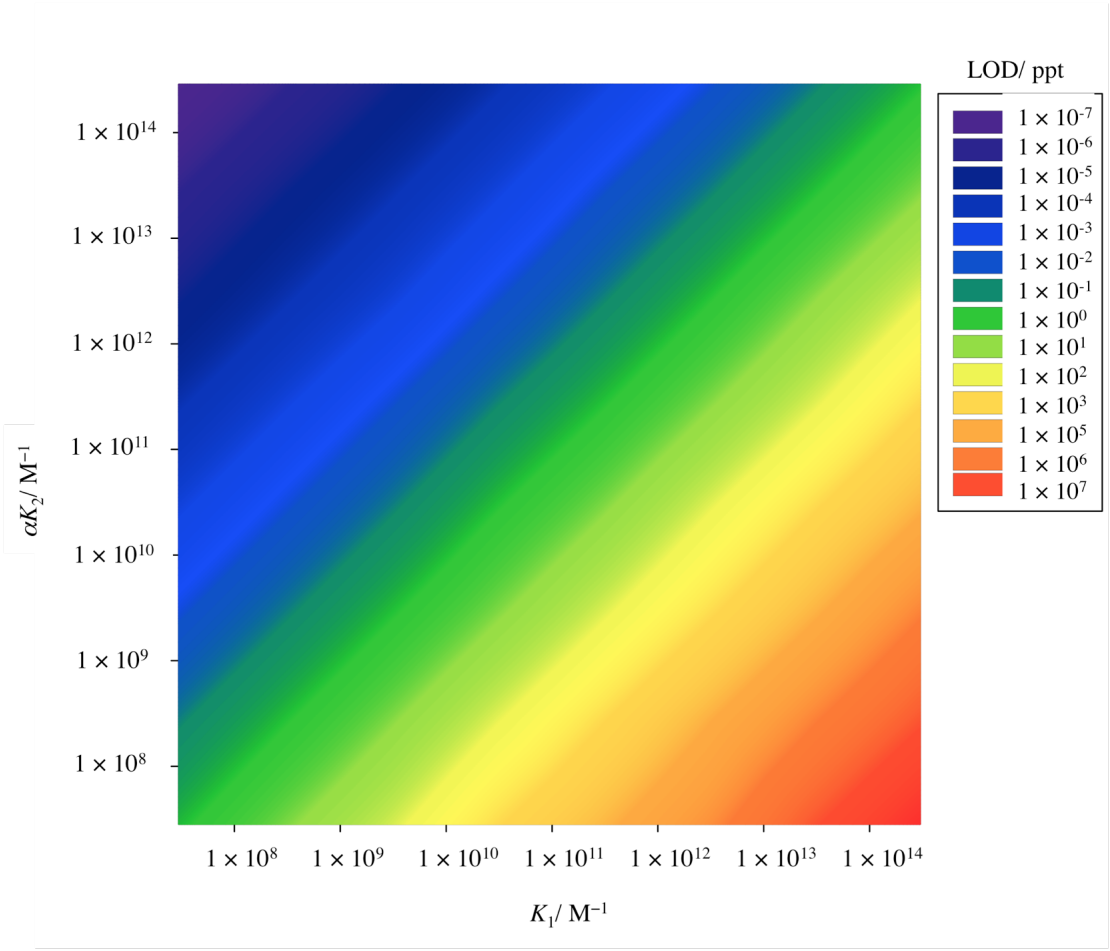

Fig. 3.8. Simulation of LOD based on Eq. (8) with respect to K_1 and αK_2

LOD is calculated from Eq. (9), $\mathrm{LOD} = \dfrac{15K_1[Ab-AuNP]_{total}\Delta\theta_{Ab-AuNP,\max}}{85\alpha K_2\Delta\theta_{1ppm,Ab-AuNP}}$.

In summary, Ab labeled with AuNP in an indirect competitive inhibition immunoassay was examined with the aim to enhance the SPR signal change and the sensitivity. LOD of the immunoassay for the detection of clenbuterol was determined to be 0.05 ppt (0.05 pg mL^{-1}) using the primary Ab-AuNP conjugate. In contrast, LOD was only 2 ppt (2 pg mL^{-1}) for the unlabeled primary Ab, which was approximately 40 times higher than that of the Ab-AuNP conjugate. LOD is influenced by the balance between K_1 and αK_2. In particular, LOD achieved for αK_2 was one order of magnitude higher than that achieved for K_1. I proposed that LOD

can be adjusted to a required level because the affinity constants (K_1 and αK_2) are determined by the molar concentrations of the reactant and sensor surface ($\Delta\theta$ and $\Delta\theta_0$).

3. 7. Summary

This study aimed to develop a method for highly sensitive detection of clenbuterol. To achieve this goal, AuNP was used as label for antibody in an indirect competitive inhibition immunoassay. A sensitivity of 0.05 ppt (0.05 pg mL^{-1}) was achieved, which was the highest among the past reports using SPR, ELISA, amperometry and fluorescence spectroscopy. The sensitivity mechanism was elucidated by evaluation of affinity constants, which showed that dielectric constant change due to labeling did not affect the affinity constants (K_1 and αK_2) because the dielectric constant magnitude terms cancel out in the Langmuir adsorption equation. Therefore, the Langmuir adsorption isotherm for SPR sensing could be used for the calculation of K_1 and αK_2, which were estimated to be 3.0×10^{11} M^{-1} and 2.9×10^{12} M^{-1}, respectively. The affinity constants were three and four orders of magnitude, respectively, higher than those of unlabeled Ab. The enhancement of the affinity constants was caused by the molar concentration difference between the Ab-AuNP conjugates and unlabeled Ab in 1 ppm (1 μg mL^{-1}) of premixed solution. Thus, I concluded that sensitivity enchantment is caused by molar concentration difference. To understand the mechanism underlying changes in LOD, simulation was performed. I found that the requirement of LOD at the ppt (pg mL^{-1}) level is that αK_2 must be one order of magnitude higher than K_1. The results showed that LOD could be adjusted to a required level because the affinity constants can be adjusted by changing the molar masses of the reactant (Ab).

3.8 References

[1] B. Liedberg, C. Nylander, I. Lunstrom, Sens. Actuators. 4 (1983) 299–304.

[2] C. Nylander, B. Liedberg, T. Lind, Sens. Actuators. 3 (1982) 79–88.

[3] X. Guo, J. Biophotonics. 5 (7) (2012) 483–501.

[4] J. Homola, Anal. Bioanal. Chem. 377 (2003) 528–539.

[5] J. Homola, Chem. Rev. 108 (2008) 462–493.

[6] J. Mitchell, Sensors 10 (2010) 7323–7346.

[7] H.H. Nguyen, J. Park, S. Kang, M. Kim, Sensors 15 (2015) 10481–10510.

[8] S. R. Mozaz, M.P. Marco, M.J. Lopez de Alda, D. Barcelo, Pure. Appl. Chem. 76 (2004) 723–752.

[9] D.R. Shankaran, N. Muira, J. Phys. D: Appl. Phys. 40 (2007) 7187–7200.

[10] P. Sing, Sens. Actuators B 229 (2016) 110–130.

[11] E.B. Bahadir, M.K. Sezginturk, Anal. Biochem. 478 (2015) 107–120.

[12] J. Homola, S.S. Yee, G. Gauglitz, Sens. Actuators B, 54 (1999) 3–15.

[13] Suherman, K. Morita, T. Kawaguchi, Appl. Surf. Sci. 332 (2015) 229–236.

[14] D.R. Shankaran, K.V. Gobi, N. Muira, Sens. Actuators B 121 (2007) 158–177.

[15] K.V. Gobi, M. Sasakai, Y. Shoyama, N. Muira, Sens. Actuators B 89 (2003) 137–143.

[16] A. Karczmarczyk, M. Dubiak-Szepietowska, M. Vorobii, C. Rodriguez-Emmenegger, J. Dostalek, K. Feller, Biosens. Bioelectron. 81 (2016) 159–165.

[17] T. Kawaguchi, D.R. Shankaran, S.J. Kim, K.V. Gobi, K. Matsumoto, K. Toko, N. Miura, Talanta 72 (2007) 554–560.

[18] A. Losoya-Leal, M.C. Estevez, S.O. Martinez-Chapa, L.M. Lechuga, Talanta 141 (2015) 253–258.

[19] J.S. Mitchell, Y. Wu, C.J. Cook, L. Main, Anal. Biochem. 343 (2005) 125–135.

[20] J. Wang, A. Munir, H.S. Zhou, Talanta 79 (2009) 72–76.

[21] L. Zhou, A. Zhu, X. Lou, D. Song, R. Yang, H. Shi, F. Long, Anal. Chem. Acta. 905 (2016) 140–148.

[22] T. Kawaguchi, D.R. Shankaran, S.J. Kim, K. Matsumoto, K. Toko, N. Muira, Sens. Actuators B 133 (2008) 467–472.

[23] M.J. Know, J. Lee, A.W. Wark, H.J. Lee, Anal. Chem. 84 (2012) 1702–1707.

[24] X. Liu, Y. Yang, L. Mao, Z. Li, C. Zhou, X. Liu, S. Zheng, Y. Hu, Sens. Actuators B 218 (2015) 1–7.

[25] B. Wenger, K. Kugelbrey, H. Gao, H. Sigrist, G. Voirin, Biosens. Bioelectron. 34 (2012) 94–99.

[26] S. Szunerits, J. Spadavecchia, R. Boukherroub, Rev. Anal. Chem. 33(3) (2014) 153–164.

[27] J.W. Choi, D.Y. Kang, Y.H. Jang, H.H. Kim, J. Min, B.K. Oh, Colloid. Surf A: Physicochem. Eng. Aspects 313–314 (2008) 655–659.

[28] T. Springer, M.L. Ermini, B. Spackova, J. Jablonku, J. Homola, Anal. Chem. 86 (2014) 10350–10356.

[29] MaxSignal Clenbuterol ELISA Test Kit, Available at: <http://www.biooscientific.com/Hormone-residue-test-kits/MaxSignal-Clenbuterol-ELISA-Test-Kit> (accessed 02.10.2016)

[30] S. Zeng, D. Baillargeat, H. Ho-Pui, Y. Ken-Tye, Chem. Soc. Rev. 43 (2014) 3426-3452.

[31] D.D. Jeremy, A.J. Cheryl, S.M. Tompkins, A.T. Ralph, Analyst 136 (2011) 3083–3090.

[32] B. Saha, T.H. Evers, W.J. Prins, Anal. Chem. 86 (2014) 8158–8166.

[33] X. Ren, F. Zhang, F. Chen, T. Yang, Food Agr. Immunol. 20 (2009) 333–344.

[34] S. Li, J. Zhang, W. Deng, X. Shen, S. Song, C. Fan, Electroanalysis 25 (2013) 867–873.

[35] Y. Tang, Z. Gao, S. Wang, X. Gao, J. Gao, Y. Ma, X. Liu, J. Li, Biosens. Bioelectron. 71 (2015) 44–50.

[36] Y. Li, P. Qi, X. Ma, J. Zhong, Eur. Food Res. Technol. 239 (2014) 195–201.

[37] Y. Wu, M. Yao, X. Fang, Y. Yang, X. Cheng, Appl. Biochem. Biotechnol. 177 (2015) 1327–1337.

Chapter 4

Strategy of Signal Amplification and Sensitivity Enhancement

4.1 Introduction

Immunoassay is an analytical technique based on the specific interaction between antibodies and their cognate antigen (analyte). Immunoassays are widely used for analyte analysis in different methods such as enzyme-linked immunosorbent assay (ELISA) [1,2], chemiluminescence [3-5], flurescence [6], electrochemiluminescence [7], and electrochemical methods (such as amperometric, potentiometric, impedimetric and capacitometric) [8-11]. The advantages of these methods are mainly their specificity and sensitivity with $ngmL^{-1}$ [12,13]. However, these methods suffered with a number of significant drawbacks like labeling of antigen or antibody, long incubation period (≥2-6 h), signal-off tendency, extensive sample handling and need trained personnel. Although, immunocromatographic assay possess some advantages in terms of user friendly, rapid and low cost; however, the major limitations are pretreatment of sample is required and low signal intensity [12,14]. Despite some advantages, the use of quartz crystal microbalance (QCM) biosensor for the determination of low level of analyte is still encumbered by its low intrinsic sensitivity [12,15]. On the other hand, surface plasmon resonance (SPR) biosensor has inherent advantages such as label-free detection, high sensitivity, reusability, quick analysis, small amount of sample, real-time monitoring and thus affinity constants of immunoreaction, etc. [16]. Therefore, SPR biosensor is considered as an important analytical tool in the field of environmental monitoring,

clinical and medical diagnosis, food safety, homeland security and agriculture monitoring by academic and industrial scientists [17-20].

Depending on SPR response to binding of an analyte to a surface, an analyte can be detected with a direct, sandwich or indirect competitive inhibition competitive immunoassay [17,21,22]. Typically, sandwich (Antibody-analyte-antibody) immunoassay is widely used for analysis of medium and large molecular weight analytes such as DNA, proteins, peptides and nucleic acids [12,23,24]. This immunoassay gives the highest level of sensitivity and specificity because of the use of a couple of match antibodies. However, sandwich immunoassay suffers from fundamental limitations that the molecule to be measured must have large enough to have two distinct epitopes to be bounded. To overcome this defect, indirect competitive inhibition immunoassay received increased attention for the detection of small molecule by researchers. Based on the inhibition principle, analyte is immobilized onto sensor surface. After that, the sensor surface is exposed to a solution of analyte mixed with a specific antibody (Ab), and SPR monitors the immunoreaction of high molecular weight unbound Ab to the sensor surface. Therefore, a high signal and a pronounced sensitivity are expected.

Indirect competitive inhibition immunoassay based on SPR biosensor has been reported for the detection of small molecule [22, 25-33]. For instance, Suherman et al. [31] reported the detection of β-agonists using primary immunoreaction. Although they achieved a ppt level limit of detection, however the signal change was significantly low. One of the key factors for success of an immunoassay especially for the detection of small molecule is the signal amplification. Because noise sources such as temperature and pressure variations and variations in the composition of the bulk liquid may result in signal drift approximately 10 mdeg. This phenomenon limits

the practically achievable detection limit [34]. From the standpoint of signal amplification, Kawaguchi et al. [27] developed indirect competitive inhibition immunoassay by modifying immunosurface with Au-nanoparticle (AuNP) for the detection of TNT. They reported 4-times higher signal amplification compared to the unmodified sensor surface, however the limit of detection (LOD) was comparable. In the previous chapter, I labeled anti-clenbuterol Ab with AuNP and used in the detection of clenbuterol (Clb, MW 277 g mol^{-1}), a small analyte. Even though, I developed a fast (< 5 min) detection process with a high sensitivity of 0.05 ppt (50 ppq), the highest signal change was 13.4 mdeg [35]. This signal change is not sufficient in terms of signal drift effect for the practical application. It has therefore been a significant challenge to simultaneously achieve both highly sensitive (a high signal and a low LOD) and raid immunoassays of small molecules.

A conventional amplification using secondary Ab (Ab_2) labeled with large particle such as AuNP, quantum dots and latex particle used to apply the sandwich immunoassay [12,24,36]. Due to their high mass, high dielectric constant and electromagnetic coupling between AuNP and Au film, AuNP labeled Ab_2 have been widely used in a variety of works [12,24,37,38].

In this study, I proposed secondary immunoreaction using secondary Ab labeled with AuNP (Ab_2-AuNP) in indirect competitive inhibition immunoassay for the detection of clenbuterol for the first time. I prepared the sensor surface using self-assembly method, since it is well known that this method dramatically promoted the stability of the sensor surface. However, the orientation of recognition molecule onto sensor surface affects the immunoreaction. Consequently, the affinity constant is changed, which control the overall sensitivity of the indirect competitive inhibition immunoassay. In the past study, it was reported that lay-down structure produced a

low affinity constant and high sensitivity using primary immunoreaction [32]. Thus, it is logical to assume that the orientation of recognition molecule onto sensor surface might affect the secondary immunoreaction. Therefore, I compared the sensing performance using the low affinity and the high affinity sensor surface aiming to investigate the effect of sensor surface structure on the secondary immunoreaction. Furthermore, the affinity constants of secondary immunoreaction were evaluated and compared for secondary Ab_2 or Ab_2-AuNP conjugate for the first time.

4.2 Fabrication of immunosurface

SPR sensograms of the immunosurface fabrication process were illustrated in Fig. 4.1. In order to fabricate the low and high affinity sensor surfaces, 0.1 mM and 5 mM DSP of methanolic solutions were injected, respectively. The flow rate was 5 μL min^{-1} and the loop volume was 200 μL. In this step, disulfide bond of DSP was cleaved and succinimidyl-terminated propenthiol monolayer was formed onto the sensor chip. After 40-min period of injection, the running solution was changed from methanol to phosphate buffered saline (PBS). The SPR response initially decreased and finally increased due to dielectric constant difference of PBS. Once SPR response becomes stable, a 1,000-ppm clenbuterol in PBS solution was injected. Clenbuterol replaced the succinimidyl group and immobilized by amide coupling reaction. Upon the binding of clenbuterol to the sensor surface, the SPR angle was shifted to the higher angle and stayed constant while the solution passed over the surface. The refractive index in the vicinity of the sensor surface was higher due to binding of clenbuterol on the surface as well as passing the clenbuterol solution through the surface. After that the resonance angle decreased due to a decrease in the bulk

refractive index in the vicinity of the sensor chip by replacing the clenbuterol solution with the PBS running solution.

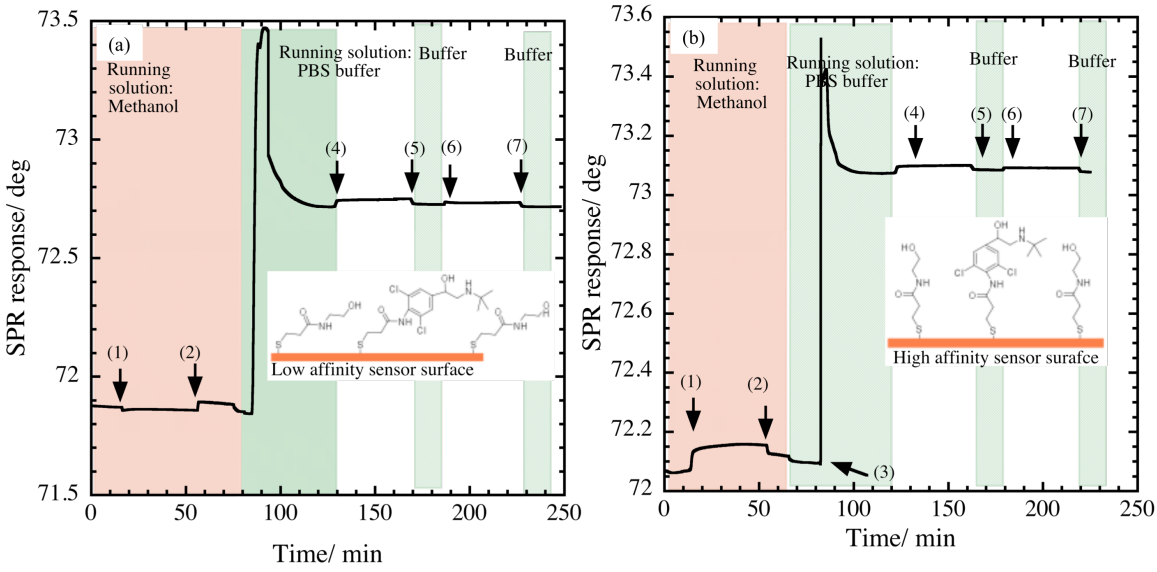

Fig.4.1. SPR sensograms represents the sensor surface fabrication process (a) low affinity sensor surface. (b) High affinity sensor surface. (1) Methanol running solution; (2) Injection of DSP in methanolic solution (0.1 and 5 mM DSP corresponds to low and high affinity sensor surface, respectively; (3) PBS buffer running solution start; (4) 1000 ppm clenbuterol in PBS solution injection; (5) PBS buffer running solution start; (6) 1000 ppm ethanolamine in PBS solution injection and (7) PBS buffer running solution.

The difference in SPR angles before the immobilization and after the final PBS wash corresponds to the amount of immobilized analyte. The maximum SPR angle shift obtained for covalent immobilization of clenbuterol on the succinimidyl terminated propenthiol monolayer was 21.8 (±2.3) mdeg for 5 mM DSP, and it corresponds to 7.87 (±0.83)× 10^{-11} mol cm^{-2}. In contrast, the surface concentration of clenbuterol was calculated to 3.80 (±0.60)× 10^{-11} mol cm^{-2} (10.5 ± 1.7 mdeg) for 0.1 mM DSP prepared sensor surface. According to [40], the amount of immobilized

receptor should keep as low as possible to avoid mass transport limitations. The recommended range for the surface concentration of immobilized receptor is 5-20 × 10^{-11} mol cm^{-2} [40]. By taking into consideration of receptor concentration, the febricated sensor surface avoids mass transport limitations. Finally, ethanolamine (1000 ppm) in PBS solution was flowed over the surface as a blocking agent in order to block unreacted *N*-hydroxy succinimide groups. The SPR angle shifts were estimated to 8.34 (±0.5) mdeg and 9.72 (±2.1) mdeg and the surface concentrations of ethanolamine were estimated to 1.36 (± 0.008) × 10^{-10} mol cm^{-2} and 1.59 (±0.034) × 10^{-10} mol cm^{-2} for 0.1 and 5 mM DSP, respectively. The binding of ethanolamine reduces the non-specific adsorption of primary and secondary antibodies introduce in the detection process.

4.3 Immunoassay

Aiming to develop the sensing performance of indirect competitive inhibition immunoassay, secondary immunoreaction was carried out. In this step, after primary immunoreaction, a standard concentration of secondary Ab (Ab_2) or Ab_2-AuNP (40 nm) conjugate solution was injected. The Ab_2 or Ab_2-AuNP conjugate will binds with the primary Ab (Ab_1) onto the sensor surface. I confirmed the reproducibility by using 3 different sensor chip (n=3) and the plots were constructed with the average data.

4.4. Results and discussion

4.4.1 Clenbuterol detection by using secondary immunoreaction

The proposed secondary immunoreaction in indirect competitive inhibition immunoassay for the detection of clenbuterol was recorded and presented in Fig. 4.2. Fig 4.2(a) and (b) represents the sonsogram for the low and high affinity sensor

surface, respectively. As seen from the sensogram, the running solution (PBS+10% ethanol) was flowed onto the sensor surface. After achieved a stable base line, the premixed solution without clenbuterol was injected at 160 s. The SPR response was initially decreased due to the difference of dielectric constant of running solution and the premixed solution. After 2 min injection of premixed solution with a flow rate 100 μL min^{-1} (loop volume 200 μL), the SPR response was increased. The same phenomena were observed from the both sansograms. Furthermore, the SPR response indicated the slow primary immunoreaction. It was assumed that the low concentration of primary Ab and short incubation time are possible reasons for the slow binding.

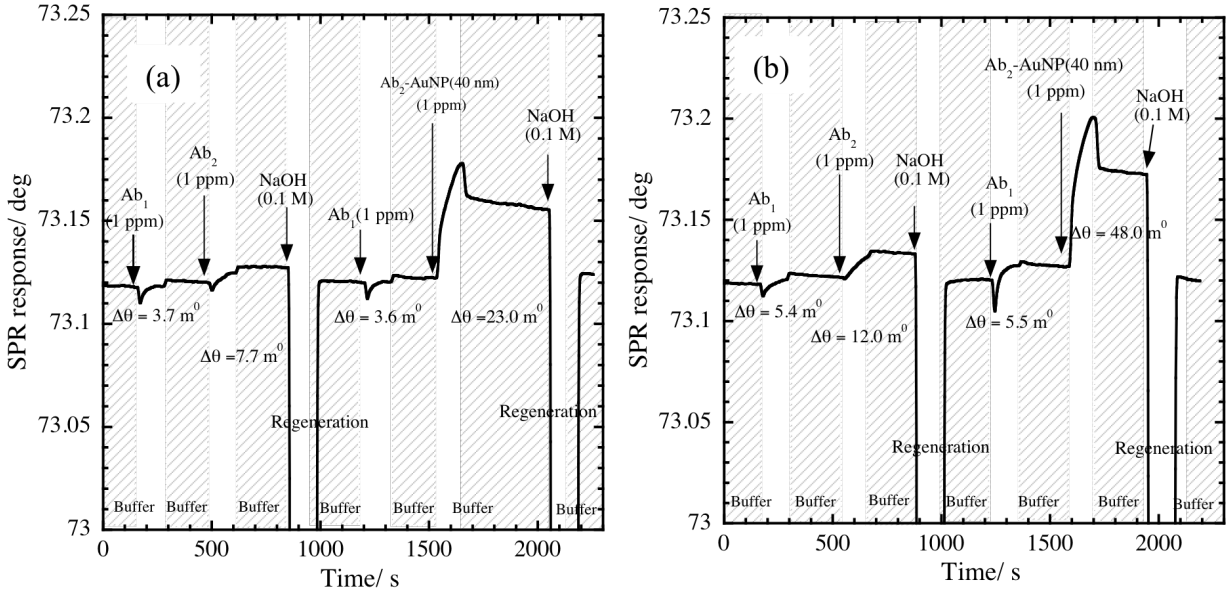

Fig.4.2. Sensogram showing affinity binding of Ab_1 and subsequent binding of Ab_2 and Ab_2-AuNP (40 nm) onto sensor surface; (a) low affinity sensor surface, (b) high affinity sensor surface.

The SPR angle shift (Δθ) was evaluated from the difference of signal change before and after the injection of premixed solution. The changes in angle shifts for primary immunoreaction were calculated to 3.7 mdeg and 5.4 mdeg for the low affinity and the high affinity sensor surface (Fig. 4.2 (a) and (b)), respectively. The corresponding surface concentrations of primary Ab were estimated to 8.2×10^{-14} mol cm^{-2} and 11.6×10^{-14} mol cm^{-2}, respectively. This result indicated that high affinity sensor surface could bind with more number of primary Ab, although the concentration of primary Ab was the same in the premixed solution.

In order to compare the affinity binding of secondary Ab onto primary Ab, Ab_2 was diluted with PBS+10% ethanol and adjusted its concentration to 1- ppm. After the primary immunoreaction the sensor surface was washed with the running solution (PBS+10%) for 200 s. Subsequently, Ab_2 was injected at 500 s and flowed over the sensor surface with already captured primary Ab for 120 min with the same flow rate as was for primary immunoreaction. As the immuno reaction goes on, the SPR response was increased and a stable line was observed at 620 s in the sensogram (Fig 4.2.). The SPR angle shift (Δθ) of the high affinity sensor surface (12.8 mdeg) was higher than that of the low affinity sensor surface (7.7 mdeg). Therefore, it was concluded that the secondary immunoreactions improved the SPR signal by 2-times compared to the primary immunoraection for the both sensor surfaces.

After the secondary immunoreaction, the sensor surface was regenerated by using 0.1 M NaOH for 2 min. This regeneration solution could remove all the primary Ab-Ab_2 pairs from the sensor surface and the SPR response returned to the base line (Fig.4.2). This result indicated that the sensor surface is stable. Subsequently, different concentrations of clenbuterol containing premixed solution were injected.

From the sensogram, it can be seen that one detection cycle takes only 360 s (including the regeneration step).

Aiming to maximize the enhancement of SPR response for the detection of clenbuterol, Ab_2-AuNP conjugate with diameter 40 nm was used. The 40-nm size of AuNPs was chosen because it provides the highest SPR signal amplification [41]. It was already demonstrated that the use of Ab_2-AuNP conjugate can amplify the SPR signal by (1) changing the refractive index at the metal-dielectric interface, (2) the electromagnetic coupling between localized surface plasmon resonance (LSPR) of nanoparticle and propagating plasmon field of the sensor surface [42]. In our system, it is difficult to measure the coupling effect; therefore, the signal enhancement was a result for the dielectric constant change. The enhanced secondary immunoreactions were represented in Fig.4.2. As shown in Fig. 4.2 (a) and (b), the SPR signal was significantly improved and the calculated SPR angle shifts were 24.4 mdeg and 55.5 mdeg for the low affinity and high affinity sensor surface, respectively. This result indicated that the high affinity sensor surface amplify SPR signal by 2.1-fold compared to the low affinity sensor surface. In comparison with the primary immunoreaction, the enhancement factor was 5.8 and 8.9 for the low affinity and high affinity sensor surface, respectively.

To evaluate the limit of detection (LOD) of the detection process, calibration plots were constructed as a function of analyte concentration. Fig. 4.3(a) and (b) shows the calibration plot for the low affinity and the high affinity sensor surface. It should be noted that each figure compares calibration plot for different immunoreaction. A similar decreasing trend with the increase of clenbuterol concentration in premixed solution and the corresponding SPR signal for primary and secondary immunoreaction were observed in the both Fig.4.3 (a) and (b). At the

sensor interface, the primary Ab in premixed solution competes with the clenbuterol in solution and immobilized clenbuterol on the sensor surface. Therefore, with the increase of clenbuterol concentration in premixed solution, the surface concentration of primary Ab was decreased due to the inhibition effect.

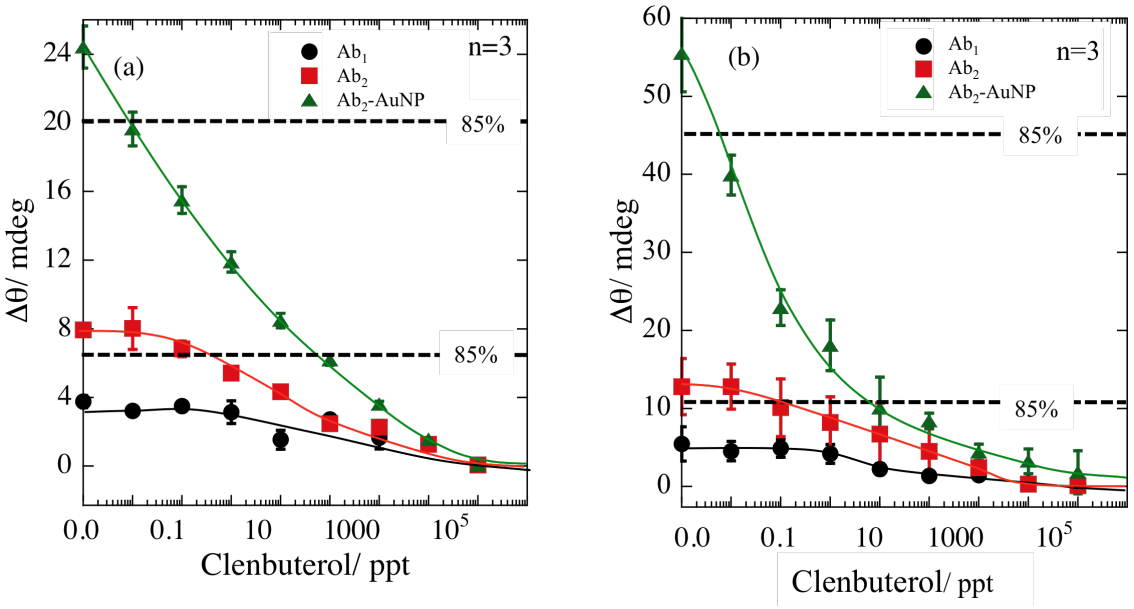

Fig. 4.3. Comparison of calibration plots obtained from primary and secondary immunoreaction. (a) a low affinity and (b) a high affinity sensor surface.

The angle shift for each detection cycle for secondary immunoreaction (unlabeled) was plotted against the surface concentration of primary Ab, as shown in Fig 4.4. The obtained slopes from the linear lines are 1.0×10^{-14} mdeg/ mol cm^{-2} and 1.3×10^{-14} mdeg/ mol cm^{-2} for low affinity and high affinity sensor surface, respectively. By comparing the slope value, high affinity sensor surface produced 1.3 times higher sensitivity than low affinity sensor surface.

The lowest and highest limit of detection was considered at 85% and 15% of inhibition from Fig.4.3, respectively [10,39] and summarized in Table.4.1. The estimated results shows that the high sensitivity with a magnitude of 7 ppq was obtained by using AuNP enhanced secondary immunoreaction for high affinity sensor

surface. It should be noted that the sensitivity of the Ab_2-AuNP was significantly better comparing to the unlabeled Ab_2. Therefore, it was concluded that the high affinity sensor surface is better than the low affinity sensor surface for the secondary immunoreaction. Compared to the recent reports represented in Table 4.2, this study shows the highest sensitivity for the detection of clenbuterol using indirect competitive inhibition immunoassay by SPR biosensor.

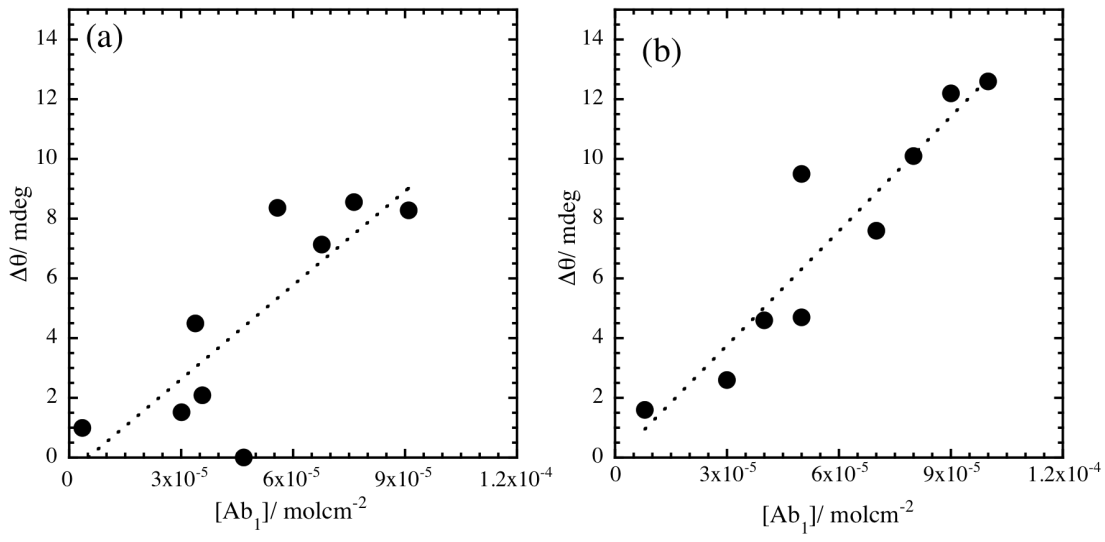

Fig. 4.4. Relationship between SPR responses for secondary immunoreaction as a function of amount of primary antibody onto sensor surface. (a) a low affinity sensor surface; (b) a high affinity sensor surface .

Table. 4.1: The lowest and highest detection limit of the secondary immunoassay.

Conjugate	Low affinity sensor surface		High affinity sensor surface	
	Low LOD	High LOD	Low LOD	High LOD
Secondary Ab	200 ppq	1 ppb	150 ppq	1.2 ppb
Secondary Ab-Au(40 nm)	10 ppq	1.1 ppb	7 ppq	0.4 ppb

Table. 4.2: Comparison of features for the detection of clenbuterol using indirect competitive inhibition immunoassay with others reports.

Immunoreaction	Bioprobes	Ab concentration	Sensitivity	Detectable range	Ref.
Primary	BSA-Clb	20 ppm	2 ppb	2-20 ppb	[37]
Primary	BSA-Clb	30 ppm (poly)	4.5 ppm	6.25-50 ppm	[42]
Primary	BSA-Clb	25 ppm (poly)	6.32 ppm	6.25-50 ppm	[38]
Primary	Clb	1 ppm (mAb)	3 ppt	3 ppt-100 ppb	[39]
Secondary (unlabeled)	Clb	1 ppm (poly)	10 ppq	10 ppq-1.2 ppb	This study
Secondary (labeled)	Clb	1 ppm (poly)	7 ppq	7 ppq-1.1 ppb	This study

4.4.2 Evaluation of affinity constant

While there was no previous report on the affinity constant determination for secondary immunoreaction in indirect competitive inhibition immunoassay, the well-established Langmuir isotherm is modified. In secondary immunoreaction, the formation of Ab_1-Ab_2 complex onto the sensor surface followed by two steps: (1) unreacted antibody in premixed solution reacts with the clenbuterol immobilized on the sensor surface through primary immureaction, and (2) injected Ab_2 binds with the reacted Ab_1 onto sensor surface by secondary immunoreaction. The secondary immunoreaction can be expressed as follows;

$$Ab_2 + Ab_{1,\,ss} \rightleftharpoons Ab_2\text{-}Ab_{1,ss} \qquad (1)$$

Here K_3 is the affinity constant for secondary immunoreaction, can be represent as:

$$K_3 = \frac{[Ab_2 - Ab_{1,ss}]}{[Ab_2][Ab_{1,ss}]} \quad (2)$$

where [Ab_2] is the molar concentration of Ab_2, expressed in mol L^{-1}. In contrast, $Ab_{1,ss}$ represents the amount of primary Ab on the sensor surface after primary immunoreaction, can be calculate from the SPR angle shift using the relationship, 1 mdeg = 1ng cm^{-2}. Assuming that unreacted $Ab_{1,ss}$ = $[Ab_{1,ss}]_0$ - $[Ab_2 - Ab_{1,ss}]$, Eq (2) can be written as:

$$K_3 = \frac{[Ab_2 - Ab_{1,ss}]}{[Ab_2]([Ab_{1,ss}]_0 - [Ab_2 - Ab_{1,ss}])} \quad (3)$$

The following equation can be derived by rearranging Eq. (3).

$$\frac{[Ab_2]_0}{[Ab_2 - Ab_{1,ss}]} = \frac{1}{K_3[Ab_{1,ss}]_0} + \frac{[Ab_2]_0}{[Ab_{1,ss}]} \quad (4)$$

In the secondary immunoreaction, standard concentration of primary Ab was premixed with different concentration of clenbuterol and then flowed over sensor surface. After that standard concentration of Ab_2 was injected. As different concentration of clenbuterol will bind with the fixed concentration of Ab_1 in the pre-mix step, consequently, $[Ab_{1,ss}]$ will be changed. When $\frac{[Ab_2]_0}{[Ab_2 - Ab_{1,ss}]}$ is plotted against $\frac{1}{[Ab_{1,ss}]_0}$, a linear relationship can be obtained and the K_3 can be evaluated from the slope. Based on the Eq. (4), the affinity constants for Ab_2 were calculated to 1.3×10^{-8} M^{-1} and 1.8×10^{-8} M^{-1} for the low affinity and the high affinity sensor surface, respectively and presented in Fig.4.5. When Ab_2-AuNP conjugate was used, the affinity constants were estimated to 2.1×10^{-8} M^{-1} and 3.9×10^{-8} M^{-1} for the low affinity and high affinity sensor surfaces, respectively. This result suggested that the higher affinity constant in the secondary immunoraection was obtained for the high affinity sensor surface compared to the low affinity sensor surface. As the sensor

surface is clenbuterol immobilized, it was in laying–down structure onto sensor surface for the low affinity sensor surface [32]. Therefore, it was assumed that the primary Ab was recognized the clenbuterol in a laying-down orientation. The Ab_2 in the secondary immunoreaction recognizes the tail (Fc part) of the primary Ab. Thereby, sufficient binding sites could not provided by the primary Ab onto low affinity sensor surface to the solution phase to interact with the Ab_2. On the other hand, the tail of the primary Ab was pointing away from the sensor surface during primary immunoraection for the high affinity sensor surface, which favored the subsequent secondary immunoreaction.

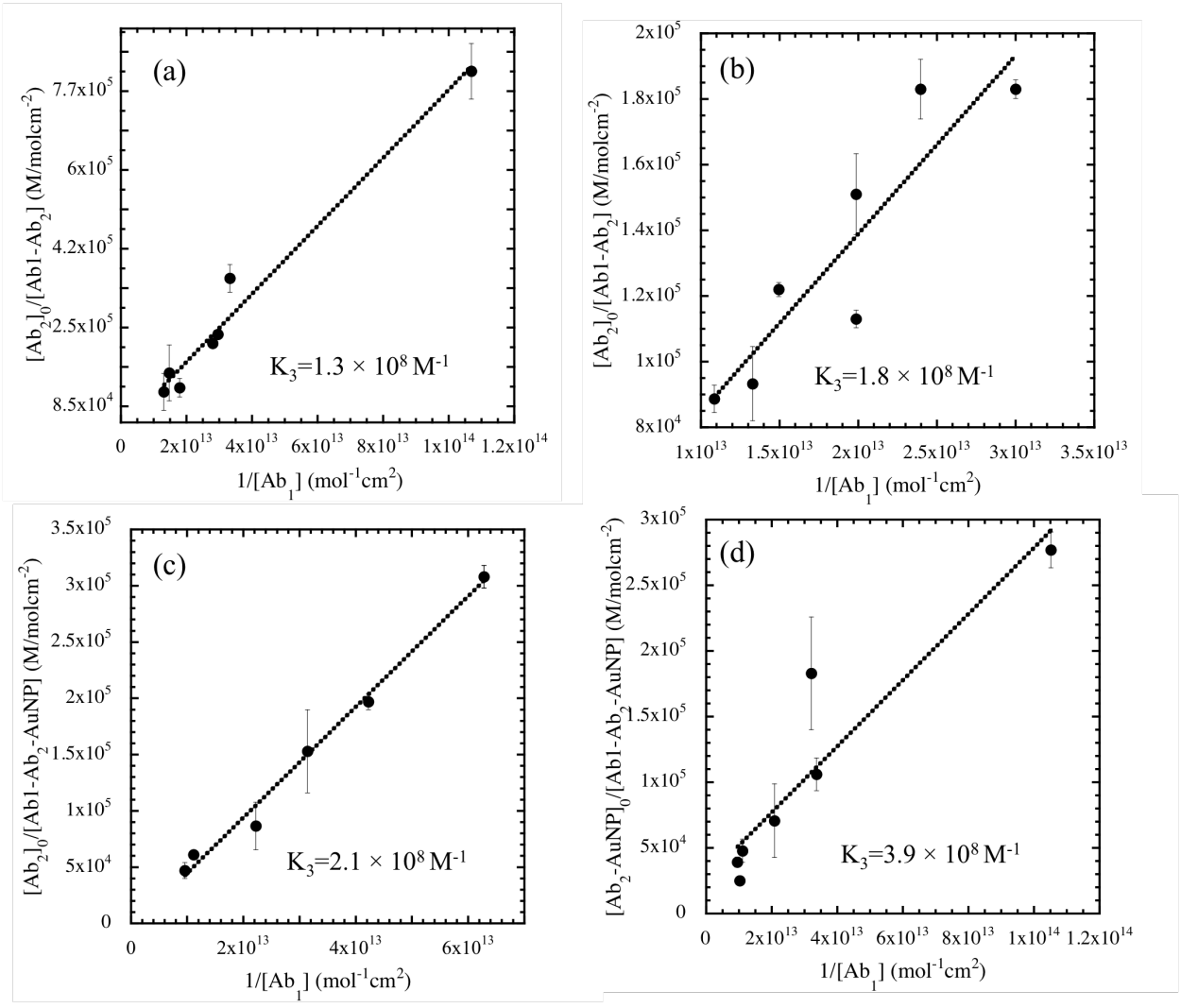

4.5. Affinity constants of secondary immunoreaction calculated using Eq. (4); (a) and (b) for unlabeled Ab_2 and (c) and (d) for labeled Ab_2 of low affinity and high affinity sensor surface, respectively.

Aiming to support this prediction, XPS study of the sensor surface was carried out after immunoreactions and presented in Fig.4.6.

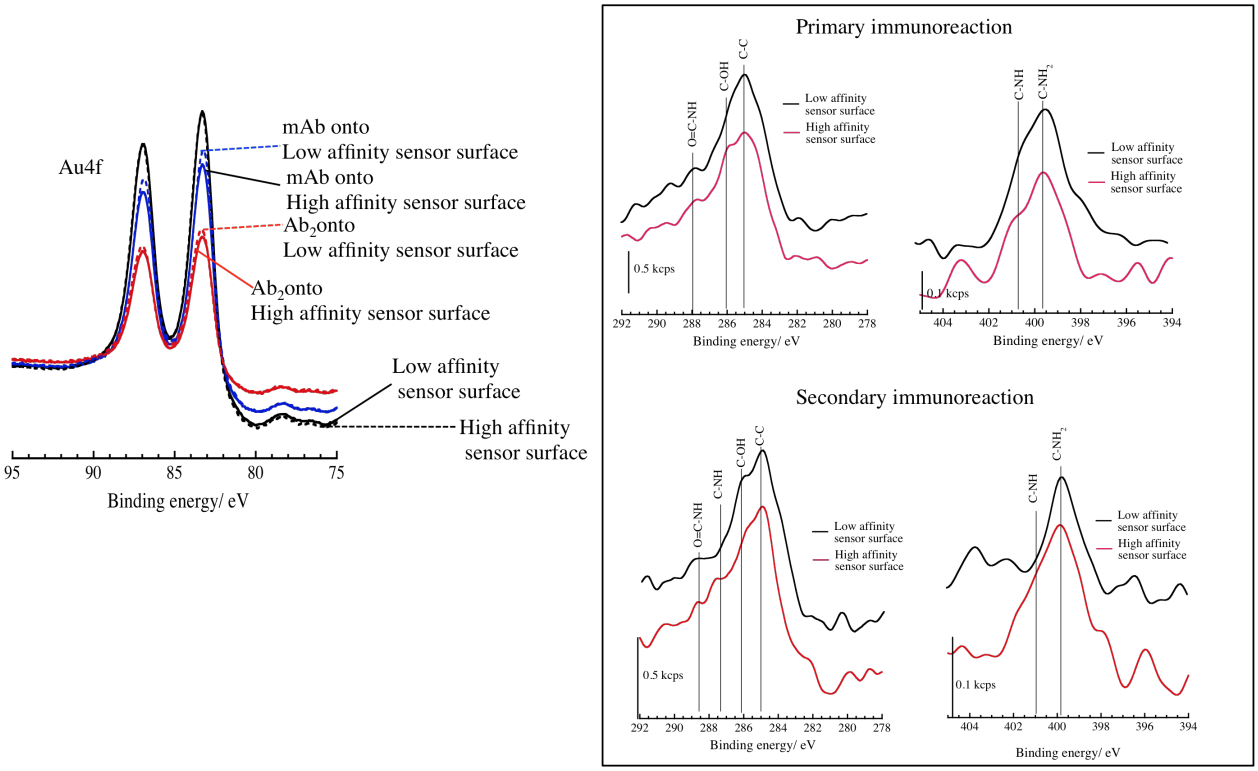

Fig. 4.6. XPS study of sensor surface after primary and secondary immunoreaction.

It was observed that the intensity of Au4f signal was decreased after primary and secondary immunioreaction. This result implies that the sensor surface become thicker after immunoreaction. In comparison of the low and the high affinity sensor surface, the high affinity sensor surface produced a bit of high intensity of Au4f signal in both of primary and secondary immunoreacted sensor surface. The low intensity of Au4f indicated the occupied area of the Au-film. A low intensity for the low affinity

sensor surface suggested that the antibody were in lay-down orientation onto the sensor surface, whereas, a standing up configuration was predicted from high intensity of Au4f signal for high affinity sensor surface. Furthermore, the presence of antibody onto the sensor surface was confirmed by the high-energy shoulder at 288.5 eV for amide (-CONH) and 286.0 eV (-C-OH, for α-amino acid) on the main C1s signal. In addition, the primary amine ($-NH_2$) peak at 399.8 eV also indicated the presence of antibody onto the sensor surface.

In conclusion, the access of binding site of clenbuterol immobilized sensor surface in primary immunoreaction was limited for low affinity sensor surface, which in turn affects the secondary immunoreaction. Consequently, a low signal was achieved for low affinity sensor surface. As a result, the high affinity sensor produced high affinity constant, which results in high sensitivity by shifting the calibration plot towards the lower analyte concentration. Therefore, it was concluded that the high affinity sensor surface produced high sensitivity of the labeled and unlabeled Ab_2 in the secondary immunoreaction.

4.5. Summary

In this study, the secondary immunoreaction was proposed in the indirect competitive inhibition immunoassay for the detection of clenbuterol. It was found that the SPR signal was amplified by 2-times by unlabeled secondary immunoreaction. Aiming to understand the effect of sensor surface structure on the secondary immunoreaction, the low affinity and high affinity sensor surface was used. The obtained results indicated that high affinity sensor surface could capture more antibodies from the solution. Consequently, the high affinity sensor surface produced higher signal compared to the low affinity sensor surface. The estimated LOD was

200 ppq and 150 ppq for the low affinity and the high affinity sensor surface, respectively. When Ab_2-AuNP (40nm) conjugate was used, the SPR signal enhancement factor was 5.8 and 8.9 compared to the primary immunoreaction for the low affinity and high affinity sensor surface, respectively. LOD for low affinity sensor surface was 10 ppq, while a 1.5-times (7 ppq) lower LOD for high affinity sensor surface were achieved in the labeled secondary immunoreaction compared to the unlabeled one. To understand the mechanism of high sensitivity of labeled secondary immunoreaction, the affinity constants of the immunotreactions ware calculated based on the Langmuir isotherm. It was found that the high affinity constants of Ab_2-AuNP conjugate result in the high sensitivity compared to the unlabeled Ab_2.

4.6. References

[1] L. Wu, C. Xu, C. Xia, Y. Duan, C. Xu, H. Zhang, J. Bao, Antib. Immunodiagn. Immunother. 33 (2014) 330–333.

[2] G.G. Gutiérrez-Zúñiga, J.L. Hernández-López, Anal. Chim. Acta. 902 (2016) 97–106.

[3] W. Baeyens, S. Schulman, A. Calokerinos, Y. Zhao, A. Campana, K. Nakashima, D. De Keukeleire, J. Pharmaceut. Biomed. 17 (1998) 941–953.

[4] Z. Fu, H. Liu, H. Ju, Anal. Chem. 78 (2006) 6999–7005.

[5] Z. Yang, Z. Xie, H. Liu, F. Yan, H. Ju, Adv. Funct. Mater. 18 (2008) 3991–3998.

[6] Z. Sheng, H. Han, D. Hu, J. Liang, Q. He, M. Jin, R. Zhou, H. Chen, Chem. Commun. 46 (2009) 2559–2561.

[7] H. Huang, J. Li, J.-J. Zhu, Anal. Methods. 3 (2011) 33–42.

[8] X. Sun, Y. Zhu, X. Wang, Food Control. 28 (2012) 184–191.

[9] J. Zhou, J. Zhuang, M. Miro, Z. Gao, G. Chen, D. Tang, Biosens. Bioelectron. 35 (2012) 394–400.

[10] L. Zeng, Q. Li, D. Tang, G. Chen, M. Wei, Electrochim. Acta. 68 (2012) 158–165.

[11] Y. Zhang, D. Zhou, Expert Rev. Mol. Diagn. 12 (2012) 565–571.

[12] X. Pei, B. Zhang, J. Tang, B. Liu, W. Lai, D. Tang, Anal. Chim. Acta. 758 (2013) 1–18.

[13] J.V. Samsonova, V.A. Safronova, A.P. Osipov, Talanta 132 (2015) 685–689.

[14] E. B. Bahadir, M. K. Sezinturk, TrAC - Trends Anal. Chem. 82 (2016) 286–306.

[15] A. Karczmarczyka, K. Hauptb, K. Fellera, Talanta 166 (2017) 193–197.

[16] E. Helmerhorst, D.J. Chandler, M. Nussio, C.D. Mamotte, Clin. Biochem. Rev. 33 (2012) 161–173.

[17] J. Homola, Chem. Rev. 108 (2008) 462–493.

[18] D.R. Shankaran, K. Matsumoto, K. Toko, N. Miura, Sens. Actuators B Chem. 114 (2006) 71–79.

[19] E.B. Bahadir, M.K. Sezginturk, Anal. Biochem. 478 (2015) 107–120.

[20] J. Homola, S. Yee, G. Gauglitz, Sensors Actuators, B Chem. 54 (1999) 3–15.

[21] M.C. Estevez, M. Alvarez, L.M. Lechuga, Laser Photon. Rev. 6 (2012) 463–487.

[22] D.R. Shankaran, K.V. Gobi, N. Muira, Sens. Actuators B 121 (2007) 158–177.

[23] D. Habauzit, J. Armengaud, B. Roig, J. Chopineau, Anal. Bioanal. Chem. 390 (3) (2008) 873–883.

[24] J. Shen, Y. Li, H. Gu, F. Xia, X. Zuo, Chem. Rev. 114 (2014) 7631–7677.

[25] J. Mitchell, Sensors. 10 (2010) 7323–7346.

[26] S. J. Kim, V. Gobi, H, Tanaka, Y. Shoyama, N. Miura, Sens. Actuators B 130 (2008) 281–289.

[27] T. Kawaguchi, D. R. Shankaran, S. J. Kim, V. Gobi, K. Matsumoto, K. Toko, N. Miura, Talanta 72 (2007) 554–560.

[28] D. A. Taylor, J. Ladd, S. Etheridge, J. Deeds, S. Hall, S. Jiang, Sens. Actuators B 130 (2008) 120–128.

[29] J. Wang, A. Munir, S. H. Zhou, Talanta 79 (2009) 72–76.

[30] M.C. Estevez, J. Belenguer, S. Gomez-Montes, J. Miralles, A. M. Escuela, A. Montoya, L. M. Lechuga Analyst, 137 (2012) 5659–5665.

[31] Suherman, K. Morita, T. Kawaguchi, Biosens. Bioelectron. 67 (2015) 356–363.

[32] Suherman, K. Morita, T. Kawaguchi. Appl. Surf. Sci. 332 (2015) 229–236.

[33] Suherman, K. Morita, T. Kawaguchi, Sens. Actuators B 210 (2015) 768–775.

[34] N. Granqvist, A, H. Anning, L. Eng, J. Tuppurainen, T. Viitala, Sensors 13 (2013) 15348–15363.

[35] D. C. Kabiraz, K. Morita, T. Kawaguchi, Talanta 172 (2017) 1–7.

[36] L. Zhou, A, Zhu, X. Lou, D. Song, R. Yang, H. Shi, F. Long, Anal. Chim. Acta. 905 (2016) 140–148.

[37] Y. Iludag, I. E. Tothill, Anal. Chem. 84 (2012) 5898−5904.

[38] T. Springer, M. L. Ermini, B. Spackova, J. Jablonku, J. Homola, Anal. Chem. 86 (2014) 10350−10356.

[37] Y. Li, X. Mao, M. Zhao, P. Qi, J. Zhong, Eur. Food Res. Technol. 239 (2014) 195–201.

[38] M. Yao, Y. Wu, X. Fang, Y. Yang, H. Liu, Anal. Biochem. 475 (2015) 40–43.

[39] Suherman, K. Morita, T. Kawaguchi, Applied surface science, 332 (2015) 229–236.

[40] R. Karlsson, A. Michaelsson, L. MAttsson, J. Immunol. Methods. 145 (1991) 229–240.

[41] S. Zeng, D. Baillargeat, H. Ho-Pui, Y. Ken-Tye, Chem. Soc. Rev. 43 (2014) 3426–3452.

[42] Y. Wu, M. Yao, X. Fang, Y. Yang, X. Cheng, Appl. Biochem. Biotechnol. 117 (2015) 1327–1337.

Chapter 5

A Sensitive Detection of Clenbuterol in Urine Sample by Using Surface Plasmon Resonance Biosensor

5.1. Introduction

β-agonists are used as medicine for pulmonary diseases and asthma [1]. These drugs are also used as growth-promoting agents to stimulate the growth of muscular tissues, when they administrated in amounts above the therapeutic level. Among other family members of β-agonists, clenbuterol has been reported as the most often illegally used by athletes and meat producer [2,3]. The residue of clenbuterol remained in meat tissue. After accumulation in body it may causes cardiac disease, nausea, fever and specific cell deaths [1,5]. At present, the use of clenbuterol in animal feed is prohibited in the United States, China and most of EU countries. However, the misuse of clenbuterol in the animal farm and in professional athletes has been often reported [3]. In addition, food poisoning in terms of clenbuterol is reported in many countries such as Mexico, Portugal, China, France, Spain, Italy and the United states [6]. The limit of detection of clenbuterol residue set by the EU is 0.1 μg/kg for muscle, 0.5 μg/kg for liver and kidney, and 0.05 μg/kg for bovine milk [7]. To date, gas chromatography/mass spectrometry (GC/MS) and liquid chromatography with mass spectrometry (LC-MS), enzyme linked emmunosorbent-based assay (ELISA) and immmunochromatographic immunoassay are the main analytical method for monitoring clenbuterol [8-10]. Although those techniques can meet the detection limit set by EU, however those methods are expensive, long detection

period, and operators are required to be well trained. Therefore, the existing methods are difficult to conduct in rapid and on-site monitoring.

In order to monitoring the illegal use of clenbuterol in animal farming, urine is popular specimen. Because sample can collect in a noninvasive way from live animal in the farm. After the oral administration of clenbuterol, the excretion rate in urine is 22-49% [11]. As clenbuterol is a small molecule, indirect competitive inhibition immunoassay is useful [12-18]. Surface plasmon resonance (SPR) biosensors are a promising alternative to the present analytical methods combined with the immunoassay technique [19-23]. However, the challenging aspect of the SPR biosensor for real sample analysis is the non-specific adsorption. This problem is caused by the presence of non-target entities in real sample. For example, urine sample contains a lot of large and small molecules such as proteins, fats, vitamins, hormones, metabolites, minerals etc [24]. Those entities can block the reaction sites of receptor and biorecognition molecules in immunoassay. Aiming to eliminate inhibitors from urine sample, Johasson et al. [24] employed molecular weight cut-off filtration process. However, the SPR signal loss was approximately 65% due to non-specific adsorption for urine sample compared to the ideal buffer solution. Therefore, an efficient sample pretreatment is needed.

In this study, I proposed a simple and organic solvent free pretreatment method using monolithic silica spin column that has recently become commercially available [25-27]. Clenbuterol spiked with filtered urine sample. The primary and secondary immunoreaction is employed for the detection of clenbuterol. In the case of secondary immunoreaction, secondary antibody labeled with 40 nm AuNP (Ab_2-AuNP) is used. Furthermore, pH effect on secondary immunoassay is also investigated.

5.2 Fabrication of immunosurface

In the previous chapter, it was found that sensor surface prepared with 5 mM DSP in methanol shows the best SPR signal and a low limit of detection for secondary immunoreaction. Therefore, sensor surface was prepared by using 5 mM DSP in methanolic solution. The sensor surface fabrication process carried out into three steps. First, dithiobis (succinimidyl) propeonate (5 mM) was flowed over the Au surface and Au surface was covered by *N*-Hyderoxysuccinimidyl terminated propenthiol through self-assembly process. Consequently, clenbuterol (1000 ppm) in PBS solution is allowed to flow and clenbuterol attached onto the sensor surface through amide coupling reaction. Finally, ethanolamine (1000 ppm) in PBS solution was injected in order to block unreacted *N*-Hydroxysuccinimide group. Therefore, the sensor surface was composed of clenbuterol-propenthiol and ethanolamine-propenthiol. The maximum SPR angle shift obtained for covalent immobilization of clenbuterol on the succinimidyl terminated propenthiol monolayer was 21.8 (±2.3) mdeg and it corresponds to 7.87 (±0.83)× 10^{-11} mol cm^{-2}. Similarly, 3.80 (±0.60)× 10^{-11} mol cm^{-2} and 1.59 (±0.034) × 10^{-10} mol cm^{-2} for clenbuterol and ethanolamine, respectively. All the solutions were injected at a flow rate 5 μL min^{-1} and the loop volume 200 μL.

5.3 Urine sample pretreatment

Urine sample of cow was collected from the Field Science Center for Northern Biosphere, Hokkaido University. 10 mL of collected urine was taken into 15 mL centrifuge tube. Then, 10 μg of clenbuterol was added to 5 mL urine sample and the

concentration of urine sample was 2 ppm. Another 5 mL Urine was used as blank (for control experiment).

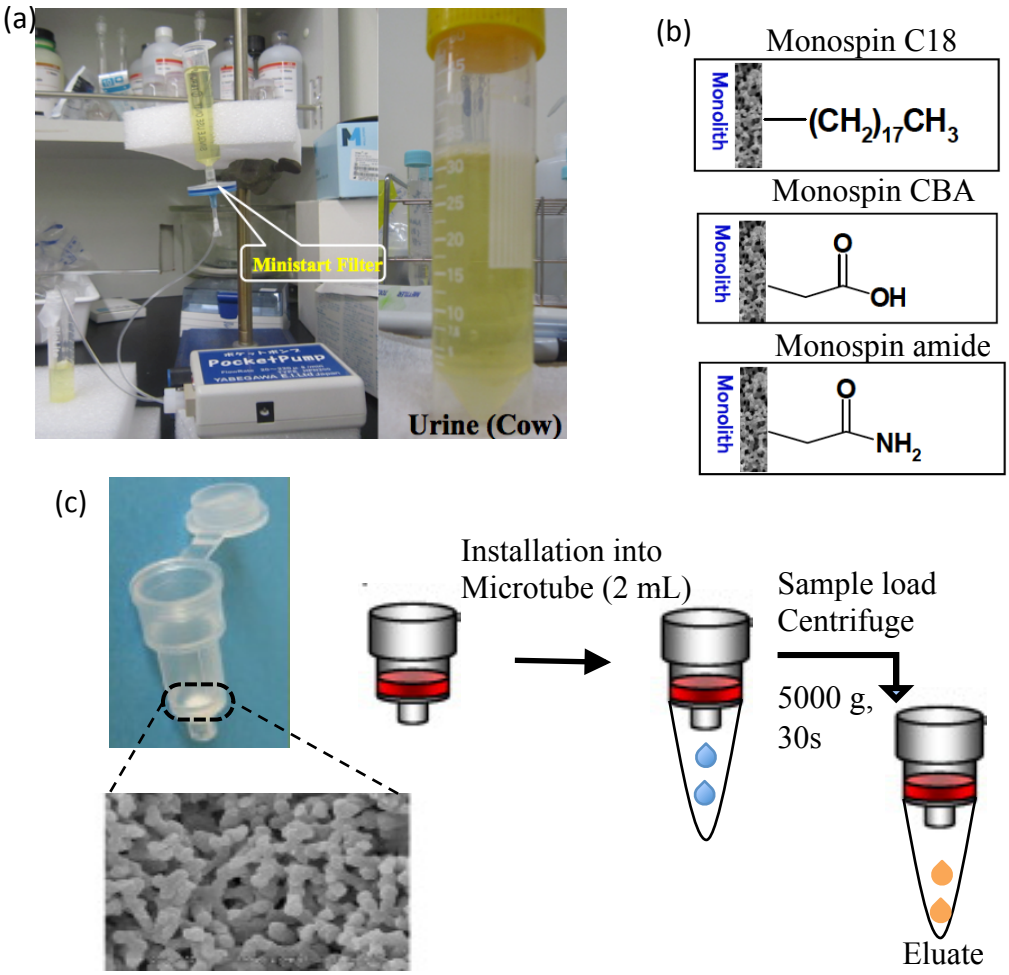

Fig. 5.1. Summery of filtration procedure (a) physical filtration using minisart syringe filter, (b) Chemical structure of monospin filter (c) Chemical filtration by using minospin filter for clenbuterol spiked urine sample.

In the pretreatment process, physical and chemical filtration was carried out. For physical filtration, Minisart syringe filter (pore size 0.2 μm) along with a pocket pump (Yabegawa Co. Lid, Japan) was used. The filtration process is illustrated in Fig. 5.1 (a). For the chemical filtration, three different functional groups terminated Monospin C18, Monospin amide and monospin CBA (Fig. 5.1 (b) were used. The

filtration process is presented in Fig.5.1 (c). After that, the pH of urine samples (both spiked and blank sample) was adjusted to 7.4 by 2-fold dilution using PBS solution. Finally, 0.01 ppt to 100 ppb clenbuterol (Clb) in urine sample were prepared through a serial dilution using blank sample as a solvent. Fig. 5.2 shows the sample preparation flow chart.

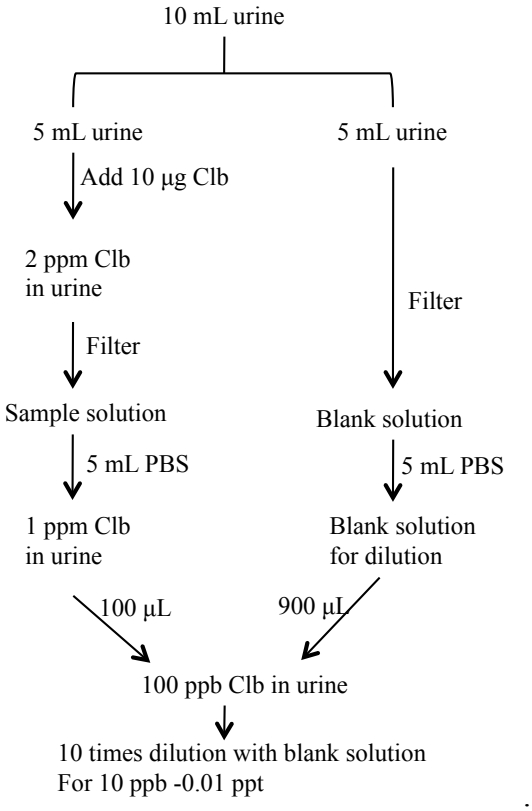

Fig. 5.2. Clenbuterol spiked urine sample preparation process.

5.4 Immunoassay format

Aiming to monitor clenbuterol in the complex urine solution, the indirect competitive inhibition immunoassay was used. In briefly, primary immunoreaction was carried out by injecting a premixed solution that contains 1 ppm anti-clenbuterol mouse IgG (primary Ab) and a wide range concentration (0.01 ppt – 100 ppb). After

injection the premixed solution, the sensor surface was washed with running buffer (PBS+10% ethanol) solution. Subsequently, 1 ppm of anti-mouse polyclonal Ab labeled with AuNP (Ab_2-AuNP conjugate, 40 nm) solution was injected. The Ab_2-AuNP conjugate binds with the primary Ab onto the sensor surface.

5.5 Results and Discussion

5.5.1 Comparison of filtration process

In order to compare the filtration process, matrix effect in the immunoassay was examined. Control experiment using primary immunoreaction was carried out and the obtained results were compared with the results of buffer solution. A fixed concentration of antibody (2 ppm) was premixed (1+1) with the blank urine sample prior to injection. The sensogram is presented in the Fig. 5.3.

As seen from Fig. 5.3(a), once a stable base line was achieved, the premixed solution was injected onto the sensor surface with a flow rate of 100 μL/ min. The SPR signal is initially decreased due to difference of dielectric constant of running buffer and the premixed solution. When reaction is goes on, it was observed that the antibody binding to the clenbuterol onto sensor surface is slow downed for urine solution compared to the buffer solution. This phenomenon can be explained as matrix components can adhere to the sensor surface clenbuterol or to the antibody in premixed solution. Another possible reason is the diffusion of antibody to the sensor surface might be hindered by the matrix components. After 2 min injection, the SPR signal reached at a higher level compared to the base line in running buffer solution. Then the running buffer solution was started to flow onto the sensor surface and the washing process was carried until obtaining a stable signal. A significant decreasing trend of SPR signal was observed for urine sample filtered by using minisart represented in Fig.5.3 (a). While the SPR signal was stabled in PBS buffer, as there

was no inhibitor and specific interaction occurred there. Therefore, decreasing trend in the washing step was caused due to desorption of some matrix components from sensor surface those are loosely attached.

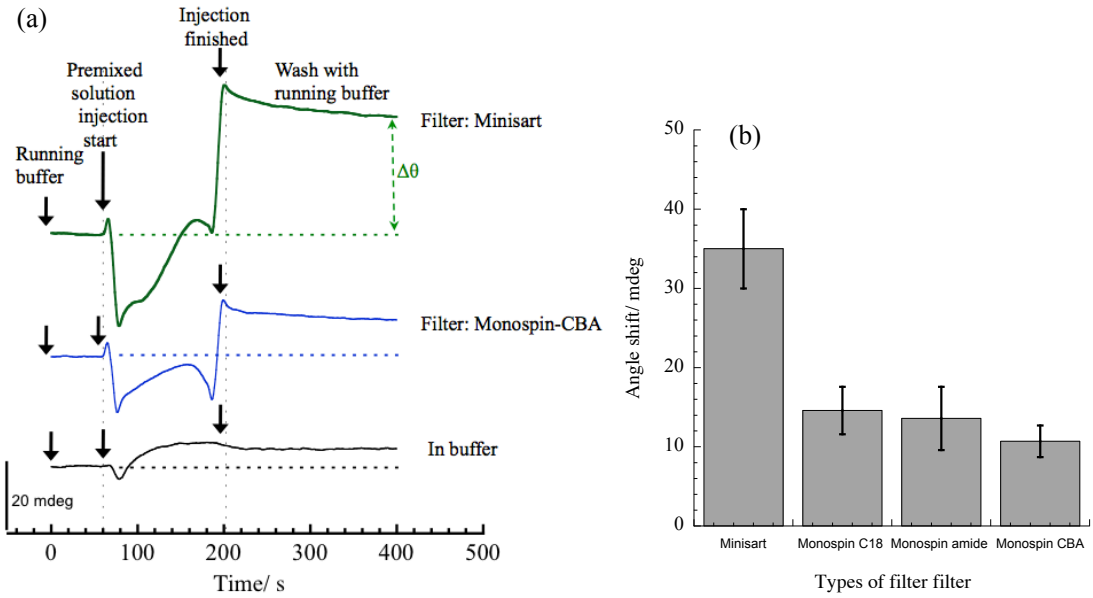

Fig.5.3. Comparison of SPR signal change; (a) Sensogram for premixed (urine + Clenbuterol Ab) solution injection, (b) Comparison of signal change for different filter.

The change in SPR signal was estimated from the signal before and after sample injection. Results are shown in Fig. 5.3 (b). A large SPR angle shift with a magnitude of 35 mdeg was estimated for minisart filter. The amount of proteins (antibody or matrix components) can be calculated from the angle shift. This result implies that 35.0 ng cm^{-2} (1 mdeg = 1 ng cm^{-2} [29]) protein including antibodies and other large molecules in urine sample was adsorbed onto the sensor surface. In contrast, the amount of bonded antibody onto sensor surface was 6.1 ng cm^{-2} (6.1 mdeg) in buffer solution. This result indicated that approximately 6-times higher SPR signal than that of in PBS buffer solution was caused by the non-specific adsorption.

The non-specific adsorption usually caused by larger components such as proteins and fat aggregates, which bind to the sensor surface increasing the total response by adding to the specific antibody response.

Aiming to evaluate functional group effect, there different types functional group equipped with monospin filter were compared. Monospin C18, monospin amide and monospin CBA are bonded with octadecyl, amide and carboxyl acid, respectively. It was found that the SPR angle shift was decreased to 10.1 mdeg (Fig.5.3 (b)), when large molecules were removed from the sample through monospin filters. Therefore, filtration process using monospin filter was more efficient compared to the minisart filter. It was assumed that during the urine sample filtration, a hydrophobic-hydrophobic interaction might occur between protein molecules of urine sample and octedecyl of monospin C18. On the other hand, amide and carboxyl functional group of monospin filter can capture small matrix components through a hydrophilic–hydrophobic interaction. As the hydrophobic part is the central part of the amino acids, therefore it can be predicted that the hydrophilic charge groups are located onto the surface side where as hydrophobic residues are on the interior side of protein molecule. As a result, hydrophilic-hydrophilic interaction dominated over the hydrophobic-hydrophobic interaction. However, monospin filter couldn't completely remove the non-specific adsorption. Between the hydrophilic fictional groups, monospin CBA shows less matrix effect compared to the monospin amide. Therefore, monospin CBA was used for the following experiment.

5.5.2 pH effect on secondary immunoassay

pH of cow urine is highly dependent on physical condition such as pregnancy, illness and feed. For example, pH may fall less than 5 when anionic salt are being

feed too heavily. Due to lack of enough minerals in feed, urine pH can be above 7. It should be noted that the ideal value of pH of cow urine is 6-7 [30]. Furthermore, the mean urine pH of beef cow is 7.27 [30]. In this study, urine samples were collected from 5 different dairy cows and pH was measured. The average pH was 8.15 (±0.10), which is consistent with the reported value of 8.10 for dairy cow [30]. Therefore, pH range was set up 3.5 to 8.5 with an interval of 1 in this experiment.

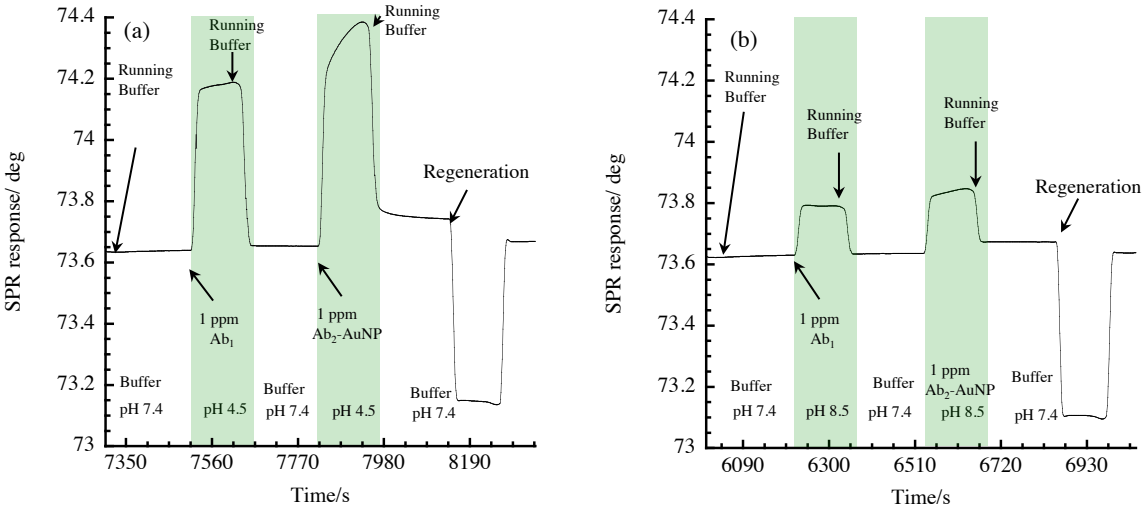

Fig.5.4. SPR response of primary and secondary immunoreactions (a) pH 4.5 and (b) pH 8.5.

To understand the effect of pH on SPR response, pH-dependent buffer solution was prepared. Sodium dihydrogen phosphate (NaH_2PO_4) and disodium hydrogen phosphate (Na_2HPO_4) was added to the phosphate buffer saline (PBS) solution (pH 7.4) aiming to decrease or increase the pH, respectively. The flow rate (100 µL/min) of running solution onto the sensor surface and experimental temperature (25°C) were kept constant. Initially the sensor surface was equilibrated with running buffer (PBS+10% ethanol, pH 7.4) and the baseline was established. Fig.5.4 shows the effect of pH on SPR response by switching the pH 7.4 to pH 4.5 and 8.5. It was observed from Fig. 5.4 (a) that the SPR signal on injection of primary

antibody (Ab, 1 ppm) showed angle shift with a magnitude of 12.2 (±1.8) mdeg, where as it was 4.2 (±0.3) mdeg for pH 8.4 (Fig. 1B). Generally, an increase in SPR angle shift reflects the increase the mass density at the sensor surface. The obtained result indicated that approximately 3-times higher amount of primary Ab (4.2 ng cm^{-2} to 12.2 ng cm^{-2}) was adsorbed onto the sensor surface from an acidic solution compared to the pH 8.4. The similar effect was found for secondary immunoreaction. As seen from Fig. 5.5 indicated that at lower pH level the total SPR angle shift (primary immunoreaction + secondary immunoreaction) was increased. Interestingly, the angle shift was dramatically increased when pH down from 5.5. These results clearly demonstrated when antibody (both the primary Ab and Ab_2-AuNP conjugate) mixed with lower pH solution, due to protonation of charge of antibody surface being changed (pI value of IgG is 6.4-7.6). Therefore, the inter antibody-antibody interaction resulting aggregation, consequently mass density increased accordingly.

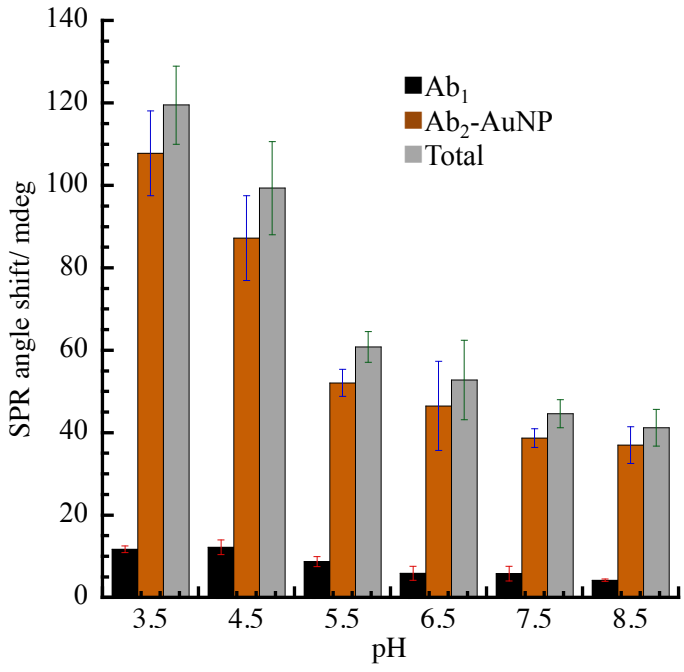

Fig.5.5. SPR angle shift for secondary immunoassay as a function of pH.

5.5.3 Inhibition effect:

Aiming to determine of inhibitors, artificial urine sample was prepared according to Japan Industry standard (JIS T3214). The composition of artificial urine for 100 ml in water is presented in Table 5.1. The pH of the artificial urine was 6.83.

Table 5.1. Composition for artificial urine ((JIS T3214).

Chemicals	Amount/g
Urea	2.5
NaCl	0.9
Sodium hydrogen phosphate	0.25
NH_4Cl	0.3
Potassium dihydrogenphosphate	0.25
Creatinine	0.2
Sodium sulfite	0.3

To compare the SPR response for filtered and unfiltered urine sample, monospin CBA filter was used. The premixed solution was prepared by adding 1 ppm primary Ab into filtered and without filtered of artificial urine sample, respectively. The SPR response was compared upon injection the premixed solution onto sensor surface and presented in the Fig. 5.6. It was found that the filtered sample generated 4.5 (±0.6) mdeg of SPR angle shift, while it was 4.2 (±0.3) mdeg for unfiltered sample. Therefore, no significant difference in angle shift was observed for the both cases. In contrast, approximately 35.0 mdeg SPR angle shift was obtained for real urine sample for physical filtration. Therefore, it was concluded that there was no inhibitor in the artificial urine.

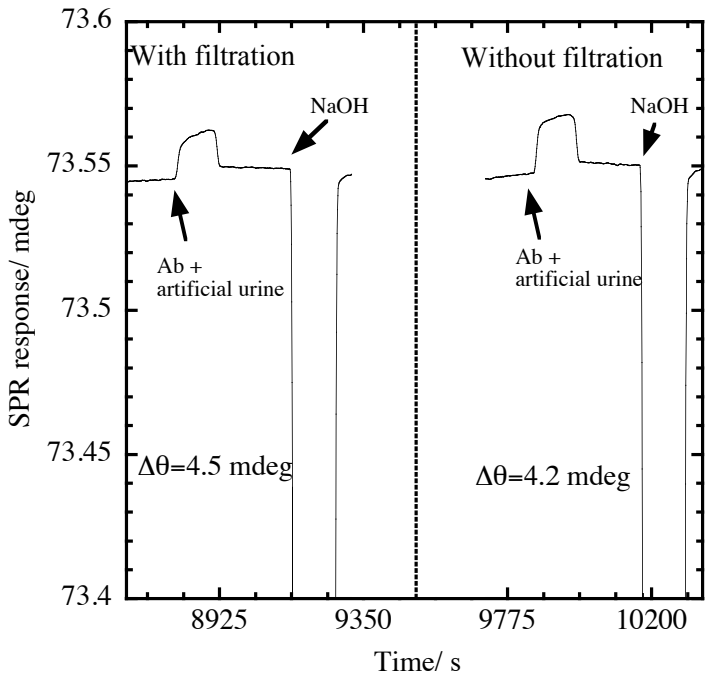

Fig. 5.6. Comparison of SPR response for filtered and without filtered artificial urine sample by using primary immunoreaction.

5.5.4 Clenbuterol detection:

The detection principle was indirect competitive inhibition immunoassay, where antibodies with unoccupied binding sites are quantified through their ability to bind to analyte immobilized onto sensor surface. As the primary Ab could not generate sufficient SPR signal, amplification step using Ab_2-AuNP conjugate was carried out using secondary immunoreaction. Fig. 5.7 shows a representative sensogram of clenbuterol spiked urine sample for the secondary immunoreaction followed by primary immunoreaction. As seen from Fig.5.7, 1 ppm primary Ab (anti-clenbuterol Ab) was premixed with the urine solution and injected at 2900 s. After the primary immunoreaction, 1 ppm Ab_2-AuNP was injected. The SPR signal was increased due to binding of primary Ab onto sensor surface. After 120 s injection of Ab_2-AuNP conjugate, the sensor surface was washed with the running buffer solution. Then the sensor surface was regenerated with 0.1 M NaOH solution. One detection

cycle takes only 1000 sec. It was found that the highest SPR signal with a magnitude of 45 mdeg was obtained.

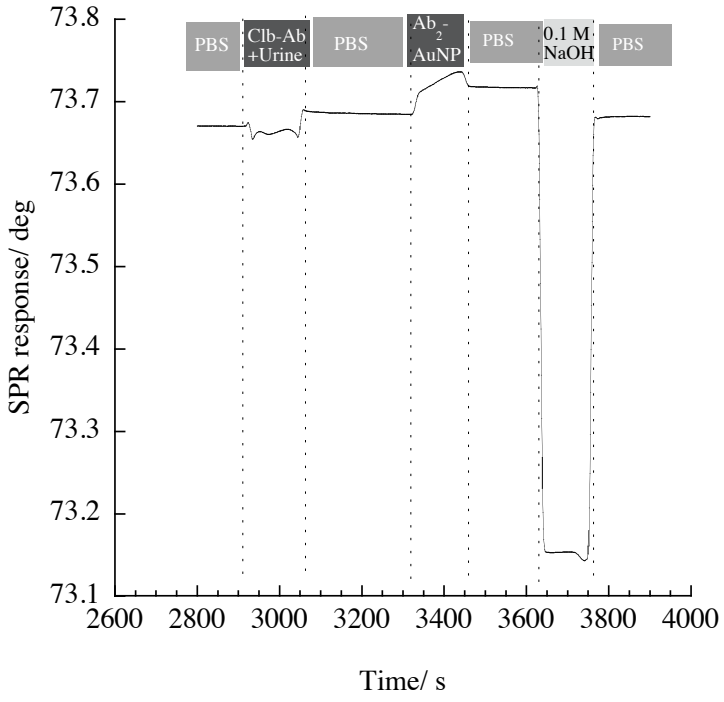

Fig. 5.7. SPR sensogram represents the angle change for primary and secondary ummoreaction. Urine sample was filtered using monospin CBA. The flow rate was 100 μL/min. 0.1 M NaOH was the regeneration solution.

The same sensor surface was used for the premixed solution containing different concentration (0.01 ppt-100 ppb) of clenbuterol spiked urine sample. The estimated angle shifts are used to construct calibration plot and illustrated in Fig.7.8. The limit of detection was estimated to 20 ppq in urine sample using Ab_2-AuNP conjugate, while a 3-times lower LOD (7 ppq) was estimated in the PBS solution. Higher LOD in comparison to the assay established in ideal buffer solution indicated some non-specific adsorption of matrix component in urine solution affect the sensitivity. However, the obtained LOD is one order lower than the maximum allowed level of

clenbuterol set by the EU commission. Therefore, the immunoassay technique could be considered as a fast and sensitive tool for the detection of clenbuterol in the urine sample.

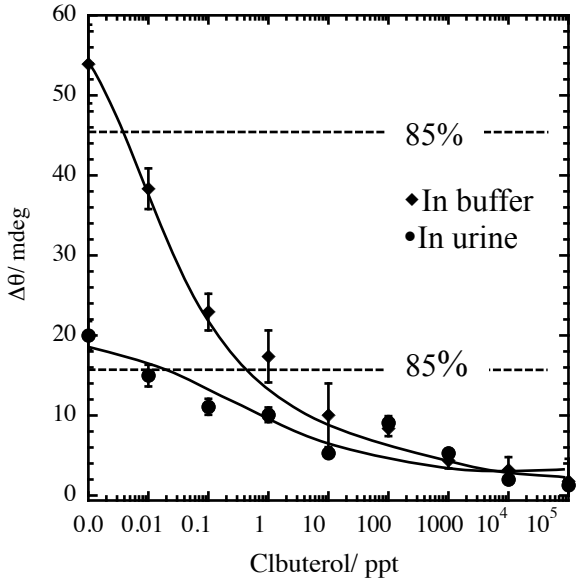

Fig.7.8. Comparison of calibration plot performed in ideal PBS buffer solution and in urine filtered with monospin CBA.

5.6 Summary

In this study, I compared between physical filtration and chemical filtration for urine. The filtered urine sample was spiked with clenbuterol. The clenbuterol spiked urine samples were then tested using developed indirect competitive inhibition immunoassay. It was estimated that a 6-times higher SPR signal was obtained for primary immunoreaction for the physical filtration of urine sample compared to the buffer solution. Therefore, a high non-specific adsorption was found for physical filtration using minisart filter. On the other hand, the obtained results indicated that chemical filtration by using monospin filters were effective. Among the three types of functional group (octadecyl, amide and carboxyl acid) modified monospin filter,

carboxylic acid group modified monospin CBA provided the best result. However, a few amount of non-specific adsorption was observed for monospin filter. The investigation of pH effect implies that lower pH resulted in aggregation of antibody, consequently abrupt angle shift was observed. Furthermore, no inhibitor was found in the artificial urine. Thereby, it was concluded that the proteins in urine sample acted as main inhibitor in SPR immunosensing. Furthermore, a low limit of detection with 20 ppq was achieved by using Ab_2-AuNP. The important aspect of the immunoassay was the urine sample diluted just 2-times. It was suggested that the low limit of detection as well as short detection time would be an alternative to the conventional methods.

5.7 References

[1] P. Taylor, C.T. Elliott, W.J. Mccaughey, H.D. Shortt, Food Addit. Contam. 10 (1993) 231–244.

[2] B. Bo, X. Zhu, P. Miao, D. Pei, B. Jiang, Y. Lou, Y. Shu, G. Li, Talanta 113 (2013) 36–40.

[3] X. Li, M. Zhou, M. Turson, S. Lin, P. Jiang, X. Dong, Analyst 138 (2013) 3066–3076.

[4] C.A. Ricks, R.H. Dalrympale, P.K. Baker, D.L. Ingle, J. Anim. Sci. 59 (1984) 1247–1255.

[5] G. Brambilla, A. Loizzo, L. Fontana, M. Strozzi, A. Guarino, V. Soprano, J. Am. Med. Assoc. 278 (1997) 635–640.

[6] Q. Fu, J. Lianga, C. Lana, K. Zhoua, C. Shia, Y. Tanga, Sens. Actuators B 203 (2014) 683–689.

[7] Council Directive 96/22/ EEC, Off. J. Eur. Union, L 125, 23.5 (1996) 3–9.

[8] X.B. Chen, Y.L. Wu, T. Yang, J. Chromatogr. B Anal. Technol. Biomed. Life Sci. 879 (2011) 799–803.

[9] J. Blanca, P.Muñoz, M.Morgado, N. Méndez, A. Aranda, T. Reuvers, H. Hooghuis, Anal. Chim. Acta 529 (2005) 199–205.

[10] MaxSignal Clenbuterol ELISA Test Kit, Available at: <http://www.biooscientific.com/Hormone-residue-test-kits/MaxSignal-Clenbuterol-ELISA-Test-Kit> (accessed 02.10.2016)

[11] O. Peñuela-Pinto, S. Armenta, F.A. Esteve-Turrillas, M. de la Guardia, Microchem. J. 134 (2017) 62–67.

[12] S. J. Kim, V. Gobi, H, Tanaka, Y. Shoyama, N. Miura, Sens. Actuators B 130 (2008) 281–289.

[13] T. Kawaguchi, D. R. Shankaran, S. J. Kim, V. Gobi, K. Matsumoto, K. Toko, N. Miura, Talanta 72 (2007) 554–560.

[14] D. A. Taylor, J. Ladd, S. Etheridge, J. Deeds, S. Hall, S. Jiang, Sens. Actuators B 130 (2008) 120–128.

[15] J. Wang, A. Munir, S. H. Zhou, Talanta 79 (2009) 72–76.

[16] M.C. Estevez, J. Belenguer, S. Gomez-Montes, J. Miralles, A.M. Escuela, A. Montoya, L.M. Lechuga, Analyst. 137 (2012) 5659–5665.

[17] Suherman, K. Morita, T. Kawaguchi, Biosens. Bioelectron. 67 (2015) 356–363.

[18] Suherman, K. Morita, T. Kawaguchi, Appl. Surf. Sci. 332 (2015) 229–236.

[19] A. Namera, A. Nakamoto, M. Nishida, T. Saito, I. Kishiyama, S. Miyazaki, M. Yahata, M. Yashiki, M. Nagao, M., J. Chromatogr. A, 1208 (2008), 71–75.

[20] E. B. Bahadir, M. K. Sezinturk, TrAC - Trends Anal. Chem. 82 (2016) 286–306.

[21] A. Karczmarczyka, K. Hauptb, K. Fellera, Talanta 166 (2017) 193–197.

[22] E. Helmerhorst, D.J. Chandler, M. Nussio, C.D. Mamotte, Clin. Biochem. Rev. 33 (2012) 161–173.

[23] J. Homola, Chem. Rev. 108 (2008) 462–93.

[24] M.A. Johansson, K.E Hellenas 129 (2004) 438–442.

[25] M. Tsunoda, C. Aoyama, S. Ota, T. Tamura, T. Funatsu, Anal. Methods. 3 (2011) 582–585.

[26] A. Namera, A. Takeuchi, T. Saito, S. Miyazaki, H. Oikawa, T. Saruwatari, M. Nagao, J. Sep. Sci. 35 (2012) 2506–2513.

[27] M. Tsunoda, M. Hirayama, K. Ohno, T. Tsuda, Anal. Methods. 5 (2013) 5161–5164.

[28] D. C. Kabiraz, K. Morita, T. Kawaguchi, Talanta 172 (2017) 1–7.

[29] E. Estenberg, B. Persson, H. Rooks, C. Urbaniczky, J. coll. Int. Sci. 143 (1991) 513–526.

Chapter 6

6.1 Summary and Conclusion

The increasing numbers of potential hazardous materials in the food products call for a rapid and sensitive analytical technique for monitoring real sample. However, a low signal, a low sensitivity and matrix effect are the main impediment for the promising SPR biosensor in practical application. The knowledge about the LOD determining factor, effect of sensor surface structure on the immunoreaction and appropriate matrix management of biological sample has been discussed.

In chapter 3, the anti-clenbuterol mouse IgG (primary Ab) was labeled with Au-nanoparticle (Ab-AuNP conjugate). The SPR immunoassay using Ab-AuNP conjugate produced an extremely low limit of the detection (LOD) with a magnitude of 0.05 ppt (0.05 pg mL^{-1}), which was 40-times lower than that of unlabeled Ab. To identify the key factor in determining the LOD of the indirect competitive inhibition immunoassay, affinity constants of the surface immunoreaction (K_1) and of the premixed solution (αK_2) were evaluated. I found that the dielectric constant change due to AuNP labeling of Ab did not affect on the affinity constants, because all the amplification magnitude terms canceled out from the equation. The simulation plot of LOD with respect to K_1 and αK_2 showed that a K_1 one order of magnitude lower than αK_2 produced a ppt-level LOD. Because the affinity constants are determined by the molar concentrations of reactant and product, the molar mass of the Ab or Ab-AuNP conjugate in the sample solution containing 1 ppm (1 μg mL^{-1}) highly affects the constants. Consequently, molar mass adjustment can be used to adjust the LOD in an indirect competitive inhibition immunoassay as needed for a practical application.

In chapter 4, aiming to achieve a high SPR signal and a high sensitivity, secondary immunoreaction by using anti-mouse IgG (Ab_2) was employed. The SPR

response was enhanced by 2-fold for the secondary immunoreaction (unlabeled) compared to the primary immunoreaction. Furthermore, the affinity constant of the sensor surface influenced the secondary immunoreaction. The high affinity constant sensor surface produced a high SPR signal and a high sensitivity in the secondary immunoreaction. The highest SPR response was achieved with a magnitude of 55.5 mdeg, which was 2-times higher than that of the low affinity sensor surface (24 mdeg) for Ab_2-AuNP conjugate. In comparison between the Ab_2-AuNP and Ab_2, the Ab_2 (unlabeled secondary Ab) produced a limit of detection (LOD) of 150 ppq (150 fg mL^{-1}), while it was improved by more than one order of magnitude to 7 ppq (7 fg mL^{-1}) by applying Ab_2-AuNP conjugate for the high affinity sensor surface. Furthermore, the obtained results indicated that the affinity constant of the secondary immunoreaction increased with increasing the sensor surface affinity constant. It was considered that the Ab_2 in the secondary immunoreaction recognized the tail of primary Ab for the high affinity sensor surface, which results in the high response, high affinity constant and consequently the high sensitivity of the detection process.

In chapter 5, a highly sensitive immunosensing of clenbuterol in a real urine sample was developed. However, the real sample may contain many kinds of inhibitors. There are challenges for real sample analysis, even though the high sensitivity was realized in an ideal condition. In this study, the indirect competitive inhibition immunoassay with secondary immunoreaction optimized in above chapters was employed for detection of clenbuterol. Although the sensitivity of 7 ppq was achieved in ideal condition using PBS buffer solution, SPR did not respond to the primary Ab of clenbuterol in non-pretreated urine. First, in order to eliminate the pH effect, the pH was adjusted by mixing with PBS buffer solution (1:1). The pH of sample solution became always 7.4 by the buffer effect. Next, the filtration methods

for urine of cows were investigated. Although very high SPR response was obtained, the sensor surface could not be regenerated again. It was suggested that the high non-specific adsorption of inhibitors was caused for physical filtration. Therefore, it was concluded that the physical filtration could not removed the inhibitors. Subsequently the chemical filtration method was examined. Three types of silica filter modified with functional group (octadecyl, amide and carboxyl acid) were employed for urine sample. All three filters showed the removal performances. This result implied that the inhibitors chemically interrupted the immunoreaction. It was noticed that the carboxylic acid group modified silica filter provided the best filtration among three filters. It was found that the highest SPR signal with a magnitude of 45 mdeg was obtained. The obtained sensitivity for urine solution was almost comparable to the sensitivity obtained in the buffer solution. Furthermore, a low limit of detection with 20 ppq was achieved by using secondary immunoreaction using Ab_2–AuNP conjugate. Therefore, it was suggested that the low limit of detection as well as short detection time would be an alternative to the conventional methods.

From the development of indirect competitive inhibition immunoassay, the following concluding points are as follows:

- The primary antibody (anti-clenbuterol mouse IgG) was labeled with AuNP (Ab-AuNP) and successfully employed in the immunoassay.
- LOD simulation was constructed from affinity constant.
- A ppt-level LOD is produced by adjusting K_1 to one order of magnitude lower than αK_2.
- Affinity constant of sensor surface influenced the SPR signal and sensitivity.
- A high affinity constant sensor surface was better compared to a low affinity sensor surface for secondary immunoreaction.

- The physical filtration did not worked well, while the chemical filtration reduced the matrix effect.
- 20 ppq clenbuterol in urine sample could be detected by only 2-time dilution.

Finally, the developed fast sample pretreatment process and the use of AuNP in indirect competitive inhibition immunoassay produced 20 ppq limit of detection for clenbuterol in urine sample. Therefore, it can be expected that the developed immunoassay technique could provide a reliable detection and quantification of clenbuterol in other real sample analysis, which will be helpful to ensure quality of human health.